

XXII  
INTERNATIONAL WORKSHOP ON  
OPTICAL WAVE & WAVEGUIDE THEORY  
AND NUMERICAL MODELLING

NICE, FRANCE  
JUNE 27 & 28, 2014

ABSTRACT BOOK





# The XXII International Workshop on Optical Wave & Waveguide Theory and Numerical Modelling

## ORGANIZERS

### TECHNICAL COMMITTEE

- Trevor Benson, University of Nottingham, UK
- Jiri Ctyroky, Institute of Electronics and Photonics, Czech Republic
- Manfred Hammer, University of Twente, Netherlands
- Andrei V. Lavrinenko, COM-DTU, Lyngby Kgs., Denmark
- John Love, Australian National University, Canberra, Australia
- Andrea Melloni, DEI-Politecnico di Milano, Italy
- Olivier Parriaux, Lyon University, Saint-Etienne, France
- Reinhold Pregla, Fern Universität, Hagen, Germany
- Ivan Richter, Czech Technical University, Prague, Czech Republic
- Christoph Wachter, Fraunhofer IOF, Jena, Germany

### LOCAL ORGANIZING COMMITTEE 2014

- Anne-Laure Fehrembach, Institut Fresnel, Aix-Marseille University, France
- Gilles Renversez, Institut Fresnel, Aix-Marseille University, France
- Nicolas Bonod, Institut Fresnel, CNRS, Marseille, France
- Claire Guéné, Communication Manager, Aix-Marseille University, France
- Emilie Carlotti, Administrative & Financial Manager, Institut Fresnel, CNRS, Marseille, France
- Marc DeMicheli, Laboratoire de Physique de la Matière Condensée, Nice, France
- Pierre Aschieri, Laboratoire de Physique de la Matière Condensée, Nice, France

### INFORMATION

<http://www.fresnel.fr/owtnm2014/>





OWTNM 2014  
XXII International Workshop on  
Optical Wave & Waveguide Theory and Numerical Modelling

OWTNM local organizing committee from the CLARTE research team, Institut Fresnel

Nice, France, 27 & 28 June 2014



# Acknowledgments

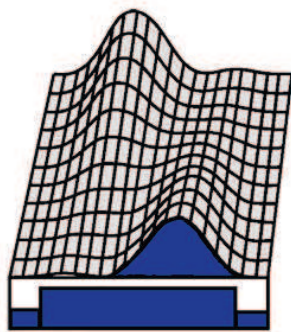
The organizers thank for their interest and support:

- The University of Nice-Sophia Antipolis which provides amphitheatres and staff members on its Saint Jean d'Angély campus
- The Faculty of Science of the Aix-Marseille University for its funding
- The CNRS region administration for the management of the inscriptions by its online tool "Azur Colloque"
- The Optitec association for its funding
- C'Nano PACA GDR CNRS 3196 for its funding
- Phoenix Software for its sponsorship
- Photon Design for its sponsorship
- Manfred Hammer of the University of Twente for his numerous advices
- Trevor Benson of the University of Nottingham for his advices about the special issue
- Frédéric Forestier, computer engineer at the Institut Fresnel, for his help on the website



**Phoenix Software**

Solutions for Micro and Nano Technologies



**Photon  
Design®**

# Preface

This XXII International Workshop on Optical Wave & Waveguide Theory and Numerical Modelling (OWTNM) is localized in Nice in the Saint Jean d'Angély campus. It will be held on 27<sup>th</sup>-28<sup>th</sup> of June 2014. As every two years, it is collocated with the bi-annual conference ECIO which will take place from the 24<sup>th</sup> up to the 27<sup>th</sup> of June. The local organizing committee is mainly composed of researchers and administrative staff of the Institut Fresnel which is localized in Marseille. The organizers hope and expect that this edition of OWTNM will be as successful as the previous meetings. The workshop will host eight oral sessions including the joint session with ECIO ensuring thirty talks, and the usual poster session with forty one posters that will be displayed over the whole event.

The website of the workshop is available at the following link:

<http://www.fresnel.fr/owtnm2014>

Marseille, 7<sup>th</sup> June 2014.

For the local organizing committee of OWTNM 2014:

Anne-Laure FEHREMBACH, Gilles RENVERSEZ, and Nicolas BONOD

# Contents

|  |           |
|--|-----------|
| <b>Programme with full poster list</b> | <b>5</b>  |
| <b>Oral presentations</b>              | <b>11</b> |
| <b>Poster presentations</b>            | <b>43</b> |
| <b>Author index</b>                    | <b>85</b> |

# **Programme**

**Workshop schedule**

**Full poster list**

**9h00-10h30 : Waveguides**

- O-1.0 *Functional PT-symmetric waveguide systems*  
H. Benisty (invited), A. Lupu and A. Degiron
- O-1.1 *Numerical analysis of pump propagation and absorption in specially tailored double-clad rare-earth doped fiber*  
P. Koška, P. Peterka
- O-1.2 *Orthonormal complex hybrid guided mode Coupling over a discontinuity in a plasmonic waveguide*  
A. Karabchevsky, M.N. Zervas, J.S. Wilkinson
- O-1.3 *Modified effective index method to fit in 2D case the phase and group index of 3D silicon photonic wire waveguide*  
A. Tsarev

**11h00-12h30 : Joint Session with ECIO-MOC**

- O-2.0 *Plasmonic and metamaterial waveguides and components for nanophotonics*  
A.V. Zayats (invited)
- O-2.1 *Ultracompact photonic crystal integrated circuits: connecting tiny devices to achieve high-performances*  
S. Malaguti, G. Bellanca (invited), S. Trillo
- O-2.2 *An enhanced wavelength tolerant design for the Generation of N-partite single photon W-states*  
K. Thyagarajan

**14h00-15h30 : Metamaterials and nonlinear optics**

- O-3.0 *Metamirrors: full control of reflection from composite sheets*  
S. Tretyakov (invited), V. Asadchy, Y. Ra'di
- O-3.1 *Guiding self-collimated beams in photonic band gap metamaterials*  
E. Centeno, J. Arlandis
- O-3.2 *Photon management by nonlinear coupling in nanostructures*  
A. Popov, S.A. Myslivets, V.V. Slabko, M.I. Shalaev, I.S. Nefedov
- O-3.3 *Nonlinear switching in optically induced waveguide arrays*  
D. Diebel, D. Leykam, M. Boguslawski, P. Rose, C. Denz, A.S. Desyatnikov

**16h00-17h15 : Scattering**

- O-4.0 *Geometric resonances in waveguides and sub wavelength nanowire gratings: Scattering "anomalies" and Optical forces*  
J.J. Sáenz (invited)
- O-4.1 *Scattering in optical waveguides: a comprehensive model for radiative losses and backreflections*  
D. Melati, F. Morichetti, A. Melloni
- O-4.2 *Modelling of a roughened sidewall ring resonator add drop filter*  
R. Mansoor, H. Sasse, A. Duffy

**17h15-18h30 : Methods and Modelling 1**

- O-5.0 *Modelling realistic plasmonic nanostructures: Field enhancement and beyond*  
O. J.F. Martin (invited)
- O-5.1 *Leaky modes in a non dissipative plasmonic waveguide with a bounded cross Section*  
A.-S. Bonnet-Ben Dhia, C. Carvalho, S. Chesnel, P. Ciarlet Jr.
- O-5.2 *Advanced modal method for computing modes of waveguides with trapezoidal cross section*  
G. Granet

**8h30-10h15 : Methods and Modelling 2**

- O-6.0 *Numerical modeling of time-domain nanophotonic applications using a discontinuous finite element type method*  
C. Scheid, S. Lanteri (invited), R. Léger, J. Viquerat
- O-6.1 *A Dirichlet-to-Neumann approach for the exact computation of guided modes in photonic crystal waveguides*  
S. Fliss
- O-6.2 *A multigrid solver with adaptive time-stepping for the WDM SOA response*  
J. Bos, C. Vagionas, R. Stoffer
- O-6.3 *An eigenmode expansion technique for modeling Kerr-nonlinear waveguide structures*  
J. Petráček
- O-6.4 *Modeling of nonlinear nanoplasmonic and nanophotonic directional couplers*  
P. Koška, P. Kwiecien, I. Richter, J. Čtyroký

**10h45-12h30 : Posters session**

**13h45-15h15 : Gratings and spectral filtering**

- O-7.0 *Subwavelength gratings for the filtering of light (spectral, spatial and polarization)*  
R. Haidar (invited), P. Bouchon, P. Chevalier, J. Jaeck, Q. Lévesque, F. Pardo, J.-L. Pelouard, C. Tardieu, G. Vincent
- O-7.1 *Coupled-wave analysis of the unexpectedly low-loss plasmon-triggered switching between orders diffracted by a metal grating*  
E. Mounkala, A.V. Tischenko, O. Parriaux
- O-7.2 *Optical quasimodes and their application to infrared spectral filtering*  
B. Vial, G. Demésy, A. Nicolet, F. Zolla, M. Commandré, T. Begou, C. Hecquet, S. Tisserand, F. Bedu, H. Dallaporta
- O-7.3 *Tunability of plasmonic surface lattice resonances via experiments and numerical mode analysis*  
A. Abass, S.R.K. Rodriguez, J. Gomez Rivas, B. Maes

**15h45-17h15 : Photonic devices and applications**

- O-8.0 *The relevance of group delay for refractometric sensing*  
H. J.W.M. Hoekstra (invited) and M. Hammer
- O-8.1 *Thermo-plasmonic optical switches at telecom wavelengths*  
J.-C. Weeber, K. Hassan, M. Nielsen, T. Bernardin, S. Kaya, C. Finot, J. Fatome
- O-8.2 *Modeling of microring resonators with high dispersion induced by a one dimensional photonic crystal*  
D. Urbonas, M. Gabalis, S. Malaguti, A. Parini, G. Bellanca, R. Petruskevicius
- O-8.3 *Second Order Sensitivity Analysis for a Photonic Crystal Waveguide Bend*  
Z. Hu, Y.-Y. Lu

## List of posters

- P-01 *A rigorous analytical approach using MoM for testing air gap tuning effects*  
L. Djouablia, A. Labbani, A. Benghalia
- P-02 *Tunability of absolute photonic band gaps in two- dimensional photonic crystals based on CdSe particles embedded in TiO<sub>2</sub>matrix*  
A. Labbani, L. Jouablia, A. Benghalia
- P-03 *Numerical Simulation of resonance structures with FDTD Algorithms Based on GPU B-CALM and CPU Meep*  
D. Urbonas, M. Gabalis, R. Petruskevicius
- P-04 *Determination of the equivalent step index of direct laser written waveguides*  
L. Huang, F.P. Payne
- P-05 *Computing waveguide modes by the pseudospectral modal method*  
D. Song, Y.-Y. Lu
- P-06 *Morris-index screening technique to assess parameters incertitude in microring-based Optical Networks-on-Chip*  
A. Parini, G. Bellanca
- P-07 *A vectorial solver for the reflection of semi-confined waves at slab waveguide discontinuities for non-perpendicular incidence*  
M. Hammer
- P-08 *The fundamentals of multi-splitting filtering technology*  
A. Tsarev
- P-09 *The propagation of the optical signal along a silicon wire in the presence of multiple weak tunnel reflections*  
E. Kolosovsky, A. Tsarev
- P-10 *The Approximation Functions Method for nonlinear Volterra integral equations*  
A. Nerukh, D. Zolotariov, T. Benson
- P-11 *Full-vectorial finite-difference analysis of ferroelectric BaTiO<sub>3</sub> device*  
X. Hu, R. Orobtschouk
- P-12 *Mono and multielectrode SOA structure optimization for wide optical bandwidth operation*  
P. Morel, R. Breno, F. Lelarge, T. Motaweh, A. Lagrost
- P-13 *Study of optical properties of textured Si solar cell with micro pillars*  
F.J. Cabrera-Espana, B.M.A. Rahman, A. Agrawal
- P-14 *Perfectly Matched Layers in negative index metamaterials*  
E. Bécache, P. Joly, V. Vinales
- P-15 *Dielectric tensor retrieval for gyrotropic 3D photonic crystals*  
A.A. Shcherbakov, A.V. Tishchenko
- P-16 *Plasmon resonances on metal sphere aggregates in a dielectric matrix*  
S. Bakhti, N. Destouches, A. V. Tishchenko
- P-17 *Explanation of ultra narrow-band reflection from a 1d grating based on a modal method and symmetry considerations*  
T. Kämpfe, A.V. Tischenko, O. Parriaux
- P-18 *Analytical model for the field of microstructured optical fibers: evaluation and enhancement*  
D.K. Sharma , A. Sharma
- P-19 *Approximate method for modal analysis of nanoscale surface plasmon-polariton waveguides*  
K. Gehlot, A. Sharma
- P-20 *Characteristics of dual-core hybrid plasmonic liquid crystal photonic crystal fiber*  
B.M. Younis, A.M. Heikal, M. Farhat, M. Abdelrazak, S.S.A Obayya
- P-21 *Polarization characteristics of elliptical spiral plasmonic photonic crystal fiber*  
F.F.K. Hussain, A.M. Heikal, M.O.H. Farhat, J. El-Azab, W.S. Abdelaziz, S.S.A. Obayya
- P-22 *Blocked Schur for noniterative bidirectional beam propagation method*  
A.M.A. Saeed, S.S.A. Obayya
- P-23 *Compact TM-pass polarizer based on Silicon-on-Insulator photonic wire*  
A.I.H. Azzam, S.S.A. Obayya
- P-24 *3D-active beam propagation method to simulate QD-polymer waveguides*  
I. Suárez, J.P. Martínez-Pastor

- P-25 *Spectral Model of non-linear phenomena in a Power-Over-Fiber system*  
L. Ghisa-Telescu, F. Audo, H. Prod'homme, A. Perennou, P. Quintard, M. Guegan
- P-26 *Analysis of surface plasmon polariton modes on a metal thin film covered with uniaxially anisotropic material*  
H.-H. Liu, H.-C. Chang
- P-27 *Design and analysis of a coupled strip-slot waveguide structure for dispersion compensation*  
N. Ashok, V. Rastogi, V. Mann
- P-28 *Low-frequency photonic bands in metallic lattices: a tightbinding description*  
K. Wang
- P-29 *"Talbot Effect" in the Time Domain*  
E. K. Sharma, J. Anand
- P-30 *Optimization of micro-structured waveguides in Lithium Niobate*  
M. Dubov, H. Karakuzu, S. Boscolo
- P-31 *Studies on dipolar interactions in arrays of sub-wavelength plasmonic nanoparticles*  
J. Fiala, P. Kwiecien, I. Richter
- P-32 *Analysis of plasmonic slot waveguide couplers in linear and nonlinear regimes*  
J. Petráček, P. Kwiecien, I. Richter, Y. Ekşioğlu
- P-33 *Nonlinear metal slot waveguides: bifurcations and higher order modes*  
W. Walasik, Y.V. Kartashov, G. Renversez
- P-34 *Modeling of a cavity-resonator-integrated guided-mode resonance filter*  
N. Rassem, A.-L. Fehrembach, E. Popov
- P-35 *Vertical Mode Expansion Method for diffraction of light by biperiodic circular cylindrical structures*  
X. Lu, H. Shi, Y.-Y. Lu
- P-36 *Geometrical interpretation of Fano resonances in plasmonic nanostructures*  
V. Grigoriev, S. Varault, G. Boudarham, B. Rolly, B. Stout, J. Wenger, N. Bonod
- P-37 *Polarizability tensors of metallic U-shaped scatterers*  
S. Varault, B. Rolly, G. Boudarham, G. Demésy, B. Stout, N. Bonod
- P-38 *Coherent perfect absorption of light by nanoparticles*  
V. Grigoriev, N. Bonod, J. Wenger, B. Stout
- P-39 *Controllable emission directivity with a hybrid magnetic-electric dielectric Scatterer*  
J. Benedicto, B. Rolly, J.-M. Geffrin, R. Abdeddaim, B. Stout, N. Bonod
- P-40 *Polarization-dependent spectra of photonic crystal with anisotropic plasmonic defect layer*  
S. Moiseev, V.V. Ostatochnikov, D. Sementsov
- P-41 *Controlling interface reflectance by plasmonic composite structure*  
S. Moiseev



# **Oral presentations**

## Functional PT-symmetric waveguide

H. Benisty (IOGS-LCF, Palaiseau), A. Lupu and A. Degiron (IEF, Orsay)

[\\*henri.benisty@institutoptique.fr](mailto:henri.benisty@institutoptique.fr)

Parity-Time (PT) symmetry was conceptualized as a quantum mechanics (QM) interrogation, namely how far operators with real eigenvalues can deviate from mathematical Hermiticity[1]. The answer is that by adding what we call in this community gain and loss in equal amounts to the diagonal terms, i.e. adding opposite imaginary terms (think of two coupled waveguides and their traditional coupled-mode 2x2 matrix), there is a range of parameters where eigenvalues remain real. Indeed, J. Ctyroky et al. [2] had come to remark this already in 1996. The added QM-inspired vocabulary may seem somewhat impressive to us, comprising terms such as "broken symmetry", "exceptional point", "gauge transform", but these offer as many hints to where these concepts may lead and are attractive for young physicists [3-6].

With a more practical view, we started to devise in 2011 whether coupling of a gain waveguide to a fixed-loss waveguide, a situation bound to occur with lossy plasmonic waveguide, provides similar intriguing features. The answer is yes with modest provisions, going a step beyond a formerly known no-gain limit also called "passive PT-symmetry"[7-9].

Two less obvious points on these PT symmetric systems came after stirring ideas and models, notably around the switching behaviour and the possible "spatial non reciprocity" :

- (i) the gain modulation essentially provides plasmonic guide systems with a crucial tuning ingredient they are missing: electro-refractive tuning, which is clearly too weak compared to the short paths typical of plasmonic waveguides;
- (ii) PT-symmetry exploits the loss-gain combination in a clever combination not intuitive from just loss compensation since, for instance, some fixed losses will be shown to lower the gain modulation needed for switching a two-channel. guide pair.

Other intriguing features allowed by the interplay of PT-symmetry and Bragg periodicity will be briefly presented.

- [1] C. M. Bender and S. Boettcher, "Real spectra in non-Hermitian Hamiltonians having PT symmetry," *Physical Review Letters*, vol. 80, pp. 5243-5246, Jun 1998.
- [2] H. P. Nolting, G. Sztefka, M. Grawert, and J. Ctyroky, "Wave Propagation in a Waveguide with a Balance of Gain and Loss," in *Integrated Photonic Conference*, Boston, 1996, pp. IMD5-1.
- [3] C. E. Rüter, K. G. Makris, R. El-Ganainy, D. N. Christodoulides, M. Segev, and D. Kip, "Observation of parity-time symmetry in optics," *Nature Phys.* 6, 192–195 (2010).
- [4] M. Kulishov, J. M. Laniel, N. Bélanger, J. Azaña, and D. V. Plant, "Nonreciprocal waveguide Bragg gratings," *Opt. Express* 13, 3068–3078 (2005).
- [5] Z. Lin, H. Ramezani, T. Eichelkraut, T. Kottos, H. Cao, and D. N. Christodoulides, "Unidirectional invisibility induced by PT -symmetric periodic structures," *Phys. Rev. Lett* 106, 213901 (2011).
- [6] L. Feng, Y.-L. Xu, W. S. Fegadolli, M.-H. Lu, J. E. Oliveira, V. R. Almeida, Y.-F. Chen, and A. Scherer, "Experimental demonstration of a unidirectional reflectionless parity-time metamaterial at optical frequencies," *Nat. Mater.* 12, 108–113 (2012).
- [7] H. Benisty, A. Degiron, A. Lupu, A. De Lustrac, S. Chénais, S. Forget, M. Besbes, G. Barbillon, A. Bruyant, S. Blaize, and G. Lérondel, "Implementation of PT-symmetric devices using plasmonics: principle and applications," *Opt. Express* 19, 18004-18019 (2011).
- [8] H. Benisty, C. Yan, A. Degiron, and A. T. Lupu, "Healing near-PT-symmetric structures to restore their characteristic singularities: Analysis and examples," *J. Lightwave Technol.* 30, 2675-2683 (2012).
- [9] A. Lupu, H. Benisty, and A. Degiron, "Switching using PT-symmetry in plasmonic systems: positive role of the losses," *Opt. Express* 21, 21651-21668 (2013).

## Numerical analysis of pump propagation and absorption in specially tailored double-clad rare-earth doped fiber.

P. Koška<sup>1,2,\*</sup>, P. Peterka<sup>1</sup>

<sup>1</sup>*Institute of Photonics and Electronics AS CR, v.v.i, Prague, Czech Republic*

<sup>2</sup>*Faculty of Nuclear Sciences and Physical Engineering, CTU in Prague, Czech Republic*

\*<mailto:koska@ufe.cz>

The full-vector FEM-BPM was used to reveal non-intuitive processes in pump propagation in a double-clad fiber with cross section that allows easy splicing of pump and signal fibers with the active fiber. Real size of the fiber and winding of the fiber is included in the model.

### Summary

We present a numerical analysis of multi-mode pump absorption in recently proposed double-clad fiber with stadium-like cross section of the inner cladding and asymmetrically placed rare-earth-doped core [1]. Such a cross section allows easy splicing of the multimode pump fiber and singlemode signal fiber to the double-clad fiber. The full-vector finite element beam propagation method (FEM-BPM) was used as a numerical tool [2]. The method and the model are described in detail. Stability and accuracy of FEM-BPM was improved to correctly simulate field propagation in such a structure on long distance. It is also necessary to excite the structure by arbitrary field profile. Definite set of functionals satisfying unisolvence condition together with hybrid edge-nodal finite element basis is presented. This set of functionals enables decomposition of arbitrary field profile to the finite element mesh.

There were several analyses addressing pump absorption efficiency in double-clad fibers with irregular cladding geometry [3]. These analyses were based on high order speckle-like mode statistics and chaotic ray approximation. All these studies assumed straight fiber, which is impractical case. In our study we present analysis of real-size structure including curvature of the fiber caused by winding of the fiber on a reel. To simulate the curvature we used the transformation of the refractive index profile.

### Results

The stability and accuracy of FEM-BPM was improved. The performance of stadium-like fiber is compared to circular fiber. Over 75 % of pump energy is absorbed in 3 m of the rare-earth-doped fiber with core absorption of 4200 dB/m and cladding-core area ratio of 342. The results show that the stadium-like fiber has much better pump absorption efficiency than the circular one.

### References

- [1] P. Peterka, et al, *Amplifier performance of double-clad Er/Yb-doped fiber with cross-section tailored for direct splicing to the pump and signal fibers*, In Tech. Digest OFC'07, p. JWA12, Anaheim, USA, March 25-29, 2007
- [2] D. Schulz, C. Glingener, M. Bludszweit, E. Voge, *Mixed finite element beam propagation method*, Light-wave Technology, Journal of, vol. 16, pp. 1336-1342, 1998
- [3] P. Leproux, S. Février, V. Doya, P. Roy, D. Pagnoux, *Modeling and Optimization of Double-Clad Fiber Amplifiers Using Chaotic Propagation of the Pump*, Optical Fiber Technology, vol. 6, pp. 324–339, 2001

# Orthonormal Complex Hybrid Guided Mode Coupling over a Discontinuity in a Plasmonic Waveguide

A. Karabchevsky<sup>1,\*</sup>, M. N. Zervas<sup>1</sup>, J. S. Wilkinson<sup>1</sup>

<sup>1</sup>*Optoelectronics Research Centre, University of Southampton, Southampton SO17 1BJ, United Kingdom*

\*[A.Karabchevsky@soton.ac.uk](mailto:A.Karabchevsky@soton.ac.uk)

We generalized an expression for expansion coefficients to determine the orthonormal complex hybrid guided mode coupling over a small step discontinuity which allowing prediction of the localised surface intensity on a plasmonic waveguide for design of devices for integrated surface-enhanced spectroscopy.

## Introduction

Waveguide surface sensing measurements require maximization of surface optical intensity. Plasmonic waveguides (PWGs) formed from a dielectric waveguide with an absorptive overlayer of a noble metal can exhibit high surface localization and therefore high surface intensity. PWGs are usually illuminated from the uncoated input waveguide as shown in the schematic in Fig 1a. The transmittance of such a device has been modelled previously for the slab waveguide case [1]. In this study, we extend a predication of transmittance through the structures with 2D confinement of a guiding layer reported elsewhere [2] using a more general expression for the expansion coefficients describing the coupling between transmitted orthonormal complex hybrid guided mode (OCHGM) amplitudes and a distribution of a surface intensity which is superimposed in Fig 1a.

## Results

Fig. 1b and Fig 1c show the calculated transmittance at 633 nm through the PWG as a function of refractive index of an ambient and power carried by the three guided modes, respectively, within gold region, neglecting backscattering and a multiple reflections. The mapped surface intensity is detailed in Fig. 1d. The guided mode intensity distributions  $|E_y(x,y)|^2$  at  $z=0 \mu\text{m}$  for a gold-coated waveguide region, calculated using FEM at a wavelength of 620 nm are shown in Fig. 1e.

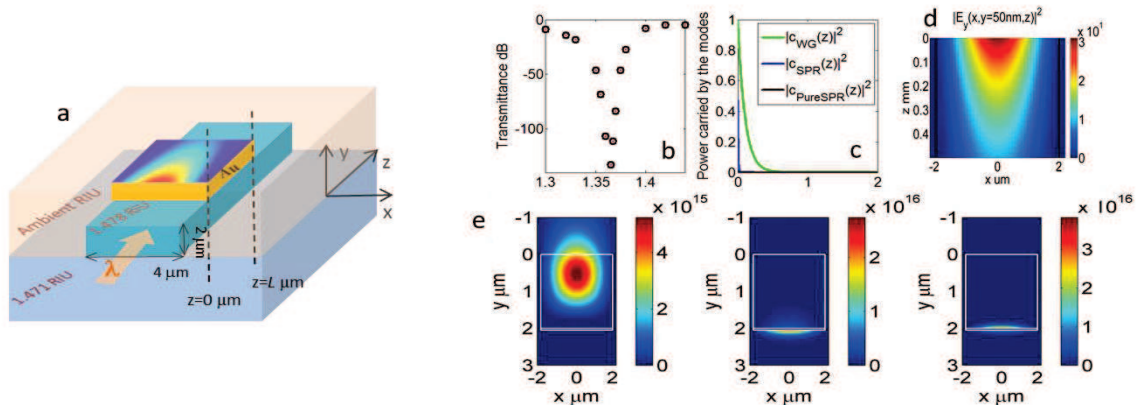


**Fig. 1.** (a) Schematic of a waveguide with calculated surface intensity distribution  $|E_y(x,y=50\text{nm},z)|^2$  enlarged in (d); (b) calculated transmittance; (c) calculated powers carried by the modes within the Au-coated region, (e)  $|E_y(x,y)|^2$  of the three guided modes obtained using FEM for a Au-coated region.

## Conclusion

We have introduced a general expression for the expansion coefficient of any two OCHGM at a step of discontinuity and applied this to the introduction of a thin absorptive overlayer to predict device transmittance and surface intensity on PWGs. This model provides the basis for designing high-sensitivity refractometers and integrated optical devices for surface-enhanced spectroscopies.

## References

- [1] J. Čtyroký et al., *Sensors and Actuators B*, 54, 66-73, 1999
- [2] A. F. Milton and W. K. Burns, *IEEE Journal of Quantum Electronics*, 13, 828-835, 1977

## Modified effective index method to fit in 2D case the phase and group index of 3D silicon photonic wire waveguide

A. Tsarev<sup>1,2\*</sup>

<sup>1</sup>*A.V. Rzhanov Institute of Semiconductor Physics SB RAS, Novosibirsk, Russia*

<sup>2</sup>*The Novosibirsk State University, Novosibirsk, Russia*

\*[tsarev@isp.nsc.ru](mailto:tsarev@isp.nsc.ru)

We set up a modified effective index method (MEIM) which correctly describes in 2d case both the phase and the group indexes in 3d silicon wire waveguide, typically used in silicon photonics in thin silicon-on-insulator (SOI) structures. The prove of concept has been obtained by direct 2d and 3d FDTD modeling.

### Summary

Three dimensional (3d) optical waveguide structures are typically modeling by 2d analogies under effective index method (EIM). The principal limitation of EIM comes from the fact that real 3d waveguide with 2 different cross dimensions ( $h$  and  $W$ ) is examined by 2d waveguide with the only one size parameter ( $w$ ). This produces an error in studying impulse excitation by FDTD method, due to wrong group index determined by EIM. We overcome this limitation by introducing a modified effective index method (MEIM) [1, 2] which correctly describes in 2d case both the phase and the group indexes in 3d strip waveguide. New MEIM utilizes the combined index profile with the two spatial parameters, namely, the central part with index  $N_{Si}$  has the width  $w$  (nearly waveguide height  $h$ ) and it is mainly responsible for the group index  $N_g$ . The base part has the same with  $W$  as in 3d waveguide and refractive index  $N_b$  which is mainly responsible for the phase index  $N_p$ . By variation of  $w$  and  $N_p$  it is possible to fit in a wide wavelength range the effective index of combined 2d waveguide to the mode index of 3d waveguide. Numerical experiments of ring resonator, Fabry-Perot (FP) and asymmetric Mach-Zehnder (MZ) interferometers by FDTD [1, 2] prove that the modified EIM gives much better agreement with the test 3d simulation as it provides the best fitting both the phase and the group indexes. For example, MEIM provides about 1% error in FSR in comparison to 29% and 34% error for EIM in FP and MZ interferometers, respectively.

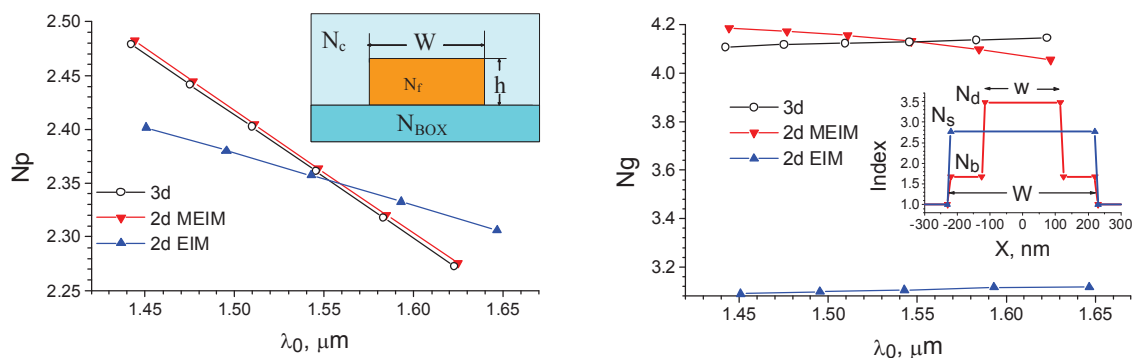


**Fig. 1.** Group and phase indexes as a function of optical wavelength  $\lambda_0$  and index profiles for different cases.

### References

- [1] A. Tsarev, "Modified effective index method to fit the phase and group index of 3D photonic wire waveguide," *Opt. Lett.*, 38, 293-295 (2013).
- [2] A. Tsarev, "Numerical modeling of optical multiplexer on SOI constructed by multiple coupled waveguides," *J. Sel. Top. Quantum Electron.* 20, no.4, pp.1,8, July-Aug. 2014.

## Plasmonic and Metamaterial Waveguides and Components for Nanophotonics

Anatoly V. Zayats<sup>1,\*</sup>

<sup>1</sup>*Department of Physics, King's College London, Strand, London WC2R 2LS, United Kingdom*

[\\*anatoly.zayats@kcl.ac.uk](mailto:anatoly.zayats@kcl.ac.uk)

Plasmonic waveguides based on metal, dielectric or metamaterial nanostructures will be overviewed focusing on their active functionalities. Nonlinear, opto-mechanical and electro-optical properties of the waveguides will be considered for applications in optical information processing and data storage.

Surface plasmon polaritons (SPPs) offer a unique opportunity to localize optical signals on subwavelength scales. Plasmonic waveguides attract significant attention for prospective information delivery and manipulation in integrated photonic circuitry. Waveguide design allows one to control the field confinement and dispersion of guided waves and engineer the required properties advantageous for one or another active application, e.g., optimisation of stimulated emission or field enhancement needed for loss compensation or all-optical signal control, respectively.

In this talk, we will overview various plasmonic waveguides focusing on their active functionalities such as amplification of surface plasmon polaritons, opto-mechanical, electro-optical and nonlinear effects [1-10]. Dielectric-loaded and hyperbolic-metamaterial-based plasmonic waveguides will be considered for applications in optical information processing and high-density data storage.

### References

- [1] A. S. Shalin, P. Ginzburg, P. A. Belov, Yu. S. Kivshar, A. V. Zayats, *Nano-opto-mechanical effects in plasmonic waveguides*, *Laser Phot. Rev.*, vol. 8, pp. 131-136, 2014.
- [2] P. V. Kapitanova, P. Ginzburg, F. J. Rodríguez-Fortuño, D. S. Filonov, P. M. Voroshilov, P. A. Belov, A. N. Poddubny, Yu. S. Kivshar, G. A. Wurtz, A. V. Zayats, *Photonic spin Hall effect in hyperbolic metamaterials for polarization-controlled routing of subwavelength modes*, *Nat. Comm.*, vol. 5, 3226, 2014
- [3] P. Ginzburg, A.V. Krasavin, A.V. Zayats, *Cascaded second-order surface plasmon solitons due to intrinsic metal nonlinearity*, *New J. Phys.*, vol. 15, 013031, 2013.
- [4] D. Fedyanin, A. V. Krasavin, A. Arsenin, A. V. Zayats, *Surface plasmon polariton amplification upon electrical injection in highly-integrated plasmonic circuits*, *Nanoletters*, vol. 12, pp. 2459–2463, 2012.
- [5] A. V. Krasavin, Th. Ph. Vo, W. Dickson, P. M. Bolger, A. V. Zayats, *All-plasmonic modulation via stimulated emission of co-propagating surface plasmon polaritons on a substrate with gain*, *Nano Lett.* vol. 11, pp. 2231-2235, 2011.
- [6] A. V. Krasavin, S. Randhawa, J.-S. Bouillard, J. Renger, R. Quidant, A. V. Zayats, *Optically-programmable nonlinear photonic component for dielectric-loaded plasmonic circuitry*, *Opt. Exp.*, vol. 19, pp. 25222-25229, 2011; S. Randhawa, A. V. Krasavin, T. Holmgaard, J. Renger, S. I. Bozhevolnyi, A. V. Zayats, R. Quidant, *Experimental demonstration of dielectric-loaded plasmonic waveguide disk resonators at telecom wavelengths*, *Appl. Phys. Lett.* 98, 161102, 2011.
- [7] A. V. Krasavin, A. V. Zayats, *Photonic signal processing on electronic scales: electro-optical field-effect nanoplasmonic modulator*, *Phys. Rev. Lett.*, vol. 109, 053901, 2012; A. V. Krasavin, A. V. Zayats, *Electro-optic switching element for dielectric-loaded SPP waveguides*, *Appl. Phys. Lett.*, vol. 97, 041107, 2010; A. V. Krasavin, A. V. Zayats, *All-optical active components for dielectric-loaded plasmonic waveguides*, *Opt. Comm.*, vol. 283, pp. 1581-1584, 2010.
- [8] A. V. Krasavin, A. V. Zayats, *Guiding light at the nanoscale: numerical optimisation of ultra-subwavelength metallic wire SPP waveguides*, *Opt. Lett.*, vol. 36, 3127-3129, 2011; A.V. Krasavin, A.V. Zayats, *Numerical analysis of long-range SPP modes in nanoscale plasmonic waveguides*, *Opt. Lett.*, vol. 35, pp. 2118-2120, 2010.
- [9] D. O'Connor, M. McCurry, B. Lafferty, A. V. Zayats, *Plasmonic waveguide as an efficient transducer for high-density data storage*, *Appl. Phys. Lett.*, vol. 95, 171112, 2009.
- [10] A. D. Neira, G. A. Wurtz, P. Ginzburg, A. V. Zayats, *Ultrafast all-optical modulation with hyperbolic metamaterial integrated in Si photonic circuitry*, *Opt. Exp.*, to be published.

# Ultracompact photonic crystal integrated circuits: connecting tiny devices to achieve high-performances

Stefania Malaguti, Gaetano Bellanca and Stefano Trillo

<sup>1</sup> *University of Ferrara, Ferrara, Italy*  
*gaetano.bellanca@unife.it*

**Abstract:** PhC technology is expected to play an important role in the future of optical telecommunication devices. Results relevant to the design and fabrication of a  $4 \times 25$  Gbit/s WDM Receiver and of a 100 Gbit/s OTDM Receiver are presented.

**Introduction.** In the last years, the rapid advances in science and technology, with the disrupting advent of Internet in daily life, have transformed significantly the world of communication and computing. The demands of consumers for higher speeds and greater capacities appear unending. Photonic chips are set to play an important role in the development of future communication and information technologies. Photons (carriers of optical signals) have important fundamental properties that make them superior to electrons (carriers of electrical signals) for representing and transmitting data, as demonstrated by long distance communication networks. However, as the bandwidth increases, the advantages of optics even holds for very short transmission distances, such as between high-speed processors in a computer, and ultimately, across individual computer chips. Although electronics continues to remain unbeaten for performing high-level data processing (such as that performed by modern computers), the growth in performance is today falling short of earlier predictions: electrical interconnects, in fact, are the key factor limiting the speed and the integration level of electronic circuits. Faster switching is possible with current transistor technology, but it takes too much power and generates too much heat to send information across the chip at higher data rates. Photonics has therefore a crucial role to play in global interconnects, but this is a difficult challenge as, to be competitive, the size and power consumption of traditional photonic devices must be reduced by more than two orders of magnitude. Photonic Crystals (PhCs) based technology seems to address these issues and be able to provide devices capable of meeting these challenges. In the framework of the European Project COPERNICUS, researches of different institutions developed the technology needed to provide 100 Gbit/s WDM and OTDM receivers based on PhCs. The main steps needed to get devices that can satisfy these challenging specifications and ensure the required performances, are summarized in the following.

**Modeling.** Effective designs for complex devices as the ones based on PhCs requires accurate theoretical modeling and simulation tools. To achieve the expected results, a wide range of steady-state and time-domain approaches have been developed. In particular, the Finite Difference in the Time Domain (FDTD) has proven to be accurate for simulating linear responses of the investigated components<sup>1</sup>. However, other approaches were pursued, in particular for nonlinear modeling<sup>2</sup> and coupling with electrical/thermal simulations<sup>3</sup>.

**Material Engineering.** For device fabrication, III-V semiconductor PhC membranes have been used<sup>4,5</sup>. This platform is ideally suited for both wavelength filtering/routing, high-speed/low power optical switching and detection. In particular, GaAs and InP technology were pursued. GaAs has the key advantage of a short carrier lifetime, which is attractive for AOGs, whereas InP is compatible with active telecom devices such as InGaAs photodetectors/laser/amplifiers. For the planar technology, both air-bridged and Benzocyclobutene (BCB)-encapsulated PhC membranes were pursued. The former for AOGs<sup>6</sup>, whereas the latter for WDM devices with integrated photodetectors<sup>7</sup>.

**Device Fabrication and Measurements.** Fig. 1 (on the left) shows an example of a 4-channel WDM Receiver. The fabrication of this component required the design of both the key elements (the PhC cavities) and the optical circuitry (waveguides, bends, tapers). Optimizations of each component is fundamental to guarantee a device that satisfies the challenging specifications and ensures the required performances. The same figure reports also (on the right) the eye diagram evaluations at the different ports of the receiver<sup>8</sup>.

# An enhanced wavelength tolerant design for the Generation of $N$ -partite single photon $W$ -states

**K. Thyagarajan<sup>1</sup>, Surajit Paul<sup>2</sup>**

*Department of Physics, Indian Institute of Technology Delhi, New Delhi – 110016, India*

[<sup>1</sup>ktarajan@physics.iitd.ac.in](mailto:ktarajan@physics.iitd.ac.in)

[<sup>2</sup>surajitpaul26@gmail.com](mailto:surajitpaul26@gmail.com)

**Abstract:** Recently integrated optic solutions for generation of  $N$ -partite  $W$ -state have been proposed using a 1-D array of ' $N$ ' identical single mode optical waveguides. The proposed design exhibits very low tolerance to the input wavelength. Here we propose an alternative design of a waveguide array consisting of  $(2N-1)$  waveguides to create ' $N$ ' partite  $W$  state that exhibits much greater tolerance to the input wavelength thus making it easy for experimental realization.

It is well known that entanglement plays a crucial role in various phenomena in the field of quantum computation<sup>1</sup>, quantum cryptography<sup>2-3</sup>, teleportation<sup>4</sup>, quantum key distribution etc. Among various kinds of non-classical entangled states,  $W$  states are important as their entanglement is less fragile against loss of any qubit whereas the other class of entangled states i.e. GHZ states become fully separable after qubit loss<sup>5</sup>. For the realization of such non-classical  $W$  states, quantum optics provides an elegant platform<sup>6</sup>.

Recently integrated optic solutions for generation of  $W$ -states have been proposed using a 1-D array of  $N$  identical single mode optical waveguides, which are coupled via nearest neighbor interaction<sup>7</sup>. The flow of a single photon through such structure is governed by a set of Heisenberg equation of motion:

$$i \frac{d\hat{a}^\dagger}{dz} = K\hat{a}^\dagger \quad (1)$$

where  $\hat{a}^\dagger$  is the creation operator representing the  $z$  dependence of the field in each of the waveguides and given by  $\hat{a}^\dagger = [\hat{a}_1^\dagger, \hat{a}_2^\dagger, \dots, \hat{a}_N^\dagger]^T$  and  $K$  is the coupling matrix representing the coupling co-efficient between adjacent waveguides. Solution of eqn. (1) gives the evolution of the  $z$ -dependence of the field as

$$\hat{a}^\dagger(z) = e^{-iKz} \hat{a}^\dagger(0) \quad (2)$$

Here the term  $e^{-iKz}$  acts as the  $z$ -evolution operator corresponding to the  $z$ -dependence of field in each waveguide. It is well known that for an array consisting of three equally spaced identical waveguides, for a single photon incident in the central waveguide a three partite  $W$ -state is formed at a propagating distance  $z_0 = \left[ \tan^{-1}(\pm\sqrt{2}) + n\pi \right] / \sqrt{2}\kappa_0$ . The major problem with the above mentioned design is that the tolerance to the wavelength of the input single photon for the generation of the  $W$ -state is very critical. Figure 1 shows the variation of probability of finding the photon in an array of 3 equally spaced ( $d = 12\mu\text{m}$ ) identical waveguides as a function of input wavelength, for a device of length  $z = 2.48\text{ cm}$  designed to provide a  $W$ -state at  $\lambda_0 = 1\mu\text{m}$ . Even a change of the input wavelength by  $\pm 0.5\text{ nm}$  ( $\approx \pm 0.05\%$ ) leads to deviation from the  $W$  state with variation in probabilities of about  $\pm 0.5\%$ . Such critical tolerance can lead to problems in practical applications of such devices.

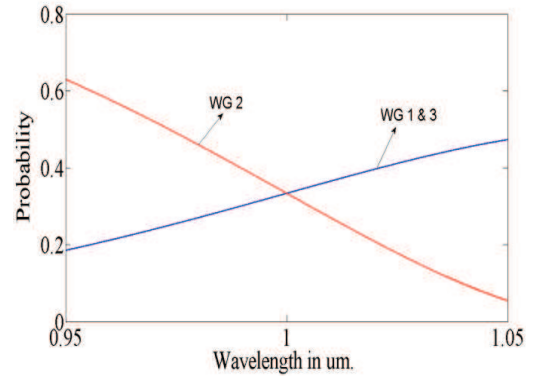


*Fig. 1: Wavelength variation of probability of finding a single photon in an array of 3 equally spaced waveguides*

## Metamirrors: Full control of reflection from composite sheets

S. Tretyakov<sup>1</sup>, V. Asadchy<sup>1,2</sup>, Y. Ra'di<sup>1</sup>

<sup>1</sup>Department of Radio Science and Engineering, Aalto University, P. O. Box 13000, FI-00076 Aalto, Finland

<sup>2</sup>Gomel State University, Department of Physics, Sovyetskaya Str. 104, 246019, Gomel, Belarus

*viktar.asadchy@aalto.fi*

We will overview our recent work on metasurfaces for full control of the phase of plane waves reflected from electrically (optically) thin sheets. This becomes possible using engineered artificial full-reflection layers (metamirrors) as arrays of electrically small resonant bi-anisotropic particles.

Metamirror is an electrically thin (“one-particle-thin”) layer which has zero transmission coefficient and controllable reflection phase [1]. Our investigations of the necessary polarization properties of the unit cells of the structure have shown that reciprocal and lossless bi-anisotropic particles with omega magnetoelectric coupling are the appropriate building blocks for the most general metamirrors. The required bi-anisotropic coupling can be realized by selecting an appropriate shape of dipolar particles sitting in each unit cell of the planar metamirror array. For the microwave frequency range metal wire particles can be used, and we have demonstrated by simulations the metamirror responses of some example designs. Fig. 1 shows spatial distribution of reflected and transmitted power densities for an example of a focusing metamirror. The structure is an electrically dense array of wire omega particles (also shown on the picture). Note that the focal distance of this lens is smaller than the wavelength. For infrared and optical frequencies, low-loss high-contrast dielectric structures of the appropriate symmetry can be possibly used for the same purpose.

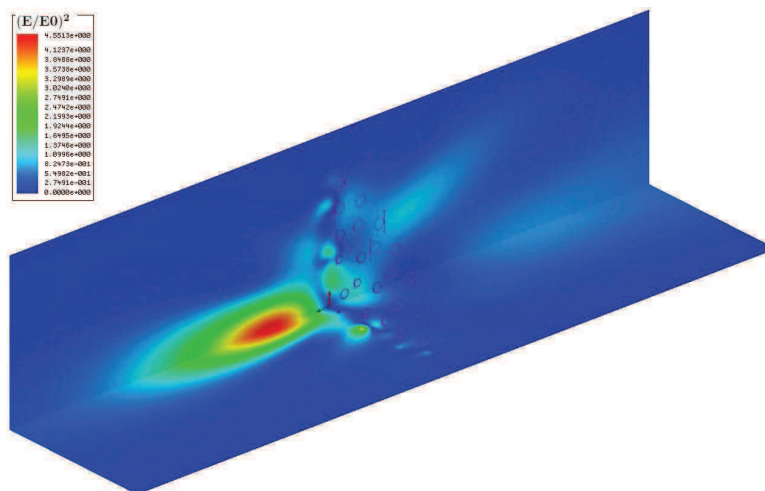


Fig. 1. Plane-wave illumination of a focusing metamirror.

It is important to note that a properly designed single layer of bi-anisotropic particles possessing omega coupling can fully reflect electromagnetic waves coming from different sides with arbitrary phases, and the waves reflected from the two sides of the metamirror can be tailored independently. This concept generalizes the reflectarray concept to the most general phase control of reflections from both sides of the layer using ultimately thin (one layer of dipolar inclusions) structures.

### References

- [1] Y. Ra'di, V.S. Asadchy, S.A. Tretyakov, Tailoring reflections from thin composite metamirrors. Preprint <http://arxiv.org/abs/1401.1677>.

## Guiding self-collimated beams in photonic band gap metamaterials

E. Centeno<sup>1\*</sup>; J. Arlandis<sup>2</sup>

<sup>1</sup>Institut Pascal, Université Blaise Pascal, 63177 Aubière, France

<sup>2</sup>Institut Langevin, ESPCI ParisTech, CNRS, 1 rue Jussieu, 75238 Paris Cedex 05, France

\* Emmanuel.Centeno@univ-bpclermont.fr

Resonant and slow light propagation of self-collimated beams in photonic band gap metamaterials is theoretically investigated. These layered structures combine positive and negative index materials and are realized with metamaterials or photonic crystal superlattices for GHz or THz applications.

### Introduction

Photonic crystals including positive and negative index layers have recently attracts much attention owing to their novel optical properties [1-2]. These photonic band gap metamaterials make zero-average index materials that present zero-phase delay and self-collimation effects [3-4]. At telecom frequencies, these structures named photonic crystal superlattices can be designed in all-dielectric materials with the help of 2D photonic crystal layers that mimic metamaterials [4].

### Summary

In this work, we show that beam shaping operations in metamaterials or photonic crystal superlattices can be interpreted with the same electromagnetic theory [5, 6]. The curvature of the iso-frequency curve is demonstrated to play a crucial for focalization or self-collimation effects. Guided by this theory, we demonstrate that self-collimation can be combined with slow light in photonic crystal superlattices. It is also shown that the amount of semiconductor can also be increased by a factor 10 compared to classical 2D PhCs [6]. These properties are expected to enhance light-matter interaction for nonlinear operations.

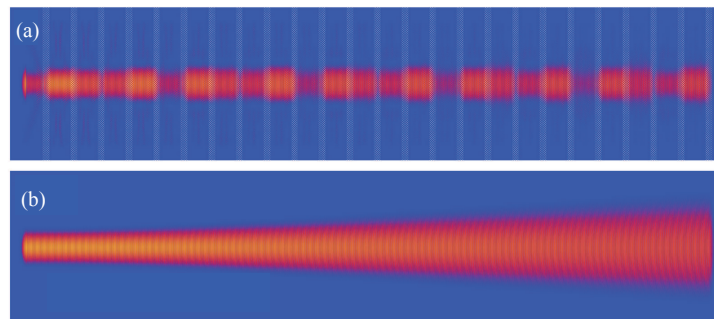


**Fig. 1.** (a) FDTD computation of a self-collimated beam propagating through a super-lattice photonic crystal.

(b) The same beam shows light diffraction in free space.

### References

- [1] J. Li, L. Zhou, C. Chan, and P. Sheng, *Photonic band gap from a stack of positive and negative index materials*, Phys. Rev. Lett. **90**, 83901 (2003).
- [2] Y. Yuan, et. al. , *Experimental verification of zero order bandgap in a layered stack of left-handed and right-handed materials*, Opt. Express **14**, 2220 (2006).
- [3] V. Mocella, et. al., *Self-Collimation of Light over Millimeter-Scale Distance in a Quasi-Zero-Average-Index Metamaterial*, Phys. Rev. Lett. **102**, 133902 (2009).

## Photon Management by Nonlinear Coupling in Nanostructures

A. K. Popov<sup>1,2</sup>, S. A. Myslivets<sup>3</sup>, V. V. Slabko<sup>4</sup>, M. I. Shalaev<sup>4</sup> and I. S. Nefedov<sup>5</sup>

<sup>1</sup> *Birck Nanotechnology Center, Purdue University, West Lafayette, IN 47907, USA, [popov@purdue.edu](mailto:popov@purdue.edu)*

<sup>2</sup> *University of Wisconsin-Stevens Point, Stevens Point, WI 54481, USA, [apopov@uwsp.edu](mailto:apopov@uwsp.edu)*

<sup>3</sup> *Institute of Physics, Siberian Branch of the Russian Academy of Sciences, 660036 Krasnoyarsk, Russian Federation, [sam@iph.krasn.ru](mailto:sam@iph.krasn.ru)*

<sup>4</sup> *Siberian Federal University,*

*660041 Krasnoyarsk, Russian Federation, [vslabko49@mail.ru](mailto:vslabko49@mail.ru), [mshalaev@buffalo.edu](mailto:mshalaev@buffalo.edu)*

<sup>5</sup> *Aalto University, FIN-00076 Aalto, Finland, [igor.nefedov@aalto.fi](mailto:igor.nefedov@aalto.fi)*

We show that particular spatial distribution of material structural elements enables extraordinary nonlinear-optical propagation processes commonly attributed to plasmonic negative-index metamaterials.

Current mainstream in fabricating bulk negative-index metamaterial (NIM) slabs relies on engineering of LC nanocircuits - plasmonic mesoatoms with negative electromagnetic response. Extraordinary coherent nonlinear optical (NLO) frequency-converting propagation processes predicted in NIMs have been realized (simulated) so far only in the microwave. This paper proposes a different paradigm which employs spatial dispersion to realize outlined processes commonly attributed to NIMs. Such opportunities are proven with numerical simulations making use of realistic models. The possibility of huge enhancement of optical parametric amplification and frequency-shifted nonlinear reflectivity has been predicted through three-wave mixing in metamaterials if one of the coupled electromagnetic waves falls in the NI frequency domain [1]. Here, we investigate manipulating properties of short contra-propagating optical pulses. Greatly enhanced NLO coupling becomes possible because phase and group velocities for one of the pulses appear contra-directed. Two options to ensure such extraordinary property commonly attributed to NIMs are investigated: waveguides with specially engineered spatial distribution of the nanoscopic building blocks, such as standing carbon nanotubes [2] or graphene nanosheets, and crystals that support optical phonons with negative group velocity [3]. Plasmonic NIMs are challenging to engineer. We show that extraordinary NLO frequency-conversion propagation processes attributed to NIMs can be mimicked in the proposed fully dielectric materials. We also show that the detrimental effects of strong losses caused by fast optical phonon damping can be eliminated in the short-pulse regime. Unparalleled properties of the proposed short-pulse process are numerically simulated and the possibility of huge enhancement of quantum conversion efficiency as well as of tailoring the duration and shapes of the generated and the transmitted fundamental pulses are predicted. Among the applications are photonic devices with advanced functional properties such as unidirectional optical amplifiers, filters, switches and cavity-free optical parametric oscillators.

**Acknowledgement.** This work was supported in parts by the NSF (Grant ECCS-1346547), by the AFOSR (Grant FA950-12-1-298), by the Presidium of the Russian Academy of Sciences (Project No 24.31), by the Russian Federal Program on Science, Education and Innovation (Grant 14.A18.21.1942), by the Siberian Branch of the Russian Academy of Sciences (Project No 23), and by the Siberian Federal University (Grant F-12).

### References

- [1] A. K. Popov and V. M. Shalaev, *Negative-index metamaterials: second harmonic generation, ManleyRowe relations and parametric amplification*, *Appl. Phys. B Lasers Opt.* **84**, 131137 (2006).
- [2] I. Nefedov and S. Tretyakov, *Ultrabroadband electromagnetically indefinite medium formed by aligned carbon nanotubes*, *Pys. Rev. B* **84**, 113410-4 (2011).
- [3] A. K. Popov, M. I. Shalaev, S. A. Myslivets, and V. V. Slabko, *Unidirectional amplification and shaping of optical pulses by threewave mixing with negative phonons*, *Appl. Phys. A* (Published on-line: November 2013). DOI 10.1007/s00339-013-8078-4

## Nonlinear switching in optically induced waveguide arrays

F. Diebel<sup>1</sup>, D. Leykam<sup>2</sup>, M. Boguslawski<sup>1</sup>, P. Rose<sup>1</sup>, C. Denz<sup>1</sup>, A. S. Desyatnikov<sup>2,\*</sup>,

<sup>1</sup> *Institut für Angewandte Physik and Center for Nonlinear Science (CeNoS),  
Westfälische Wilhelms-Universität Münster, 48149 Münster, Germany*

<sup>2</sup> *Nonlinear Physics Centre, Research School of Physics and Engineering,  
The Australian National University, Canberra ACT 0200, Australia*

\*[Anton.Desyatnikov@anu.edu.au](mailto:Anton.Desyatnikov@anu.edu.au)

We present experiments on light propagation in optically induced coupled waveguides in photorefractive media. We generate various waveguide configurations via multiplexing of Bessel beams, and explore nonlinear dynamics in double- and quadruple-well potentials, demonstrating a power-controlled optical vortex switch.

Optical induction is a versatile setting for studying the interplay between nonlinearity and discreteness in coupled waveguide arrays. Many previous experiments have explored propagation through waveguide arrays which form extended lattices, demonstrating various fundamental effects such as discrete soliton formation [1] and Anderson localization [2]. However, studies of *finite* arrays of waveguides have so far been limited, because the optical induction technique requires a nondiffracting induction beam, and in a homogeneous medium spatially localized beams typically diffract.

In this contribution, we experimentally demonstrate the optical induction of reconfigurable clusters of a few coupled nonlinear waveguides. We create the waveguides using an incoherent superposition (multiplexing) of Bessel beams [3, 4], which are crucially both spatially localized and nondiffracting. Then, we explore the linear and nonlinear dynamics of different probe beams in our induced structures.

Starting with a two-waveguide coupler, we demonstrate control over parameters such as the coupling strength, and nonlinear symmetry-breaking bifurcations. Generalizing to dynamics in a two-dimensional ring-like cluster of four waveguides, we consider the dynamics of discrete vortices. The photorefractive anisotropy leads to a periodic reversal of the vortex charge (handedness) during propagation. In the nonlinear regime, the probe beam intensity can control the period, and thereby the vortex charge at the output, realizing a power-controlled vortex switch [5].

A simple coupled mode model and numerical simulations of nonlinear wave propagation in the anisotropic photorefractive model [6] corroborate our experimental observations. Our approach may be readily generalized to other families of self-similar beams, for example self-accelerating Bessel-like beams, providing a flexible setting for exploring nonlinear dynamics in finite systems.

### References

- [1] N. K. Efremidis, S. Sears, D. N. Christodoulides, J. W. Fleischer, and M. Segev, “Discrete solitons in photorefractive optically induced photonic lattices,” *Phys. Rev. E* **66**, 1 (2002).
- [2] M. Segev, Y. Silberberg, and D. N. Christodoulides, “Anderson localization of light,” *Nat. Photonics* **7**, 197, (2013).
- [3] M. Boguslawski, A. Kelberer, P. Rose, and C. Denz, “Multiplexing complex two-dimensional photonic superlattices,” *Opt. Express* **20**, 27331 (2012).
- [4] F. Diebel, P. Rose, M. Boguslawski, and C. Denz, “Optical induction scheme for assembling nondiffracting aperiodic Vogel spirals,” *App. Phys. Lett.*, in press.
- [5] A. S. Desyatnikov, M. Dennis, and A. Ferrando, “All-optical discrete vortex switch,” *Phys. Rev. A* **83**, 063822 (2011).
- [6] A. Zozulya and D. Z. Anderson, “Propagation of an optical beam in a photorefractive medium in the presence of a photogalvanic nonlinearity or an externally applied electric field,” *Phys. Rev. A* **51**, 1520 (1995).

## Geometric resonances in waveguides and sub wavelength nanowire gratings: Scattering "anomalies" and Optical forces.

J.J. Sáenz<sup>1,2</sup>

<sup>1</sup>*Condensed Matter Physics Center (IFIMAC), Universidad Autónoma de Madrid, Spain*

<sup>2</sup>*Donostia International Physics Center (DIPC), Donostia-San-Sebastián, Spain*

\* [juanjo.saenz@uam.es](mailto:juanjo.saenz@uam.es)

Scattering from a single nanoparticle or defect inside a waveguide present a resonant response at specific geometric conditions similar to those of nanowire gratings. We discuss how these geometric resonances lead to diffraction anomalies, local field enhancements, resonant absorption or resonant radiation pressure effects.

Multiple scattering theory can be used to obtain a full analytical description of complex resonant phenomena arising in sub wavelength nanowire gratings or in single mode waveguides with small defects. The strong coupling between the dipolar field scattered by small particles and the evanescent modes (in a waveguide) or evanescent diffracted beams (in a grating) can lead to a number of interesting resonant effects.

Here we analyze the optical response of sub-wavelength nanowire gratings made of arbitrary anisotropic materials [1]. For transparent dielectric nanorods it is possible to obtain very large local field enhancements at specific resonant conditions [2]. These structures would lead to enhancement of molecular fluorescence signals without quenching. In the presence of absorption, it is possible to derive the conditions to tune the absorption/thermal emission and extinction resonances [2]. For magneto-optical dielectrics we show that there is a complex interplay between the geometric resonances of the grating and the magneto-optical Kerr effects (MOKE) response [1]. As we will show, for a given polarization of the incident light, a resonant magneto-optical response can be obtained by tuning the incidence angle and grating parameters to operate near the resonance condition for the opposite polarization.

A completely equivalent analysis was applied to study electromagnetic forces on neutral particles in hollow waveguides [3]. At the geometric resonance, the effective scattering cross section of a very small particle can be made as large as the wavelength even far from any localized plasmon-polariton resonance. A small particle can then be strongly accelerated along the guide. The presence of the two particles splits the resonance leading to a nontrivial oscillating interaction. The existence of stable, optically bound dimers under two counter-propagating (non-correlated) light modes was also discussed. In analogy with these findings, we will discuss some interesting radiation pressure effects on subwavelength nanorod gratings.

### References

- [1] H. Marinchio, R. Carminati, A. García-Martín and J.J. Sáenz, *Magneto-optical Kerr effect in resonant subwavelength nanowire gratings*, New J. Phys. **16**, 015007 (2014).
- [2] M. Laroche *et al.*, *Tuning the optical response of nanocylinder arrays*, Phys. Rev. B **74**, 245422 (2006); *Optical Resonances in One-Dimensional Dielectric Nanorod arrays: Field-induced fluorescence enhancement*, Opt. Lett. **32**, 2762 (2007).
- [3] R. Gómez-Medina *et al.*, *Resonant radiation pressure on neutral particles in a waveguide*, Phys. Rev. Lett **86**, 4275 (2001); *Unusually strong optical interactions between particles in quasi-one-dimensional geometries*, Phys. Rev. Lett **93**, 243602 (2004).

## Scattering in optical waveguides: a comprehensive model for radiative losses and backreflections

D. Melati<sup>1</sup>, F. Morichetti<sup>1</sup>, A. Melloni<sup>1</sup>,

<sup>1</sup> *Dipartimento di Elettronica, Informazione e Bioingegneria, Politecnico di Milano, Milano, Italy*  
*daniele.melati@polimi.it*

A unified model to describe both radiative losses and distributed backscattering generated by sidewall roughness independently on waveguide geometry and technology is presented. The model is in very good agreement with experimental results obtained on different types of optical waveguides, demonstrating its validity for arbitrary waveguide geometries and technologies.

### Summary

The interaction of the modes propagating in an optical waveguide with sidewall roughness causes severe impairments for the functionality of photonic circuits, acting as a source of extrinsic losses which couple part of the power to radiative modes (radiative losses,  $\alpha_r$ ) and counter-propagating modes (backscattering,  $r_b$ ). In this work we propose a unified vision on these two loss mechanisms through the formulation of the  $n_w$  model [1], which applies to arbitrary waveguide geometry or technology. The  $n_w$  model results to be in a very good agreement with existing models that individually describe radiative loss or backscattering only [2, 3]. Both contributions depend directly to the derivative of the effective index with respect to the waveguide width  $w$  through the expressions  $\alpha_r = A(\partial n_{\text{eff}}/\partial w)$  and  $r_b = B(\partial n_{\text{eff}}/\partial w)^2$ . The parameters  $A$  and  $B$  are independent on  $w$  and take into account the roughness standard deviation and correlation length. The derivative  $\partial n_{\text{eff}}/\partial w$  gives information on the “sensitivity” of the mode to the width variations produced by the sidewall roughness and hence provides a direct description of the interaction between the sidewall roughness and the optical field [4]. Figure 1 shows the measurements of the propagation losses (a) and backscattering (b) for two different types of waveguides: a SOI channel waveguide (black circles) and a InP-based rib waveguide (red squares). Results are presented as function of the normalized waveguide width  $w/w_0$ , being  $w_0$  the width limit for single mode propagation. A fit performed with the  $n_w$  model (dashed lines) is in good agreement with the experimental results both for radiative losses and backscattering.

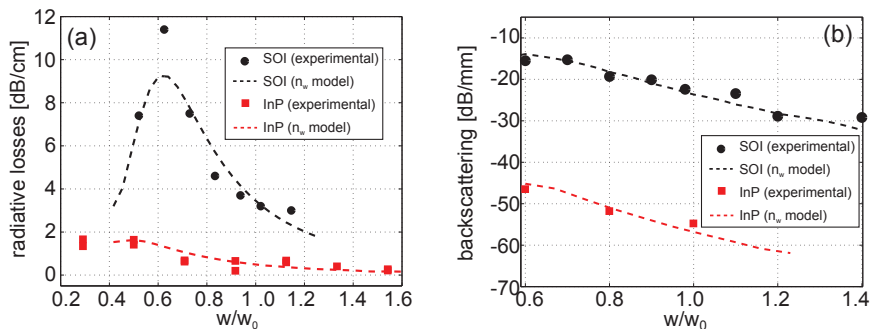


Fig. 1. Measurements (marks) of the propagation losses (a) and distributed backscatter (b) for a SOI channel waveguide and a rib InP-based waveguide. The experimental results are fitted with the  $n_w$  model (dashed lines).

The research leading to these results has received funding from the European Community’s Seventh Framework Program FP7/2007-2013 under grant agreement ICT 257210 PARADIGM.

### References

- [1] D. Melati, F. Morichetti and A. Melloni, *A unified approach for radiative losses and backscattering in optical waveguides*, to be published in Journal of Optics.
- [2] F.P. Payne and J.P.R. Lacey, *A theoretical analysis of scattering loss from planar optical waveguides*, Optical and Quantum Electronics, 26(10), 1994.
- [3] F. Ladouceur and L. Poladian, *Surface roughness and backscattering*, Opt. Lett., 21(22), Nov 1996.
- [4] D. Melati, F. Morichetti and A. Melloni, *Real photonic waveguides: guiding light through imperfections*, to be published in Advances in Optics and Photonics.

## Modelling of A Roughened Sidewall Ring Resonator Add Drop Filter

R. Mansoor\*, H. Sasse, A. Duffy

Faculty of Technology, De Montfort University, Leicester, UK.

\*P10005332 @myemail.dmu.ac.uk

A single ring resonator with a roughened sidewall is studied to characterize the effects of backscatter. An equivalent structure for it is proposed, then the through port response is derived analytically. It is then modelled using CST. The proposed analytical model is used to calculate the key parameters of the roughened ring, and extracts the backscattering parameters which are different for each resonance wavelength.

### Introduction

The optical waveguide micro-ring resonator is a promising technology for integrated photonic devices in Wavelength Division Multiplexing (WDM) networks. The roughness of the optical waveguide surface, typically experienced during manufacture, is responsible for scattering loss, and also generates a counter-propagating mode. The mutual coupling between the forward and counter-propagated modes inside the ring leads to a net power transfer, and results in a distortion to the ideal response of the filter in the form of resonance splitting.

### Results

In practice, the reflection is distributed along the ring, but can be considered as a lumped scattering point without loss of generality [1]. Fig. 1 shows the single ring model (A), with the equivalent structure (B). The through port ( $S_t$ ) response was calculated analytically using equation (1). A simulation using CST MWS [2] is performed to obtain the through port response of a roughened sidewall ring resonator. The results of the simulation and that of the analytical model (Fig. 2) are used to calculate the ring parameters by applying curve fitting using least squares error.

$$S_t = \frac{t - t_r \cdot t^3 \cdot e^{-j\theta} - t_r \cdot t \cdot e^{-j\theta} + t^3 \cdot e^{-2j\theta}}{1 - 2 \cdot t^2 \cdot t_r \cdot e^{-j\theta} + t^4 \cdot e^{-2j\theta}} \quad (1)$$

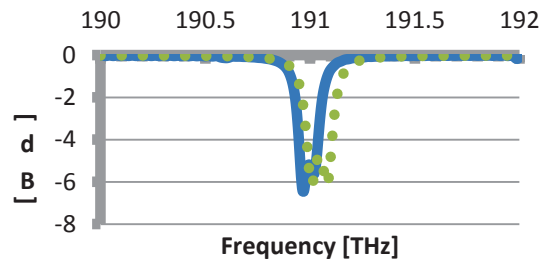
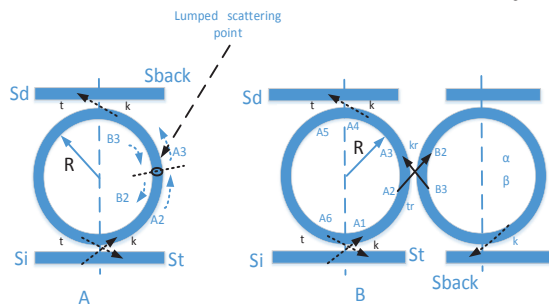


Fig. 1. The single ring resonator (A) and (B) is the equivalent structure

Fig. 2. CST (solid) and analytically (dotted) simulation through port response.

The obtained values were: coupling  $k^2=0.0943$ , reflection  $t_r=0.99327$ , and loss per round trip  $e^{-\alpha l}=0.9855$ . The roughness induced reflectivity strongly affects the resonance shape, and this model allows to extract all the ring resonator parameters in the presence of sidewall effect.

### References

- [1] B. E. Little, J. Laine and S. T. Chu, "Surface-roughness-induced contradirectional coupling in ring and disk resonators," *Opt. Lett.*, vol. 22, pp. 4-6, 1997.
- [2] (2013). *3D Electromagnetic Simulation software*. Available: [www.cst.com](http://www.cst.com).

## Modelling realistic plasmonic nanostructures: Field enhancement and beyond

Olivier J.F. Martin

*Nanophotonics and Metrology Laboratory, Swiss Federal Institute of Technology Lausanne (EPFL)*  
[www.nanophotonics.ch](http://www.nanophotonics.ch) [olivier.martin@epfl.ch](mailto:olivier.martin@epfl.ch)

The potential of modelling to guide and interpret optical experiments in plasmonics strongly depends on the ability of simulating realistic nanostructures.

Whilst numerical simulations are playing a central role in the design and analysis of plasmonic experiments, very often the underlying numerical models are limited to idealized representations of the system under study. For example, plasmonic dipole antennas are often modelled as perfect metallic nanostructures with parallelepipedic surfaces, although nanofabricated plasmonic nanostructures are usually very rough and defined by the metal grain boundaries.

In this presentation, I will describe our recent work on the modelling of realistic plasmonic nanostructures with emphasis on developing numerical tools to analyze practical experimental situations. Our approach is based on the surface integral equation (SIE) which solves Maxwell's equations in their integral form using simultaneously the electric and the magnetic fields [1]. Two appealing features of this approach are 1) the possibility of handling nanostructures with an arbitrary shape [2,3] and 2) the ease of including complex backgrounds such as surfaces or periodic structures [4]. I will present different practical examples and show how additional observables beyond the field distribution can be computed. These will include the calculation of optical forces and enhancement parameters for fluorescence and Raman spectroscopy.

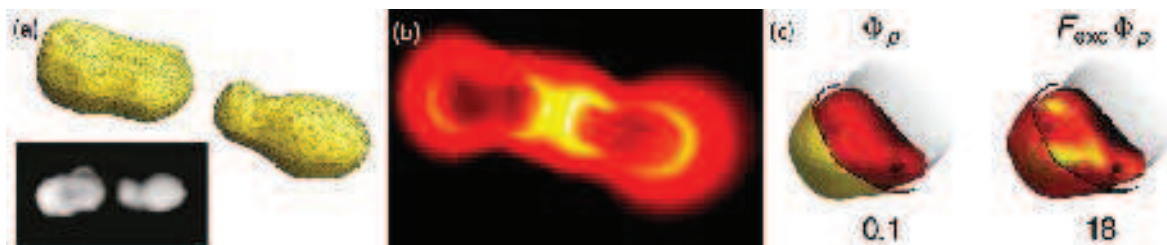


**Fig. 1.** (a) Model for a realistic plasmonic antenna obtained from the SEM image. (b) Near-field distribution at the vicinity of such the realistic antenna shown in panel (a). (c) Enhancement parameters for the fluorescence of molecules located 1nm from the surface of a realistic plasmonic nanostructure.

### References

- [1] A.M. Kern, and O.J.F. Martin, Surface integral formulation for 3-D simulations of plasmonic and high permittivity nanostructures, *J. Opt. Soc. Am. A* **26**, 732 (2009).
- [2] A.M. Kern, and O.J.F. Martin, Excitation and reemission of molecules near realistic plasmonic nanostructures, *Nano Lett.* **11**, 482 (2011).
- [3] A.M. Kern, A.J. Meixner, and O.J.F. Martin, Molecule-dependent plasmonic enhancement of fluorescence and Raman scattering near realistic nanostructures, *ACS Nano* **6**, 9829 (2012)
- [4] B. Gallinet, A.M. Kern, and O.J.F. Martin, Accurate and versatile modeling of electromagnetic scattering on periodic nanostructures with a surface integral approach, *J. Opt. Soc. Am. A* **27**, 2261 (2010).

## Leaky modes in a non dissipative plasmonic waveguide with a bounded cross section

A.-S. Bonnet-Ben Dhia<sup>1</sup>, C. Carvalho<sup>1</sup>, L. Chesnel<sup>2</sup>, P. Ciarlet Jr.<sup>1</sup>,

<sup>1</sup> *POEMS, UMR 7231 CNRS-INRIA-ENSTA, Palaiseau, France*

<sup>2</sup> *Department of Mathematics and Systems Analysis, Aalto University, Finland*  
*camille.carvalho@ensta-paristech.fr*

We study the modes of a plasmonic waveguide made of a dielectric and a metal inclusion with corners. Due to the sign-changing permittivity, it appears singular phenomena which create leakage at the corners. An original and stable numerical method involving PMLs at the corners is presented to compute and sort the modes.

### Summary

We consider a cylindrical waveguide of axis  $z$  made of a dielectric material with a cylindrical metal inclusion. The cross section of the waveguide is bounded. The metal permittivity can be modeled with the dissipationless Drude's model:

$$\epsilon(\omega) = \epsilon_\infty \left( 1 - \frac{\omega_p^2}{\omega^2} \right)$$

where  $\epsilon_\infty$  characterizes the limit behaviour at high frequency, and  $\omega_p$  is the plasma frequency. Then for frequencies  $\omega < \omega_p$ , the metal permittivity is a negative real number. We consider the time-harmonic Maxwell's equations. By looking for the modes of shape  $(\mathbf{E}, \mathbf{H})(x, y, z, t) = (E, H)(x, y)e^{i(\beta z - \omega t)}$ ,  $\beta \in \mathbb{R}$ , we study first the linearized eigenproblem (dependence in  $\omega$  of  $\epsilon$  frozen):  $A(\beta)(E, H) = \omega^2(E, H)$ . For a given  $\beta \in \mathbb{R}$ , under some conditions on  $\epsilon$  and the geometry [1], the operator  $A(\beta)$  is self-adjoint with a discrete spectrum, then the  $\omega_j^2(\beta) \in \mathbb{R}$ ,  $j \in \mathbb{N}$ , are associated to guided and evanescent modes. Besides for a metal inclusion with corners, these properties can be no longer true due to singular phenomena occurring at the corners [2, 3] called black-hole waves. In that case classical finite elements produce a real spectrum which contains both physical and spurious eigenvalues. By taking into account the black-hole waves, one can sort the eigenvalues: the real ones correspond to the guided and evanescent modes, the complex ones are associated to leaky modes. It may sound odd for a waveguide of bounded cross section to obtain leaky modes, however this is due to the black-hole waves introducing leakage at the corners. To be able to compute the modes with finite elements, we perform an original use of PMLs by putting them at the corners. Numerical results confirm that this method is efficient and stable as we refine the mesh. Once the linearized eigenproblem is fully understood, we can solve in principle the non linear eigenvalue problem.

### Acknowledgement

We thank the DGA for financial support.

### References

- [1] A.-S. Bonnet-Ben Dhia, L. Chesnel, P. Ciarlet Jr., *T-coercivity for scalar interface problems between dielectrics and metamaterials*, Math. Mod. Num. Anal., 46(2012), pp. 1363–1387.
- [2] A.-S. Bonnet-Ben Dhia, M. Dauge, K. Ramdani, *Analyse spectrale et singularités d'un problème de transmission non coercif*, C. R. Acad. Sci. Paris, Ser. I, 328 (1999), pp. 717–720.
- [3] A.-S. Bonnet-Ben Dhia, L. Chesnel, X. Claeys, *Radiation condition for a non-smooth interface between a dielectric and a metamaterial*, Math. Mod. Meth. App. Sci., 2013.

## Advanced modal method for computing modes of waveguides with trapezoidal cross section

G. Granet<sup>1,2\*</sup>

<sup>1</sup>Clermont Universités, Université Blaise Pascal

Institut Pascal, BP10448, F-63000 Clermont- Ferrand, France

<sup>2</sup>CNRS UMR 6602, F-63177 Aubière, France

\*<mailto:granet@univ-bpclermont.fr>

We use recent advances in modal methods to investigate dispersion relations and field distributions in waveguides with trapezoidal cross section and arbitrary materials.

### Summary

In recent years, many novel optical wave-guides have been designed and fabricated. Some of these wave-guides have high-index contrast and possibly sharp corners. Numerical modelling of these wave-guides require advanced numerical methods with high efficiency and accuracy especially when the wave-guides include materials with negative permittivity. The problem comes from the difficulty to enforce accurately boundary conditions with complicated geometries which in turn determines the overall effectiveness of the solver. In linear numerical methods, the wave-guide cross section is discretized and a linear matrix eigenvalue problem is derived by using the method of Moments. The effectiveness of any numerical modal method is linked with the mesh that is used to describe the geometry and by the expansion and test basis chosen in the computation. Matched coordinates allow to make the boundary of the wave-guide coincide with surfaces of coordinates which facilitates the writing of boundary conditions. Adaptive spatial resolution have also shown to be a powerful tool to improve the effectiveness of various numerical modal methods. In addition to the above geometrical aspects, using sub-domain basis like polynomials or splines allow to enforce boundary conditions rigorously.

We have developed a mode solver which incorporates together for the first time matched coordinates, adaptive spatial resolution and sub-domain basis. The determination of dispersion relations of various wave-guide with trapezoidal cross section demonstrates its effectiveness.



Fig. 1. Two waveguides with trapezoidal cross section.

### References

- [1] T.Weiss, G. Granet , N. A. Gippius, S. G. Tikhodeev , H. Giessen , *Matched coordinates and adaptive spatial resolution in the Fourier modal method*, Opt. Ex. 17, 8051-8061 (2009).
- [2] G.Granet, *Efficient implementation of the B-spline modal method for lamellar gratings*, J.Opt. A. 31, 332-337 (2014)

## Numerical modeling of time-domain nanophotonic applications using a discontinuous finite element type method

C. Scheid<sup>1,2</sup>, S. Lanteri<sup>2</sup>, R. Léger<sup>2</sup>, J. Viquerat<sup>2</sup>,

<sup>1</sup> *J.A. Dieudonné Laboratory, UMR 7351, University of Nice-Sophia Antipolis, France*

<sup>2</sup> *Nachos project-team, Inria Sophia Antipolis-Méditerranée, France*

*Stephane.Lanteri@inria.fr*

During the last ten years, the discontinuous Galerkin time-domain (DGTD) method has progressively emerged as a viable alternative to well established finite-difference time-domain (FDTD) and finite-element time-domain (FETD) methods for the numerical simulation of electromagnetic wave propagation problems in the time-domain. We discuss here about the development and application of such a DTGD method for solving the system of time-domain Maxwell equations coupled to material models relevant to nanophotonics.

### Summary

The DGTD method can be considered as a finite element method where the continuity constraint at an element interface is released. While it keeps almost all the advantages of the finite element method (large spectrum of applications, complex geometries, etc.), the DGTD method has other nice properties which explain its increasing adoption in computational electromagnetics: (1) it is naturally adapted to a compact support high order interpolation of the unknown field; (2) when the discretization in space is coupled to an explicit time integration method, the DG method leads to a block diagonal mass matrix independently of the form of the local approximation (e.g the type of polynomial interpolation) which is a striking difference with classical FETD formulations; (3) it easily handles complex meshes including multi-element as well as non-conforming meshes with hanging nodes; (4) it is flexible with regards to the choice of the time stepping scheme. One may combine the DG spatial discretization with any global or local explicit time integration scheme, or even implicit, provided the resulting scheme is stable; (5) it is naturally adapted to parallel computing more precisely, the compact nature of method is in favor of high computation to communication ratio especially when the interpolation order is increased. Numerical modeling of electromagnetic wave propagation in interaction with metallic nanostructures at optical frequencies requires to solve the system of Maxwell equations coupled to appropriate models of physical dispersion in the metal. The most used are the Drude and Drude-Lorentz models. We will discuss here about the adaptation of a DGTD initially introduced in [1] in order to deal with various dispersion models. An ADE formulation has been adopted. The resulting ADE-based DGTD method is detailed in [2] where we also study the stability and a priori convergence of the method. We first considered the case of Drude and Drude-Lorentz models and, further extend the proposed ADE-based DGTD method to be able to deal with a generalized dispersion model in which we make use of a Padé approximant to fit an experimental permittivity function. The numerical treatment of such a generalized dispersion model is also presented in [2]. In this talk, we will discuss about our efforts regarding this DGTD method in order to improve its accuracy, flexibility and efficiency in view of the numerical treatment of large-scale nanophotonics applications. Numerical results will be presented for several of 3D problems ranging from academic test problems to more realistic configurations.

### References

- [1] L. Fezoui, S. Lanteri, S. Lohrengel, and S. Piperno. Convergence and stability of a discontinuous Galerkin time-domain method for the 3D heterogeneous Maxwell equations on unstructured meshes. *ESAIM: Math. Model. Numer. Anal.*, 39(6):1149–1176, 2005.
- [2] J. Viquerat, S. Lanteri, and C. Scheid. Theoretical and numerical analysis of local dispersion models coupled to a discontinuous galerkin time-domain method for Maxwell's equations. RR-8298, 2013.

## A Dirichlet-to-Neumann approach for the exact computation of guided modes in photonic crystal waveguides

S. Fliss<sup>1</sup>

<sup>1</sup> *POems (UMR 7206 CNRS/ENSTA/INRIA)*  
*sonia.fliss@ensta-paristech.fr*

This work deals with the computation of guided modes in 2D planar Photonic Crystal (PhC) waveguides. It is a key issue in the process of designing devices in photonic communications. We propose an exact numerical method for the computation of the guided modes which is, conversely to existing methods, independent from their confinement.

### Summary

This work deals with 2D planar PhC waveguides which are obtained by introducing a line defect in a 2D planar PhCs. In optics, such defects are created to construct an (open) waveguide that concentrates light. The existence and computation of the eigenmodes is a crucial issue. This is related to a self-adjoint eigenvalue problem associated to a PDE in an unbounded domain (in the directions orthogonal to the line defect), which makes both the analysis and the computations more complex.

For the computation of the guided modes, the *Supercell method* is a well-known method. It consists in truncating the unbounded domain and making computations in the truncated domain. In practice, this approach replaces the eigenvalue problem set in an unbounded domain to an approximated one set in a bounded domain. The super-cell method has proven to be an efficient yet reliable method if the modes are well-confined, i.e. decay exponentially inside the PhCs with large decay rate. However, if the guided mode is not well-confined, the size of the truncated domain has to be sufficiently large, otherwise the computation can be wrong, and then the computational cost of the super-cell method increases significantly. Moreover, spurious eigenvalues and eigenvectors may be introduced by this numerical method.

By adapting to eigenvalue problems the construction of DtN operators originally developed for scattering problems [1], we want to offer a rigorously justified alternative to existing methods. Compared to the supercell method, the DtN method allows us to reduce the numerical computation to a small neighborhood of the defect independently from the confinement of the computed guided modes. Moreover, as the method is exact, we improve the accuracy for not-well confined guided modes. Obviously, there is a price to be paid: the reduction of the problem leads to a nonlinear eigenvalue problem of a fixed point nature [2]. However, this difficulty already has been overcome for homogeneous open waveguides for which the DtN approach is well known [3].

### References

- [1] P. Joly, J.-R. Li, S. Fliss, *Exact boundary conditions for periodic waveguides containing a local perturbation* Commun. Comput. Phys. 1 (6), 945973, 2006.
- [2] S. Fliss, *A Dirichlet-to-Neumann approach for the exact computation of guided modes in photonic crystal waveguides*, SIAM J. Sci. Comp., 35(2), B438-B461, 2013.
- [3] P. Joly and C. Poirier, *A numerical method for the computation of electromagnetic modes in optical fibres*, Math. Methods Appl. Sci., 22, 389447, 1999.

## A Multigrid Solver with Adaptive Time-Stepping for the WDM SOA response

J. Bos<sup>1</sup>, C. Vagionas<sup>2</sup>

<sup>1</sup>Phoenix Software, Enschede, The Netherlands

<sup>2</sup>Department of Informatics, Aristotle University of Thessaloniki, Thessaloniki, Greece

\*[Jan.Bos@phoenixbv.com](mailto:Jan.Bos@phoenixbv.com)

A time-domain solver for the WDM response of Semiconductor Optical Amplifiers (SOA) relying on multigrid numerical techniques, implicit time discretization schemes and a wideband steady state material gain coefficient is presented with key feature of adaptive time stepping mechanism towards efficiency.

### Introduction

Improvements in SOA modelling have traditionally relied on spatio-temporal division of the carrier-induced gain dynamics on equidistant grids and wideband gain coefficients [1]. The one-by-one explicit schemes have led to impressive quantitative experimental matching with commercial SOAs[2]. Multigrid are adopted [3] for adaptive time-steps and enhanced computational efficiency.

### Summary

Multigrid methods adopt a series of coarser grids for the free carrier densities, restricting the finest grid of traditional longitudinal SOA division to two only sectors, as shown in Fig.1(i), while maintaining grid independent convergence rates. This implies solving at once the associated system of coupled differential equations for the carrier distribution[1]. With the second order accurate implicit midpoint rule and simple step doubling scheme, adaptive time-stepping with dense time sampling at the rise/fall times only is exploited. As shown in Fig.1(ii) for wavelength conversion at 10 Gb/s bits are resolved in  $\leq O(10)$  steps/samples regardless of the bitrate and pulse shape. Adaptive time sampling is important for statistical BER analysis with long bit patterns.

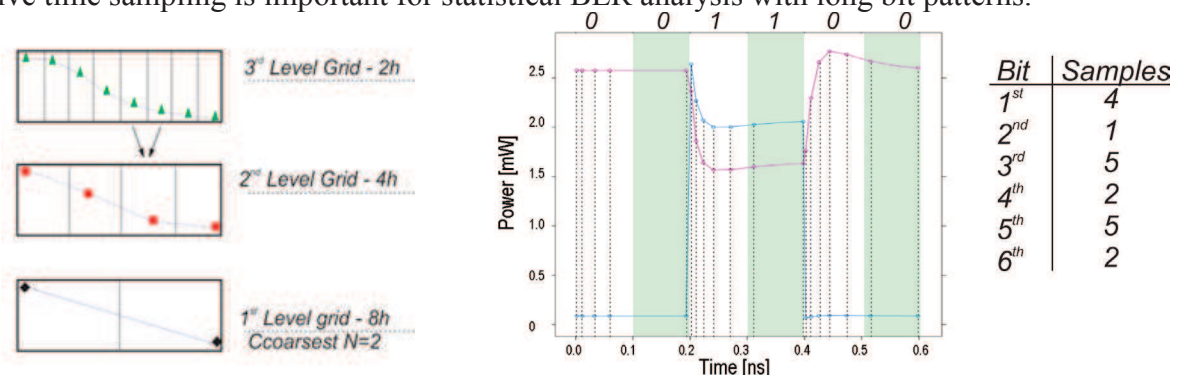


Fig. 1. Coarse grids and adaptive time sampling for the XGM SOA operation with dense samples at odd bits.

### Conclusion

Adaptive time-stepping is presented for the WDM SOA response relying on multigrid techniques.

### References

- [1] M. J. Connelly, "Wideband semiconductor optical amplifier steady-state numerical model," IEEE J. Quantum Electron., vol. 37, no. 3, pp. 439–447, Mar. 2001.
- [2] C. Vagionas, et. al., "Optical RAM and Flip-Flops Using Bit-Input Wavelength Diversity and SOA-XGM Switches," J. Lightw. Technol., vol. 30, no. 18, pp.3003–3009, Sep. 2012
- [3] J. Bos, R. Stoffer, "A Multigrid Solver for the Steady-state Solution of Rate Equations based Semiconductor Optical Amplifier Models," OWTNM, 2010

## An eigenmode expansion technique for modeling Kerr-nonlinear waveguide structures

J. Petráček

*Institute of Physical Engineering, Brno University of Technology, Technická 2, 616 69 Brno, Czech Republic*  
[petracek@fme.vutbr.cz](mailto:petracek@fme.vutbr.cz)

We present a new implementation of the eigenmode expansion technique for modeling Kerr-nonlinear waveguide structures. The formulation uses numerically stable scattering matrices and a perturbation approach based on the rigorous coupled-mode theory.

### Summary

It is well known that *linear* waveguide structures can be effectively simulated by using the eigenmode expansion techniques (EME) [1]. The approach is particularly advantageous for the structures composed of longitudinally uniform waveguides (“sections”). An extension of EME for *Kerr-nonlinear* structures has been already demonstrated [2]. The nonlinear technique uses spatial discretisation of nonlinear sections and an iterative procedure that requires a repeated calculation of eigenmodes. The aim of this work is to present an alternative approach [3], labeled as NL-EME, which solves the modal propagation in the nonlinear sections by using the rigorous coupled-mode theory. In this way, the recalculation of eigenmodes is avoided and thus one of the main advantages of EME maintained.

We consider a nonlinear waveguide structure described with the dielectric function  $\varepsilon = \varepsilon_0 + \gamma |\vec{E}|^2$ , where  $\varepsilon_0$  is the dielectric function of the linear structure and  $\vec{E}$  is the electric field. The structure is divided into the longitudinally uniform sections; i.e.  $\varepsilon_0$  and  $\gamma$  inside of any section are functions of transversal coordinates  $(x, y)$  only. The electromagnetic field in each section is expanded in terms of the linear eigenmodes, which are obtained as solutions of Maxwell’s equations for  $\varepsilon = \varepsilon_0(x, y)$ . For linear structures ( $\gamma = 0$ ), the technique follows the standard formulation which employs the scattering matrices [1]. Note that the scattering-matrix formalism is essential to prevent numerical instabilities that are related to propagation of evanescent modes.

For nonlinear structures ( $\gamma \neq 0$ ), we consider  $\gamma |\vec{E}|^2$  as a perturbation of the linear dielectric function  $\varepsilon_0$  and use the rigorous coupled-mode theory. The procedure leads to a nonlinear system of coupled differential equations accompanied with (implicit) boundary conditions. We formulate a straightforward iterative technique for solution of the system. In particular, at each iteration step, we obtain linear problem, which can be efficiently solved by using scattering matrices; in this way, the nonlinear algorithm naturally extends the linear technique.

The paper will introduce the model and theoretical formulation of NL-EME. Then we will present numerical results for typical structures (e.g. nonlinear waveguide cavity with linear DBR grating) that can be simulated. Finally, we will compare NL-EME with other established techniques.

**Acknowledgments** This work was supported by Ministry of Education, Youth, and Sports of the Czech Republic under contract LD14008.

### References

- [1] P. Bienstman and R. Baets, *Opt. Quantum Electron.*, **33**, 327-341, (2001).
- [2] B. Maes, P. Bienstman, and R. Baets, *Opt. Quantum Electron.*, **36**, 15-24, (2004).
- [3] J. Petráček, *Microw. Opt. Technol. Letters*, **55**, 2628-2631 (2013).

## Modeling of nonlinear nanoplasmonic and nanophotonic directional couplers

P. Koška<sup>1</sup>, P. Kwiecien<sup>2</sup>, I. Richter<sup>2,\*</sup>, J. Čtyroký<sup>1</sup>

<sup>1</sup>*Institute of Photonics and Electronics AS CR, v.v.i., Prague, Czech Republic*

<sup>2</sup>*Czech Technical University in Prague, Faculty of Nuclear Sciences and Physical Engineering, Department of Physical Electronics, Prague, Czech Republic*

\*[richter@fjfi.cvut.cz](mailto:richter@fjfi.cvut.cz)

Results of numerical modeling of nanophotonic and nanoplasmonic directional couplers based on slot waveguide geometry operating both in linear and nonlinear regimes obtained with several in-house and commercial software tools are presented, mutually compared and assessed.

### Introduction

Efficient nonlinear optical devices are very desirable photonic components. For their low-power operation, application of waveguides exhibiting extremely high transversal confinement is perhaps the most promising. In this paper we numerically analyze behavior of several types of nanophotonic and nanoplasmonic directional couplers based on slot waveguide geometries [1-3], both in linear and nonlinear (with Kerr-type nonlinearity) regimes.

### Waveguide geometry and numerical modeling

The transversal cross-sections of several designs of both nanophotonic and nanoplasmonic (Figs. 1c),d)) directional couplers are schematically shown in Fig. 1. In Figs. 1a),b), two alternatives of a nanophotonic coupler is designed as a pair of coupled SOI slot waveguides while the structures in Figs. 1c),d) represent two versions of hybrid dielectric-plasmonic slot waveguide (HDPSW) couplers, composed of two coupled HDPSWs. In all cases, the slot is supposed to be filled with a polymer with a very strong Kerr-type nonlinearity. Si guides with slots are then embedded either in SiO<sub>2</sub>, or – perhaps more practically – in the same polymer (Figs. 1a),c)), or in SiO<sub>2</sub> (Figs. 1b),d)). Apart from a nonlinear polymer, the nonlinearity of silicon is considered, too; while the nonlinearity of metal (gold) in the HDPSW coupler is neglected. To model linear propagation, three in-house software tools were used, namely the FEM-BPM, and two Fourier modal methods – BEX and aRCWA [4-6], developed recently. Nonlinear propagation was modeled with an in-house NL-FEM-BPM and a commercial FDTD tools, with Kerr-nonlinearity implemented.

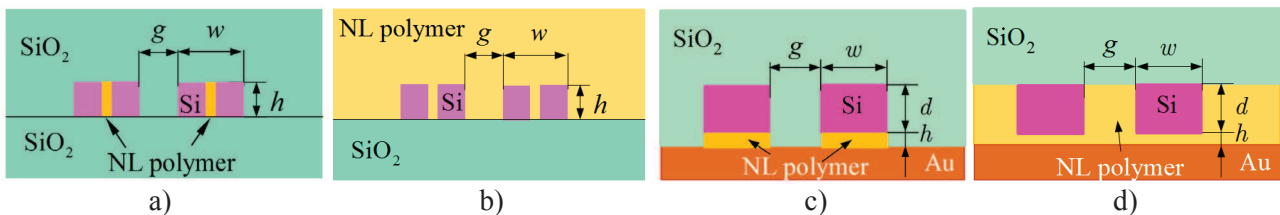


**Fig. 1.** Examples of designs of a), b) paired coupled SOI slot waveguide couplers, and c), d) plasmonic directional couplers based on HDPSW, with nonlinear polymer.

Efficiency and accuracy of modeling methods will be discussed, in both linear and nonlinear regimes, and calculated switching properties of waveguide-coupler designs will be mutually compared and assessed.

### References

- [1] T. Vallaitis, S. Bogatscher, L. Alloatti, *et al.*, *Opt. Express* **17**, 17357-17368, (2009).
- [2] M. Fujii, J. Leuthold, and W. Freude, *IEEE Photonics Technology Letters* **21**, 362-364, (2009).
- [3] J. Čtyroký, P. Kwiecien, and I. Richter, *JEOS - RP* **8**, 13024-1 - 13024-6, (2013).
- [4] P. Kwiecien, I. Richter, and J. Čtyroký, *AIP Conf. Proc.* **1475** (TaCoNa), 71-73, (2012).
- [5] B. Maes, J. Petráček, S. Burger, P. Kwiecien, *et al.*, *Optics Express* **21**, 6794-6806, (2013).
- [6] J. Čtyroký, *J. Lightwave Technology* **30**, 3699-3708, (2012).

## Subwavelength gratings for the filtering of light (spectral, spatial and polarization)

Riad Haidar<sup>1,3,\*</sup>

Patrick Bouchon<sup>1</sup>, Paul Chevalier<sup>1,2</sup>, Julien Jaeck<sup>1</sup>, Quentin Lévesque<sup>1,2</sup>, Fabrice Pardo<sup>2</sup>,  
Jean-Luc Pelouard<sup>2</sup>, Clément Tardieu<sup>1,2</sup>, Grégory Vincent<sup>1</sup>

<sup>1</sup>*ONERA, the French aerospace lab, Chemin de la Hunière, Palaiseau, France*

<sup>2</sup>*Laboratoire de photoniques et de nanostructures, CNRS, Route de Nozay, Marcoussis, France*

<sup>3</sup>*Ecole Polytechnique, Palaiseau, France*

\*[haidar@onera.fr](mailto:haidar@onera.fr)

The current trend towards compact, cost-effective and multi-purpose infrared opto-electronic systems brings the need for new conception tools and technological means. In this frame, subwavelength and plasmonic concepts open promising avenues: at a first level, for the conception of high-efficiency and compact optical elements arrays (i.e., polarizer, filter, or lens arrays) that can be brought in the vicinity of focal plane arrays, inside the confined volume of the camera; at a second level, for the integration of optical functions within the pixel of detection; and at a third level, for the enhancement of the opto-electronic properties of the elementary infrared detector. I will draw an overview of recent advances and realizations done in our lab.

### References

- [1] Compact planar lenses based on a pinhole and an array of single mode metallic slits Q. Lévesque, P. Bouchon, F. Pardo, J.-L. Pelouard, R. Haïdar, J. Eur. Opt. Soc, Rapid Publ. 8, 13071 (2013)
- [2] Metal-dielectric bi-atom structure for angular-tolerant spectral filtering E. Sakat, S. Héron, P. Bouchon, G. Vincent, F. Pardo, S. Collin, J.-L. Pelouard, R. Haïdar, Opt. Lett. 38, 425 (2013)
- [3] Optical Extinction in a Single Layer of Nanorods P. Ghenuche, G. Vincent, M. Laroche, N. Bardou, R. Haïdar, J.-L. Pelouard, S. Collin, Phys. Rev. Lett. , 143903 (2012)
- [4] Free-standing guided-mode resonance band-pass filters: from 1D to 2D structures E. Sakat, G. Vincent, P. Ghenuche, N. Bardou, C. Dupuis, S. Collin, F. Pardo, R. Haïdar, J.-L. Pelouard, Optics Express 20, 13082 (2012)
- [5] Perfect extinction in subwavelength dual metallic transmitting gratings T. Estruch, J. Jaeck, F. Pardo, S. Derelle, J. Primot, J.-L. Pelouard, R. Haïdar, Opt. Lett. 36, 3160 (2011)
- [6] Free-standing subwavelength metallic gratings for snapshot multispectral imaging R. Haïdar, G. Vincent, S. Collin, N. Bardou, N. Guerineau, J. Deschamps, J.-L. Pelouard, Appl. Phys. Lett. 96, 221104 (2010).

## Coupled-wave analysis of the unexpectedly low-loss plasmon-triggered switching between orders diffracted by a metal grating

E. Mounkala, A.V. Tishchenko, O. Parriaux

Laboratoire Hubert Curien UMR CNRS 5516, 18 Rue Prof. B. Lauras, Lyon University, F-42000 St-Etienne  
parriaux@univ-st-etienne.fr

### Abstract

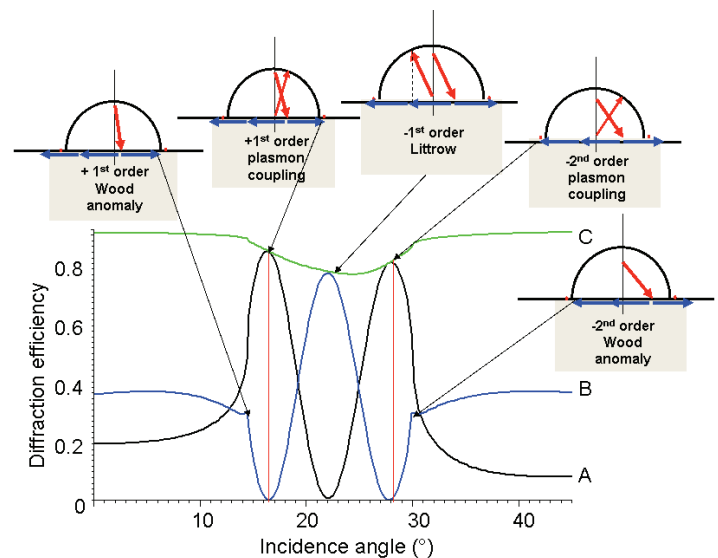
A coupled-wave formalism is developed to give a phenomenological understanding of how a +1<sup>st</sup> and -2<sup>nd</sup> order grating-coupled plasmon mode triggers the switching between the 0<sup>th</sup> and -1<sup>st</sup> diffracted orders reflected by an undulated metal surface with intriguingly low absorption loss.

### The structure and incidence conditions

The structure is a simple, rather deep sinusoidal undulation (depth/period ratio about 0.3) of a metal surface. The incidence angle  $\theta$  is in the neighborhood of the -1<sup>st</sup> order Littrow condition. The wavelength/period ratio is such that the reflected 0<sup>th</sup> and -1<sup>st</sup> diffraction orders are propagating.

### The plasmon-triggered switching effect in the angular domain

Applying the exact Chandezon method to the TM-excited structure results in the 0<sup>th</sup> and -1<sup>st</sup> order angular spectra of the figure opposite obtained with a silver grating: as expected, the -1<sup>st</sup> order (curve B) is maximum at Littrow incidence. Increasing  $\theta$  provokes a fall of the -1<sup>st</sup> order, (and an increase of the Fresnel reflection, curve A) which reaches zero (resp. a maximum) at the angle ensuring +1<sup>st</sup> order plasmon coupling. Decreasing  $\theta$  does the same at the angle of -2<sup>nd</sup> order plasmon coupling. This new effect was demonstrated experimentally and shows also in the wavelength domain at fixed angle  $\theta$  [1]. Surprisingly, plotting the energy balance versus  $\theta$  reveals that the absorption losses are small when the plasmon is excited and maximum off-resonance (curve C).



### Towards a phenomenological representation

To elucidate the coupling mechanism, and to broaden the domain where it can operate and possibly be applicable, the authors are developing a coupled-mode formalism in which the waves considered are the incident beam, the reflected 0<sup>th</sup> and -1<sup>st</sup> propagating orders, the forward- and backward-propagating plasmon modes. The formalism has now been established in the most concise form. There remains to calculate the coupling coefficients on the basis of concrete examples modeled exactly by the Chandezon method, then to check that these are relevant phenomenological parameters in that they remain essentially constant over a reasonably wide range of optogeometrical parameters.

The intended contribution will describe the developed coupled-wave formalism and explain the physics behind this low-loss plasmon-triggered free-space wave switching effect.

### References

- [1] J. Sauvage-Vincent et al., Optics Express, to be published.

## Optical quasimodes and their application to infrared spectral filtering

B. Vial<sup>1,2</sup>, G. Demésy<sup>1</sup>, A. Nicolet<sup>1</sup>, F. Zolla<sup>1</sup>, M. Commandré<sup>1</sup>, T Begou<sup>1</sup>, C. Hecquet<sup>1</sup>,  
S. Tisserand<sup>2</sup>, F. Bedu<sup>3</sup>, H. Dallaporta<sup>3</sup>

<sup>1</sup> *Université d'Aix-Marseille, CNRS, Centrale Marseille, Institut Fresnel, Marseille, France*

<sup>2</sup> *Silios Technologies, ZI Peynier-Rousset, rue Gaston Imbert Prolongée, 13790 Peynier, France*

<sup>3</sup> *Université d'Aix-Marseille, CNRS, CiNaM, UMR 7325, Campus de Luminy, Case 913, 13288 Marseille  
Cedex 9, France*

*benjamin.vial@fresnel.fr*

We present a Finite Element modal approach to study resonant interaction of light with metamaterials. This technique is applied to the design of infrared spectral filters for multispectral imaging applications. Fabrication and measurements in good agreement with numerical calculations are also reported.

Various filtering functions can be performed by bi-periodic diffractive structures patterned at a sub-wavelength scale, which shows a resonant behaviour. We have developed a modal approach based on the finite element method (FEM) adapted to diffractive structures of arbitrary geometry. If the modal analysis in bounded domains is well known, it shows to be much more difficult in the unbounded case, revealing quasimodes associated with complex eigenvalues. Through a geometrical transformation of coordinates, our method allows to treat a bounded problem where the free space is truncated by Perfectly Matched Layers (PML). This technique that allows us to find numerically an arbitrary number of eigenvalues in the complex plane. In addition, we show that it is possible to expand the solution of the problem with sources on the reduced eigenvectors basis [1]. Thus we can obtain the coupling coefficients of a plane wave of frequency, incidence and arbitrary polarization with a particular mode, giving us valuable information on the conditions of excitation of resonances of the system. We then apply these techniques to the design of several bi-periodic structures realizing different filtering functions in the infrared and study their spectral properties. Two types of filters, band cut in reflexion (with metal insulator metal metamaterial [2]) and bandpass in transmission (with annular aperture arrays [3]), have been fabricated and experimentally characterized.

### References

- [1] Benjamin Vial, Frédéric Zolla, André Nicolet, and Mireille Commandré. Quasimodal expansion of electromagnetic fields in open two-dimensional structures. *Phys. Rev. A*, 89:023829, Feb 2014.
- [2] Benjamin Vial, Guillaume Demésy, Frédéric Zolla, André Nicolet, Mireille Commandré, Christophe Hecquet, Thomas Begou, Stéphane Tisserand, Sophie Gautier, and Vincent Sauget. Resonant metamaterial absorbers for infrared spectral filtering: quasimodal analysis, design, fabrication and characterization. *Submitted to J. Opt. Soc. Am. B*, January 2014.
- [3] Benjamin Vial, Frédéric Bedu, Hervé Dallaporta, Mireille Commandré, Guillaume Demésy, André Nicolet, Frédéric Zolla, Stéphane Tisserand, and Laurent Roux. Transmission enhancement through square coaxial apertures arrays in metallic film: when leaky modes filter infrared light. *Submitted to Opt. Lett.*, March 2014.

## Tunability of plasmonic surface lattice resonances via experiments and numerical mode analysis

A. Abass<sup>1</sup>, S.R.K. Rodriguez<sup>2</sup>, J. Gomez Rivas<sup>2,3</sup>, B. Maes<sup>4,5,\*</sup>

<sup>1</sup>Solar Cells Group, ELIS, Ghent University, Ghent, Belgium

<sup>2</sup>Center for Nanophotonics, FOM Institute AMOLF, c/o Philips Research Laboratories, Eindhoven, The Netherlands

<sup>3</sup>COBRA Research Institute, Eindhoven University of Technology, Eindhoven, The Netherlands

<sup>4</sup>Micro- and Nanophotonic Materials Group, University of Mons, Mons, Belgium

<sup>5</sup>Photonics Research Group, INTEC, Ghent University-imec, Ghent, Belgium

\*[bjorn.maes@umons.ac.be](mailto:bjorn.maes@umons.ac.be)

Angle-dependent measurements on arrays of metallic nanorods are confronted with various numerical simulations. We analyze in-depth the properties of surface lattice resonances in these systems, which are coupled excitations of localized surface plasmon resonances and Rayleigh anomalies.

### Introduction

When in-plane diffraction is occurring via metallic particles, one has the possibility to excite interesting hybrid photonic-plasmonic modes. We examine the tunability, angular dispersion and field profile of these so-called surface lattice resonances via experiments and numerical simulations.

### Summary

Experimentally we vary the nanoparticle width, so that various detunings of the localized mode and the in-plane diffraction (or Rayleigh anomaly) are observed (Fig. 1 left). Numerically we can elucidate these properties via analysis, amongst others, of the eigenmode profiles, their spatial extension and the radiative properties (Fig. 1 right). The extensive range of properties such as narrow and wide spectral responses, bright and dark angular spectra etc. allows for various applications [1].

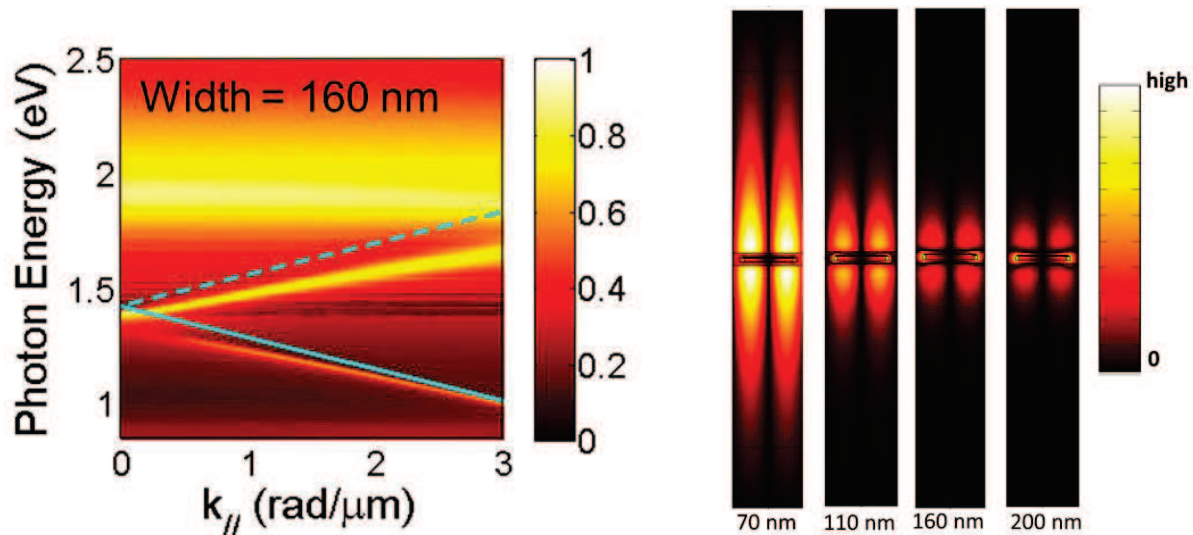


**Fig. 1.** (Left) Example of an experimental angular extinction spectrum in function of energy and propagation constant. (Right) Calculated eigenmode profile for various particle widths.

### Reference

- [1] A. Abass, S.R.K. Rodriguez, J. Gomez Rivas, B. Maes, *Tailoring Dispersion and Eigenfield Profiles of Plasmonic Surface*, ACS Photonics, 1(1), p61-68, 2014

## The relevance of group delay for refractometric sensing

Hugo J.W.M. Hoekstra,<sup>1,\*</sup> and Manfred Hammer<sup>1,2</sup>

<sup>1</sup>*Institute for Nanotechnology, University of Twente, Enschede, The Netherlands*

<sup>2</sup>*University of Paderborn, Theoretical Electrical Engineering, Paderborn, Germany*

[\\*H.J.W.M.Hoekstra@utwente.nl](mailto:H.J.W.M.Hoekstra@utwente.nl)

It is argued that the sensitivity of an optical sensing device, defined as the relative change of the transmittance for refractive index changes, is closely related to the group delay. Further, a general expression relating group delay and the ratio of the time-averaged optical energy and the input power is presented.

### Introduction

The big potential of integrated optical refractometric sensing devices is evidenced by the large number of publications in the field, showing many different device implementations owing to the large variety of application conditions, and also to the chase after devices with a high sensitivity. The aim of this paper is to consider the relevance of the different definitions used in literature for device sensitivity and also to discuss which physical quantities are relevant for a high sensitivity.

### Theory

We consider an abstract device. Assuming that the dominant noise is proportional to the transmittance, as a consequence of, for example, power fluctuations of the source, variations in detector responsivity, or mechanical instabilities, we define the sensitivity  $S$  for changes of the index  $n_l$  by

$$S = \left| \partial \ln T_m / \partial n_l \right|, \quad (1)$$

where  $T_m$  is the transmittance from the input channel to the output channel labeled  $m$ . During the conference the relevance of this definition will be compared with that of other definitions.

In our search to understand which quantities are the most relevant for high  $S$  we have considered group delay. It can be shown that for an arbitrary, non-absorbing photonic structure with given input channel with input power  $P_{in}$  the following relation holds

$$\sum_{m=1}^Q T_m \tau_{g,m}^l = \frac{1}{2} \frac{\partial(n_l \omega)}{\partial \omega} \int_{V_l} \epsilon_0 n_l |\mathbf{E}|^2 d\tau / P_{in} \quad (2)$$

where the summation runs over the  $Q$  output channels ( $m$ ), the subscript  $l$  refers to a certain material of the structure corresponding to volume  $V_l$ ,  $\omega$  is the angular frequency and  $\mathbf{E}$  is the electric field. The quantity  $\tau_{g,m}^l$  is the partial group delay for channel  $m$ , being that part of the group delay originating from the material  $l$ , which relates to the total group delay (from all  $P$  materials) via

$$\tau_{g,m} = \sum_{l=1}^P \tau_{g,m}^l \equiv -\text{Im}(\partial \ln t_m / \partial \omega). \quad (3)$$

As a byproduct of the theory we present a general relation, which holds if the output modes of the structure are not overlapping with each other or with the input field, as follows

$$\sum_{m=1}^Q T_m \tau_{g,m} = \int_V D d\tau / P_{in},$$

where  $D$  is the energy density and  $V$  the volume of the considered structure. During the presentation at the conference it will be argued that partial group delay and sensitivity can be converted into each other using a simple Mach-Zehnder like interferometric set-up.

### Conclusions

As to be elaborated during the workshop, a large *energy density* in the probed material relative to the input power enables the construction of a highly sensitive device. Further, a large *partial group delay*, originating from the 'sensing' part of the structure, is sufficient to construct a device with large sensitivity.

## Thermo-plasmonic optical switches at telecom wavelengths

J.-C. Weeber<sup>1,\*</sup>; K. Hassan<sup>1</sup>, M. Nielsen<sup>2</sup>, T. Bernardin<sup>1</sup>, S. Kaya<sup>1</sup>, C. Finot<sup>1</sup>, J. Fatome<sup>1</sup>

<sup>1</sup>LICB, Université de Bourgogne, 9 Av. A. Savary, 21078 Dijon, France;

<sup>2</sup>ITI, University of Southern Denmark, DK-5230 Niels

\*jcweeber@u-bourgogne.fr

We demonstrate thermo-optical plasmonic switches operating at telecom wavelengths. The switches rely on hybrid metallo-polymer waveguides sustaining so-called dielectric-loaded surface plasmon modes. The switches are operated by using either electrical or all-optical activation.

### Introduction

Thermal control of surface plasmon propagation is so far one of the most practical way to activate dynamic plasmonic components operating in the telecom frequency range. In this contribution, we will report on the use of dielectric-loaded surface plasmon waveguides with a sub-micron cross-section for the development of plasmonic thermo-optical switches that can be used for high-bit rate data traffic routing.

### Summary

Dielectric loaded surface plasmon waveguides (DLSPW) are comprised of a polymer ridge deposited on top of a metal film or strip. The effective index of the fundamental plasmonic (TM-like) mode sustained by such waveguides can be readily manipulated provided that the polymer features a large thermo-optical coefficient. In this work, we first demonstrate high-bit rate (10 Gb/s) propagation along DLSPWs [1] and their implementation into electrically activated ON/OFF switches based on coupled racetrack shaped resonators. Next, beyond electrical activation, we will show that, when doped with metallic nano-particles [1], polymer-based DLSPW are convenient for the development of “all-optical” routing switches (see Fig. 1). The dynamic of the response of those switches will be considered from DC to the nanosecond regime. In the last part of this work we will suggest new designs for fast plasmonic thermo-optical components featuring response and latency times in the nanosecond range improving by two orders of magnitude the bandwidth of thermo-optical routing switches as compared to currently existing devices.

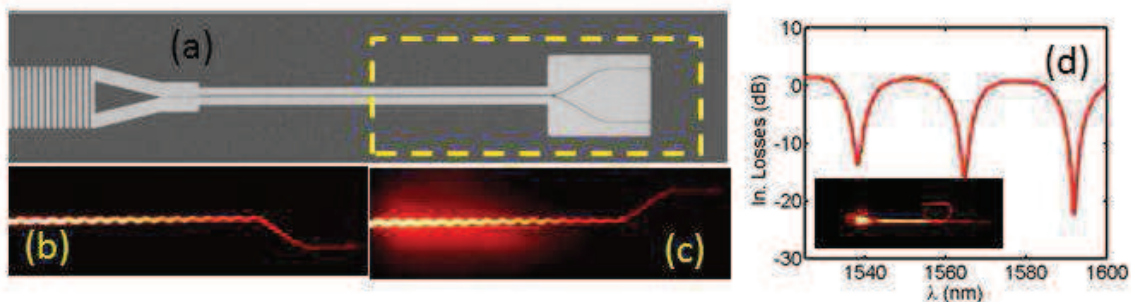


**Fig. 1.** (a) Electron microscope image of an electron-beam lithographically fabricated 1x2 DLSPW switch. The total length of the device is 120 $\mu$ m. (b) (resp. (c)) Radiation leakage microscopy images of the cold (hot) states of the swicthe at 1560nm. The activation of the swicthe is performed optically (see the elliptically shaped spot on (c)). (d) Typical spectrum of a racetrack shaped plasmonic resonator (radius 5 $\mu$ m, see inset) used for the implementation of ON/OFF thermo-optical switches.

[1] M. G-Nielsen *et al.*, *J. Lightwave Technol.* **75**, 245405 (2012)

[2] J.-C. Weeber *et al.*, *Optics Express.* **21**, 27291 (2013) (Focus issue on Surface Plasmon Photonics)

## Modeling of microring resonators with high dispersion induced by a one dimensional photonic crystal

D. Urbonas<sup>1</sup>, M. Gabalis<sup>1\*</sup>, S. Malaguti<sup>2</sup>, A. Parini<sup>2</sup>, G. Bellanca<sup>2</sup>, R. Petruskevicius<sup>1</sup>,

<sup>1</sup> Institute of Physics, Center for Physical Sciences and Technology, Vilnius, Lithuania

<sup>2</sup> Department of Engineering, University of Ferrara, Ferrara, Italy

[gysliukas@micro.lt](mailto:gysliukas@micro.lt)

We present the numerical analysis of perforated microring resonators. Transmission characteristics and performance of these devices are investigated through Finite-Difference-Time-Domain method.

### Introduction

Microring resonators have many different fields of application such as filtering, sensing and so on. One particular modification that can increase the performance of these devices is the introduction of perforations inside the core material. Analysis of such devices is sparse in literature, mostly limited to slotted [1] and perforated [2] microring resonators. We investigate the effect of periodicity in the core of the ring on transmission properties, thus opening new scenarios for possible applications.

### Results

Fig. 1(a) shows the geometry of a microring resonator with circular perforations. The aim of these perforations is to increase the volume in which the electromagnetic field of the guided wave interacts with the surrounded material. The dispersive behavior of periodic structures should also be considered. The band-gap determined by the periodic defects (Fig. 1(b)) modifies the transmission of the waveguide coupled with the ring (Fig. 1(c)). There are no propagating modes in the ring for frequencies inside the band-gap. Due to the high dispersion for wavelengths close to the band-edge, the free spectral range of the resonator is also modified. Different hole shapes can be used to achieve different results, thus making the response of the device more sensitive to perturbations. In the final work we will show how the shape of the holes can influence the response of the device.

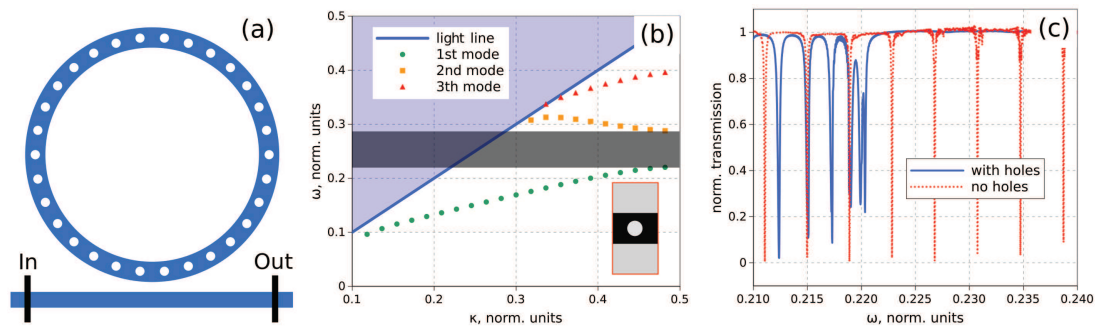


Fig. 1. (a) Geometry of the microring resonator with circular holes. (b) Band diagram of equivalent element. (c) Transmission spectra of microring resonator with holes (solid line) and without holes (dotted line).

### References

- [1] K. R. Hiremath, J. Niegemann, K. Busch, *Analysis of light propagation in slotted resonator based systems via coupled-mode theory*, Optics Express, vol. 19, no. 9, pp. 8641-8655, 2011.
- [2] D. Goldring, U. Levy, D. Mendlovic, *Highly dispersive micro-ring resonator based on one dimensional photonic crystal waveguide design and analysis*, Optics Express, vol. 15, no. 6, pp. 3156-3168, 2007.

## Second Order Sensitivity Analysis for a Photonic Crystal Waveguide Bend

Zhen Hu<sup>1</sup>, Ya Yan Lu<sup>2</sup>,

<sup>1</sup> *Department of Mathematics, Hohai University, Nanjing, Jiangsu, China*

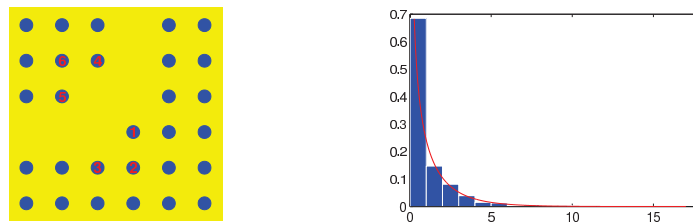
<sup>2</sup> *Department of Mathematics, City University of Hong Kong, Kowloon, Hong Kong*

*huzhen@hhu.edu.cn*

For a 90° photonic crystal waveguide bend, a second order sensitivity analysis is performed at the frequency where the transmission coefficient is nearly 1. If the radius of a rod follows a normal distribution, we show that the transmission coefficient follows a non-central  $\chi^2$  distribution approximately.

### Introduction

For practical applications of photonic crystal (PhC) devices, it is important to determine the sensitivity of device properties with respect to design parameters. Standard sensitivity analysis [1] based on the adjoint variable method calculates the first order partial derivatives of a response function with respect to the parameters. In some cases, the first order derivatives are nearly zero, and it is necessary to calculate the second order partial derivatives. We consider a 90° PhC waveguide bend (shown in the left panel of the figure below) where the background is a square lattice (lattice constant  $L$ ) of dielectric rods (radius  $0.18L$ , dielectric constant 11.56). For certain frequency, the transmission coefficient  $T$



is nearly 1, then the partial derivatives of  $T$  with respect to design parameters (such as the radii of the rods) are nearly zero, and the second order derivatives can no longer be ignored. Besides, if the radii of the rods are assumed to be random variables following certain probability distribution, we can approximate the distribution of  $T$  more accurately when the second order derivatives are available.

### Results

It is possible to efficiently analyze 2D PhC devices based on the Dirichlet-to-Neumann (DtN) maps of the unit cells [2]. We have extended the DtN-map method to calculate the first and second order partial derivatives of device properties such as the transmission coefficient  $T$ . For the 90° bend at the normalized frequency  $\omega L/(2\pi c) = 0.35$ , the first and second order derivatives ( $T'$  and  $T''$ ) with respect to the radius of the rod marked by integer 3 are  $T'(r) = 0.005782$  and  $T''(r) = -7.2801$ . If a radius of that rod has a random perturbation  $\Delta r$  which follows the normal distribution  $N(0, \sigma^2)$ , we can show that the distribution of  $T(r + \Delta r)$  is related to the non-central  $\chi^2$  distribution by

$$\left[ T(r + \Delta r) - \left( T(r) - \frac{T'^2(r)}{2T''(r)} \right) \right] / \left( \frac{1}{2} T''(r) \sigma^2 \right) \sim \chi^2 \left( 1, \left( \frac{T'(r)}{T''(r)\sigma} \right)^2 \right).$$

The above result is validated by simulations as shown in the right panel of the figure above.

### References

- [1] G. Veronis, R. W. Dutton, and S. Fan, *Optics Letters*, **29**, 2288-2290, 2004.
- [2] Z. Hu and Y. Y. Lu, *Optics Express*, **16**, 17383-17399, 2008.



# **Poster presentations**

## A rigorous analytical approach using MoM for testing air gap tuning effects on multilayered equilateral triangular microstrip antenna

L. Djouablia<sup>1,\*</sup>, A.Labbani<sup>2</sup> and A. Benghalia<sup>3</sup>

<sup>1</sup> University "20 august 1955" of Skikda, Department of Genie Electric, Technologie Faculty, Algeria.

<sup>2,3</sup> Laboratory LHS, Department of Electronic, Engineering sciences Faculty. Mentouri University, of Constantine, Algeria

<sup>1,\*</sup> Corresponding author e-mail: ln\_djouablia@live.fr

Using a new combined analytical approach, air gap tuning effects on resonant frequency and radiation field of multilayered equilateral triangular microstrip antenna will be presented in this paper. The problem is analysed in spectral domain using moment method MoM and an electric field integral equation combined with a mathematical approach.

### Introduction

Generally the value of permittivity is the most sensitive parameter in microstrip antenna performance, it must be fixed and is unchangeable, it depends on dielectric's nature only, but in some cases as microwaves domain, we need to change it without changing the media or modifying the structure. Note that, we are in front of an electromagnetic problem, a rigorous calculus using an analytical approach based on Maxwell's equations and spectral-domain method of moments combined with mathematical approach "reference element method" [1], [2] will be presented in the present study, by inserting an air gap in the substrate between the dielectric and the ground plane of an equilateral triangular patch antenna or even at the middle of the dielectric.

### Problem formulation and results

Starting from Maxwell's equations in Fourier-transform the exact Green functions formulas can be

deduced for two and three layers: 
$$G = \begin{bmatrix} G_{11} & G_{12} \\ G_{12} & G_{22} \end{bmatrix}$$

$G_{22}$ ,  $G_{12}$ ,  $G_{21}$ ,  $G_{11}$ : Parameters calculated rigorously using this approach.

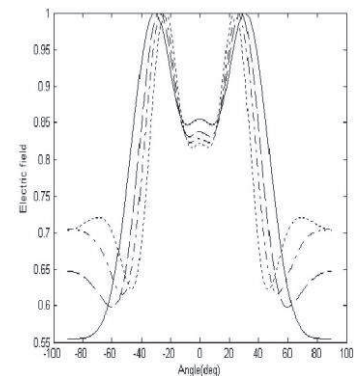
The proposed mathematical method is general and can be applied to any form can be approximated to a known form, for calculating the Fourier transform of basis functions.

### Conclusion

Although the proposed approach can give results for several resonant modes according to different parameters of the antenna. Only analysis of real part's complex resonant frequency will be presented.

### References

- [1] D. Mirshekar-Syahkal, "Spectral domain method for microwave integrated circuits", Research studies presses LTD, John Willey and sons INC, 1989.
- [2] J.Douchet and B.Zwhalen, "Calcul différentiel et intégral, fonctions réelles de plusieurs variables réelles", (2nd edition), p.140-142.



Radiation patterns around resonance versus in the plane  $\phi=0^\circ$  for different gaps.

## Tunability of absolute photonic band gaps in two-dimensional photonic crystals based on CdSe particles embedded in TiO<sub>2</sub> matrix

A. Labbani<sup>1,\*</sup>, L. Jouablia<sup>1</sup>, A. Benghalia<sup>1</sup>

*Microwave and Semiconductors Laboratory, Faculty of Engineering Sciences Department of Electronics University Constantine 1. Ain El Bey Road, 25000 Constantine, Algeria*

\*[labbame@yahoo.fr](mailto:labbame@yahoo.fr)

We investigate the photonic band gap (PBG) spectra of two-dimensional photonic crystals (2D PC's) created by square and hexagonal lattices consisting of coating CdSe rods with a thin air layer in a TiO<sub>2</sub> matrix. The square lattice of coated rods is modified by inserting a small air rod into the center of each square unit cell.

### Introduction

PCs are periodic dielectric structures designed to control and manipulate the propagation of light. One of the most interesting properties of PC's is that they can be designed to possess an absolute PBG's. Much attention has therefore, been drawn towards 2D PC's with some typical lattice types, for example square, hexagonal and complex lattices. Many attempts have been made to design various kinds of PC's to achieve a large absolute PBG. To our knowledge, only a few authors have investigated how the existence of interfacial (or cladding) layers affects the properties of PBG's [1].

### Summary

We investigate different aspect of the absolute PBG in two-dimensional square and hexagonal lattices considering an interfacial layer between the CdSe rods and the TiO<sub>2</sub> matrix. Our results show that in a square lattice a coating alone does not help to create an absolute PBG. However, we showed that adding air rod into the center of each square unit cell can produce the absolute PBG. The optimum gap is achieved by tuning the thickness of the shell layer in the two types of lattices.

### Results

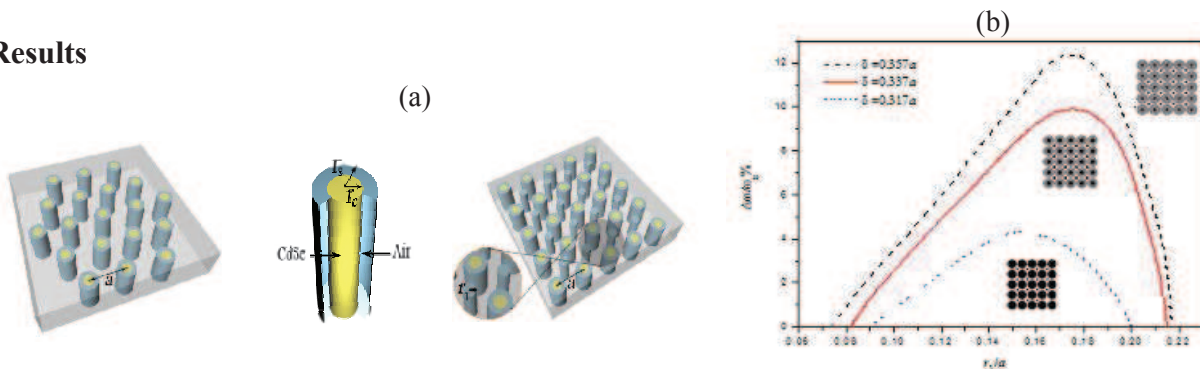


**Fig. 1.** (a) Schematic representation of the studied structures (b) Width  $\Delta\omega/\omega_g$  of the absolute PBG for the square lattice plotted as a function of radius ratio  $r_1/a$  for three thicknesses of the shell layer  $\delta = 0.357a$ ,  $0.337a$ , and  $0.317a$ .

### Conclusion

Our results suggest that the presence of the shell layer surrounding the CdSe rods has an obvious influence on the value of the absolute PBG. The optimum gap can be obtained by tuning the thickness of the coating layer for each structure.

### References

- [1] T. Trifonov *et al.*, *Analysis of photonic band gaps in two-dimensional photonic crystals with rods covered by a thin interfacial layer*, Phys. Rev. B, 2004.

## Numerical Simulation of resonance structures with FDTD Algorithms Based on GPU B-CALM and CPU Meep

D. Urbonas \*, M. Gabalis R. Petruskevicius

<sup>1</sup> *Institute of Physics, Center for Physical Sciences and Technology, Vilnius, Lithuania*  
*darius.urbonas.p@gmail.com*

We compare two Finite-difference-Time-Domain software packages. One runs the simulation utilizing Central Processing Unit (CPU), another - Graphical Processing Unit (GPU). By shifting simulation execution from CPU to GPU a significant reduction of computation time can be achieved.

### Introduction

The size of the possible simulation with Finite-Difference-Time-Domain (FDTD) method is often limited by computation time. By combining the parallel nature of FDTD algorithm with GPU reduction in computation time can be obtained. In this work we present comparison between two free FDTD software packages. One is using CPU - Meep [1]. And the other is using GPU - B-CALM [2]. Two 3D structures were analyzed: metallic rectangular cavity resonator and microring resonator based refractive index sensor. The comparison between both FDTD packages is made with regard to simulation time and numerical accuracy.

### Results

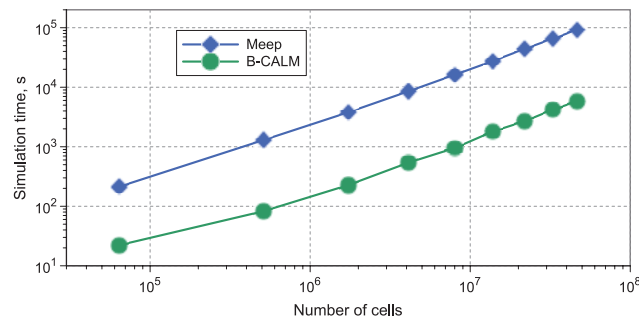


Fig. 1. Simulation time as a function of number of cells in computational domain.

Figure 1 shows the simulation time as a function of number of cells in computational domain. Observed speed up of FDTD simulation running on GPU as compared to the CPU is about 18 times. Simulation results, in numerical accuracy, agree well among both software packages.

Significant speed up of 18 times makes GPU FDTD attractive for simulations in which computational time is of the highest importance.

### References

- [1] A. F. Oskooi, D. Roundy, M. Ibanescu, P. Bermel, J. D. Joannopoulos, S. G. Johnson, *MEEP: A flexible free-software package for electromagnetic simulations by the FDTD method*, Computational Physics Communications, vol. 181, pp. 687-702, 2010.
- [2] P. Wahl, D. S. Ly-Gagnon, C. Debaes, D. A. B. Miller, H. Thienpont, *B-CALM: An open-source GPU-based 3D-FDTD with multi-pole dispersion for plasmonics*, Optical and Quantum Electronics, vol. 44, pp. 285-290, 2012.

## Determination of the Equivalent Step Index of Direct Laser Written Waveguides

L. Huang<sup>1,\*</sup> and F.P. Payne<sup>1</sup>

<sup>1</sup>*Department of Engineering Science, University of Oxford, Parks Road, Oxford OX1 3PJ, United Kingdom*

\*[leilei.huang@jesus.ox.ac.uk](mailto:leilei.huang@jesus.ox.ac.uk)

We propose a modification of the propagation mode near field technique to determine the equivalent step index of direct laser written optical waveguides.

### Introduction

The direct writing of optical waveguides using ultra-short laser pulses has attracted considerable interest because of its advantage in the fabrication of three dimensional optical structures. Determining the refractive index of the resulting waveguides is essential but difficult. One method is based on the propagation mode near field technique (PMNFT) in which the measured modal near field is used together with the wave equation to numerically determine the refractive index. This method can be inaccurate because noise in the measured near field makes numerical calculation of the second derivative in the wave equation unreliable. For many applications, a detailed knowledge of the refractive index profile is unnecessary and instead an equivalent step index (ESI) which accurately predicts the modal field is adequate. This paper presents a modification of the PMNFT to determine the ESI of direct laser written (DLW) waveguides. The optical fields computed using the resulting ESI are in very close agreement with the measured fields.

### Determination of the Equivalent Step Index

The optical near field of a DLW waveguide was measured. Noise in the resulting data was reduced by applying a digital Savitzky-Golay filter. A combination of Laguerre-Gaussian and modified Bessel functions was used to fit the measured near field in the central and cladding regions of the waveguide respectively. This, together, with the wave equation, was used to compute a first estimate of the ESI difference  $\Delta n$  and core radius  $a$ . These estimation values were used as the starting point of an optimisation process whereby the modal field of the ESI was computed and the mean square error between the computed and measured field was calculated. The optimal values of  $\Delta n$  and  $a$  were then found that resulted in a best fit that minimised the mean square error between the computed and measured fields. The optimisation routine exploited an accurate analytical expression for the modal field propagation constant for the solution of the dispersion equation. Figure 1 shows a typical example of the measured near field and the calculated one using the best fit ESI with  $\Delta n = 0.013$  and  $a = 2\mu\text{m}$ . The two field distributions agree very closely and both have a mode field diameter of  $3.5\mu\text{m}$ ; the mean square error is  $1.9 \times 10^{-3}$ .

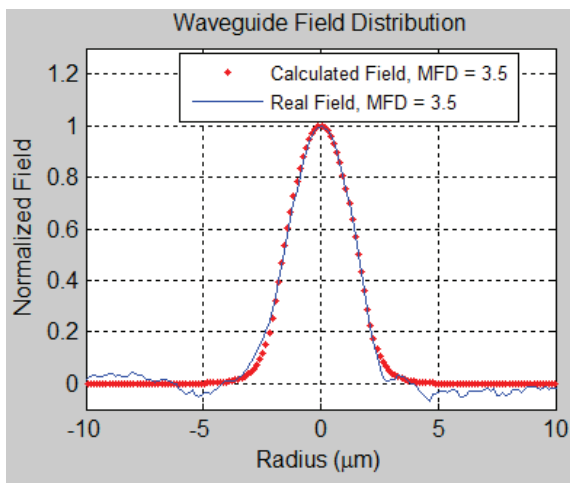


Fig. 1 Predicted and measured field distributions.

### Conclusion

We have demonstrated a modification of the PMNFT to find the ESI of the DLW waveguides. The optical fields predicted from the ESI are in extremely close agreement with the measured fields, which provide useful information for the fabrication and characterization of the written waveguides.

## Computing Waveguide Modes by the Pseudospectral Modal Method

Dawei Song<sup>1</sup> and Ya Yan Lu<sup>2</sup>

<sup>1</sup> *Department of Mathematics, Nanjing University of Aeronautics and Astronautics, Nanjing, Jiangsu, China*

<sup>2</sup> *Department of Mathematics, City University of Hong Kong, Kowloon, Hong Kong*

For waveguides with high index-contrast and right-angle corners, the classical mode-matching method (as a full vectorial mode solver) is widely used. A recently developed pseudospectral modal method (PSMM) for diffraction gratings is reformulated as a numerical variant of the mode-matching method. It is simple to implement and gives highly accurate results.

### Introduction

For optical waveguides with high index-contrast and sharp corners, if high accuracy is needed, the finite difference [1] and finite element [2] mode solvers typically produce very large matrices, and the corresponding matrix eigenvalue problems are not easy to solve. Recently, the pseudospectral modal method (PSMM) [3, 4] was developed for in-plane and conical diffraction grating problems. We extend the PSMM as a numerical variant of the mode-matching method for computing optical waveguide modes.

### The method

Consider an optical waveguide with a  $z$ -independent dielectric function  $\varepsilon(x, y)$ , where  $z$  is along the waveguide axis,  $x$  and  $y$  are the transverse variables. Assuming that the waveguide cross section can be divided into a number of vertical slices where  $\varepsilon$  depends only on  $y$ , we use the Chebyshev pseudospectral method to calculate the one-dimensional TE and TM modes for each vertical slice, expand  $E_y$ ,  $H_y$ ,  $E_z$  and  $H_z$  using the numerical eigenmodes, match the four field components on the vertical lines between the slices, and obtain the following nonlinear eigenvalue problem

$$\mathbf{F}(\beta)\mathbf{x} = \mathbf{0}, \quad (1)$$

where  $\mathbf{F}$  is a square matrix of relatively small size, and  $\beta$  appears implicitly in the matrix  $\mathbf{F}$ . To find a guided mode from Eq. (1), we determine  $\beta$  from the condition that  $\mathbf{F}(\beta)$  is a singular matrix.

### Results

We consider a classical rib waveguide where the rib width is  $w = 3.0 \mu\text{m}$ , the rib thickness is  $h = 1 \mu\text{m}$ , and the thickness of the slab is  $t = 0.5 \mu\text{m}$ . The refractive indices of the cladding, the guiding layer and the substrate are  $n_t = 1$ ,  $n_c = 3.44$  and  $n_b = 3.4$ , respectively. For the free space wavelength  $\lambda = 1.15 \mu\text{m}$ , we calculate the normalized propagation constant  $\beta/k_0$  for different values of  $N$ , where  $N$  is the total number of points for discretizing  $y$ . For  $N = 240$  and  $280$ , we obtain  $\beta/k_0 \approx 3.4131321$  and  $\beta/k_0 \approx 3.41313214$ , respectively. Notice that the matrix  $F$  is an  $(2N) \times (2N)$  matrix for the rib waveguide. Our numerical results indicate that the PSMM (as a mode solver) is simple to implement and highly accurate for waveguides with high index-contrast and right-angle corners.

### References

- [1] G. R. Hadley, *J. Lightwave Technol.* **20**, 1219-1231, 2002.
- [2] S. Selleri, L. Vincetti, A. Cucinotta, and M. Zoboli, *Opt. Quant. Electron.* **33**, 359-371, 2001.
- [3] D. Song, L. Yuan, and Y. Y. Lu, *J. Opt. Soc. Am. A* **28**, 613-620, 2011.
- [4] D. Song and Y. Y. Lu, *J. Mod. Opt.* **60**, 1729-1734, 2013.

## Morris-index screening technique to assess parameters incertitude in microring-based Optical Networks-on-Chip

Alberto Parini <sup>1,2,\*</sup>, Gaetano Bellanca <sup>2</sup>,

<sup>1</sup>Laboratory for Micro and Submicro Enabling Technologies of Emilia-Romagna Region (MIST E-R), Italy

<sup>2</sup>Department of Engineering, University of Ferrara, Italy

\*[alberto.parini@unife.fr](mailto:alberto.parini@unife.fr)

We present a statistical screening technique, based on the Morris index method, to assess the impact of technological imperfections on the performance of microring-based Optical Networks-on-Chip (ONoCs).

### Introduction

Technological processes are prone to errors and tolerances; as a result, the experimental response of a fabricated device may differ considerably from the corresponding analytical or numerical previsions. When there are many parameters subject to incertitude, the overall impact of their randomness on the output(s) is difficult to clearly assess. Statistical methods for the identifications of the most influential factors in models with many variables have been successfully applied in several physical context. Here, we specialize the low computational cost technique proposed by Morris [1] to evaluate the impact of the variability of some key geometrical parameters on the performance of Optical-Network on Chip routers.

### Results

Left panel of Fig. 1 shows the analyzed structure [2]. The bar chart on the right shows the relative degradation in the performance of the three routing paths, due to a statistical variability in the radius of the eight rings. The higher the bar, the most impacting the ring imperfection on the transmission properties through the considered path.

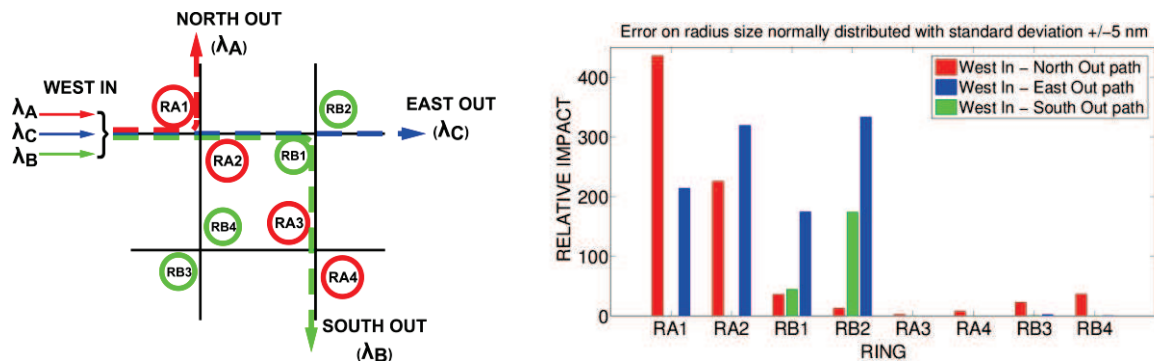


**Fig. 1.** (Left) Network under test: rings RA1, RA2, RA3, RA4 are resonant with  $\lambda_A$ , rings RB1, RB2, RB3, RB4 are resonant with  $\lambda_B$ ,  $\lambda_C$  is a through wavelength for both families. (Right) Relative impact of the radii imperfections on the optical signal-to-noise ratio of each routing path, as evaluated by the Morris method.

### Conclusion

Statistical screening techniques can provide, with a low computational cost, an insight of the impact of technological tolerances on the switching performance of complex optical networks.

### References

- [1] Max. D. Morris, *Factorial Sampling Plans for Preliminary Computational Experiments*, Technometrics, Vol. 33, No. 2. (May, 1991), pp. 161-174
- [2] X. Tan, M. Yang, L. Zhang, Y. Jiang, and J. Yang, "A generic optical router design for photonic network-on-chips," *IEEE J. Lightw. Technol.*, vol. 30, no. 3, pp. 368–376, Feb. 2012

## A vectorial solver for the reflection of semi-confined waves at slab waveguide discontinuities for non-perpendicular incidence

Manfred Hammer<sup>1,2,\*</sup>

<sup>1</sup>MESA<sup>+</sup> Institute for Nanotechnology, University of Twente, Enschede, The Netherlands

<sup>2</sup>University of Paderborn, Theoretical Electrical Engineering, Paderborn, Germany

\*[m.hammer@utwente.nl](mailto:m.hammer@utwente.nl)

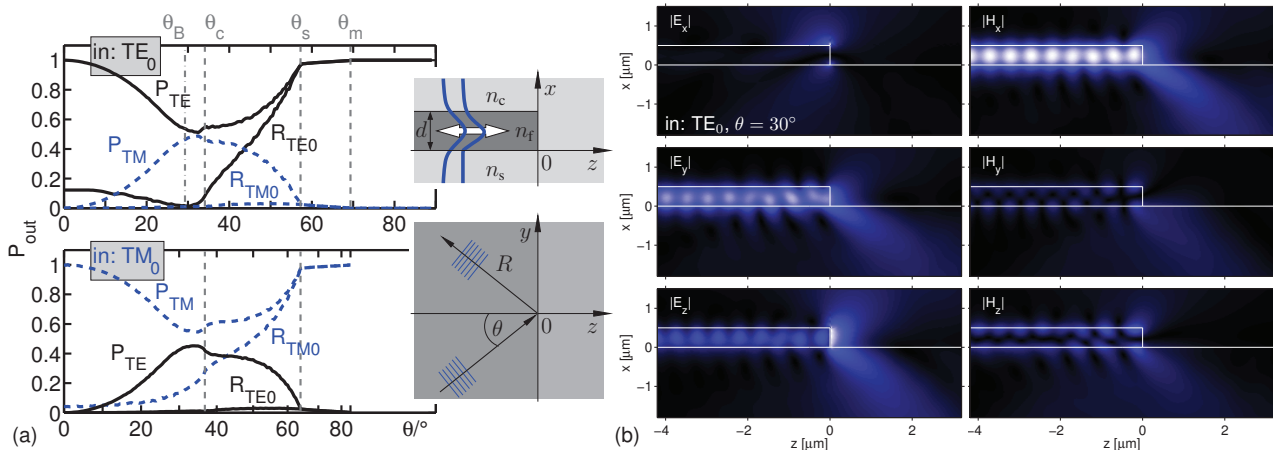
The non-normal incidence of thin-film guided, in-plane unguided optical waves on straight, possibly composite slab waveguide facets is considered. The quasi-analytical, vectorial solutions permit to inspect polarization properties of reflected and refracted guided waves, radiative losses, and full field details near the facet.

### Non-normal light incidence on a slab waveguide discontinuity

The effects of a straight transition between regions with different layering, or of a core facet, on thin-film guided, in-plane unguided light forms the basis for a series of classical integrated optical components. While scalar TE / TM Helmholtz equations apply for perpendicular incidence, for non-normal incidence one is led to a vectorial problem [1] that is formally identical to that for the modes of 3-D channel waveguides. Here, however, it needs to be solved as a parametrized, inhomogeneous system on a 2-D computational window with transparent-influx boundary conditions.

### Vectorial, quasi-analytical solutions by quadridirectional eigenmode propagation (QUEP)

As a step beyond the scalar approximation [1] and an older bidirectional approach [2], we report on a dedicated vectorial solver for — in principle — arbitrary rectangular cross section geometries, based on simultaneous expansions into slab modes along *two* orthogonal coordinate axes (QUEP, [3]). A review of general aspects (solver specifics, power balance, reciprocity, characteristic angles), will be followed by a discussion of solutions for different configurations, including the example below.



Reflection of semi-guided plane waves at a thin film facet. (a): reflected / outgoing power carried by the TE<sub>0</sub> / TM<sub>0</sub> modes ( $R_{TE0}$ ,  $R_{TM0}$ ) and by all TE / TM waves ( $P_{TE}$ ,  $P_{TM}$ ) for TE<sub>0</sub>- (top) or TM<sub>0</sub>-excitation (bottom), versus incidence angle  $\theta$ ; critical angles  $\theta_c$ ,  $\theta_s$ ,  $\theta_m$  for power being carried away by “cover”, “substrate”, and TM-fields; quasi-Brewster angle  $\tan \theta_B = n_c / n_{eff,TE0}$ . (b): e.m. components (absolute values) for TE<sub>0</sub>-excitation at  $\theta = 30^\circ$ . Parameters:  $n_s : n_f : n_c = 1.5 : 2.0 : 1.0$ ,  $d = 0.5 \mu\text{m}$ , vacuum wavelength  $\lambda = 1.55 \mu\text{m}$ .

### References

- [1] F. Çivitci, M. Hammer, and H. J. W. M. Hoekstra. *Optical and Quantum Electronics*, 46(3):477–490, 2014.
- [2] W. Biehlig and U. Langbein. *Optical and Quantum Electronics*, 22(4):319–333, 1990.
- [3] M. Hammer. *Optics Communications*, 235(4–6):285–303, 2004.

## The fundamentals of multi-splitting filtering technology

A. Tsarev<sup>1,2\*</sup>

<sup>1</sup>*A.V. Rzhanov Institute of Semiconductor Physics SB RAS, Novosibirsk, Russia*

<sup>2</sup>*The Novosibirsk State University, Novosibirsk, Russia*

*\*[tsarev@isp.nsc.ru](mailto:tsarev@isp.nsc.ru)*

The original results which construct the basis of multi-splitting filtering technology have been reviewed. The main building blocks like an excellent silicon wire crossing, modified effective index method and original design let possible to develop and study a new optical multiplexer built by multiple coupled Si-wires on SOI.

### Introduction

Silicon photonics creates a great amount of optical devices intended for different applications from telecom to sensors. None of them are ideal but each has some advantages related to the others. A brief description of original results which make the building blocks of multi-splitting (MS) photonic structures on silicon-on-insulator (SOI), which can be used as tunable filter or reconfigurable optical add drop multiplexer (ROADM), are discussed and reviewed in the paper.

### Summary

A general view of the novel multi-splitting multiplexer is shown in Fig. 1. Device examination is very complicated and the study has been divided into several separate parts, which are focused on one key point. The first part is devoted to the approach of multilayer waveguide crossing [1] which is also suitable to construct a damper. Next part discusses the modified effective index method MEIM [2] which is optimal for direct 2D modeling of the device as it correctly (with about 1% error) describes in 2D case the phase and group index of 3D silicon wire waveguide. Optimum filter design [3] takes into account a constant pass-length difference and variation of coupling strength by controlling the gap between directional couplers used as power splitters. Spectrum properties of the MS filter and its tuning by thermo-optic effect are examined by direct 2D modeling jointly by FDTD and MEIM. *Work is supported by the grant 12-07-00018a by the Russian Fund for Basic Research.*

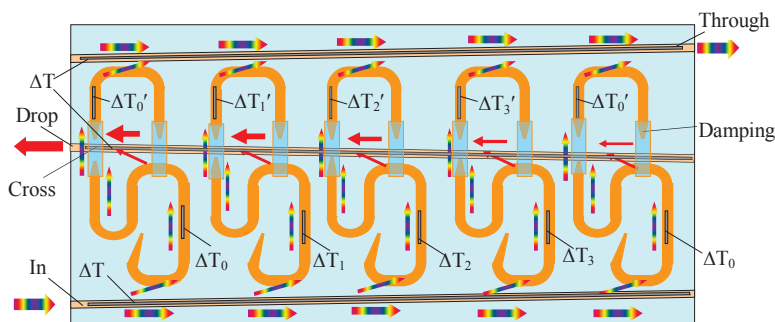


**Fig. 1.** The principle view of multi-splitting tunable multiplexer.

### References

- [1] Andrei V. Tsarev, "Efficient silicon wire waveguide crossing with negligible loss and crosstalk," *Opt. Express* 19, 13732-13737 (2011).
- [2] A. Tsarev, "Numerical Modeling of the Optical Multiplexer on SOI Constructed by Multiple Coupled Waveguides," *IEEE Journal of Selected Topics in Quantum Electronics*, vol.20, no.4, pp.1,8, July-Aug. 2014 (in press, doi: 10.1109/JSTQE.2013.2295180).
- [3] A. Tsarev, "Modified effective index method to fit the phase and group index of 3D photonic wire waveguide," *Opt. Lett.*, 38, 293-295 (2013).

## The propagation of the optical signal along a silicon wire in the presence of multiple weak tunnel reflections

E. Kolosovsky<sup>1</sup>, A. Tsarev<sup>1,2\*</sup>

<sup>1</sup>A.V. Rzhanov Institute of Semiconductor Physics SB RAS, Novosibirsk, Russia

<sup>2</sup>The Novosibirsk State University, Novosibirsk, Russia

\*[tsarev@isp.nsc.ru](mailto:tsarev@isp.nsc.ru)

The propagation of the signal in the single-mode silicon wire with multiple tunnel reflections has been examined. A possible signal interference at multiple wires crossing in silicon optical microchips is shown.

### Introduction

In silicon photonics in the design and construction of optical microchips naturally arises multiple crossings of silicon wires. To realize an efficient crossing with minimal scattering cross, we proposed [1, 2] to use the tunnel coupling through the oxide buffer layer of the optical wave from a tapered silicon wire into the adjacent polymer waveguide and back to the tapered silicon wire. For the cross direction this polymer waveguide is a tunnel insert with a very small reflection of the incident wave (of the order  $10^{-4}$ ) [2]. We are interesting what would be happen if the number of intersections with such polymer inserts become very large?

### Summary

The scheme of tunnel scattering of light by polymer inserts is shown in Fig. 1. The arrows indicate the incident (from the left) and the reflected fields. A direct numerical simulation is problematic due to a weak influence to the signal by tunneling inserts. For the simulation we used a high-precision approach based on semi-analytic method of lines (MoL) [3], which is a well-proved for the optical tasks with a high index contrast like a silicon structures.

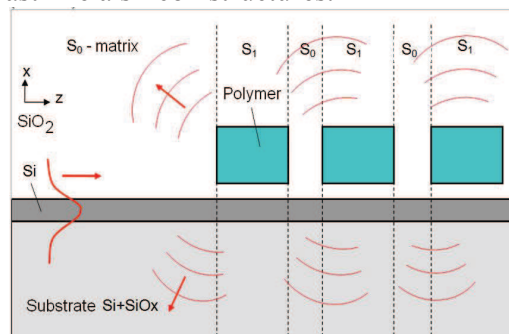


Fig. 1. The tunnel scattering by polymer inserts.

### Results

It is shown that because of the collective scattering by the tunneled reflections one can get the almost completely blocking of the optical signal, despite the small reflection by the each inserts. In the contrast to the strong Bragg gratings reflection, the scattering by the weak tunneling inserts does not lead to a strong reverse reflection of the guided mode. Thus in the case of the signal blocking the optical signal is scattered into the waveguide environment. *Work is supported by the grant 12-07-00018a by the Russian Fund for Basic Research.*

### References

1. A.V. Tsarev, "Efficient silicon wire waveguide crossing with negligible loss and crosstalk," *Opt. Express* 19, 13732-13737 (2011).
2. A. V. Tsarev, E. A. Kolosovskii, "Analysis of light propagation for a crossing of thin silicon wires using vertical tunnelling coupling with a thick optical channel waveguide", *QUANTUM ELECTRON*, 2013, 43 (8), 744–750.
3. U. Rogge and R. Pregla, "Method of lines for the analysis of strip-loaded optical waveguides", *Opt. Soc. Amer. B*, vol. 8, pp. 459–463, Feb. 1991.

## The Approximation Functions Method for Nonlinear Volterra Integral Equations

A. Nerukh<sup>1,\*</sup>, D. Zolotariov<sup>1</sup>, T. Benson<sup>2</sup>

<sup>1</sup> Kharkov National University of Radio Electronics, 14 Lenin Ave., Kharkov, 61166, UKRAINE

<sup>2</sup> George Green Institute for Electromagnetics Research, University of Nottingham, University Park, Nottingham, NG7 2RD, UK

\* [nerukh@gmail.com](mailto:nerukh@gmail.com)

The approximation functions method for the solution of a nonlinear Volterra integral equation is presented. A computer model based on the algorithm is developed and the transformation of an electromagnetic pulse in a nonlinear layer is investigated.

### Introduction

Interactions of optical pulses with active semiconductor waveguides are of significant importance in quantum electronics and optical communications technology. As a rule an exact consideration of electromagnetic processes in nonlinear media is possible only in special cases, so approximate methods are put on the forefront. In this paper the nonlinear Volterra integral equation [1] which describes electromagnetic waves in a nonlinear layer is solved by the method of approximating functions [2].

### Summary

Using the developed method the nonlinear Volterra integral equation is reduced to a system of linear algebraic equations. The Newton method for the solution of this system provides quadratic convergence. Original software for computer modeling of such an algorithm is developed and its applications to some physical phenomena are presented. In particular the transformation of electromagnetic pulses by a layer with a nonlinear medium is considered. The method developed has no limitations on the type of nonlinearity.

### Results

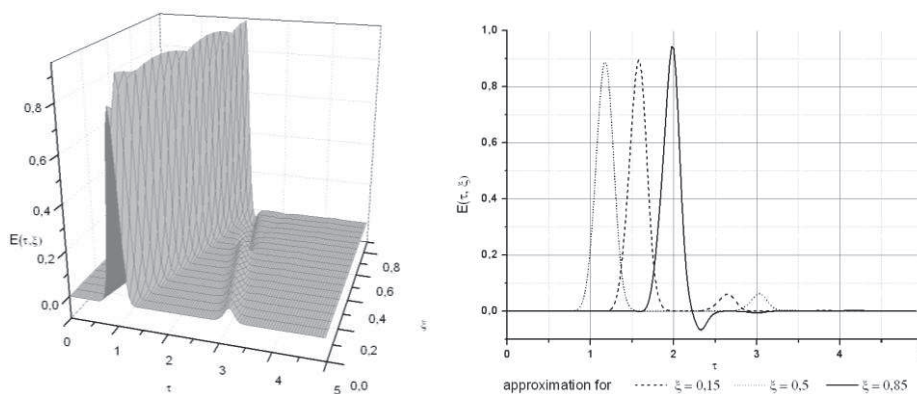


**Fig. 1.** The transformation of the Gaussian pulse in the layer with the nonlinear medium and snapshots of the pulse at various points of the layer.

### References

- [1] A.G. Nerukh, P. Sewell, T. M. Benson, *Volterra integral equations for nonstationary electromagnetic processes in time-varying dielectric waveguides*, Journal of Lightwave Technology, vol. 22, 1408-1419, 2004.
- [2] K. Maleknejad, H. Almasieh, M. Roodaki, *Triangular functions (TF) method for the solution of nonlinear Volterra–Fredholm integral equations*, Communication of Nonlinear Science in Numerical Simulations, No 15, 3293–3298, 2010.

## Full-vectorial finite-difference analysis of ferroelectric BaTiO<sub>3</sub> device

Xuan HU\*, Régis OROBTCHOUK

*Institut des Nanotechnologies de Lyon (INL), CNRS UMR5270, Université de Lyon  
Bâtiment "Blaise Pascal", 7 avenue Jean Capelle, INSA-Lyon, Villeurbanne 69621, France*

\*[xuan.hu@insa-lyon.fr](mailto:xuan.hu@insa-lyon.fr)

We present a design of slot waveguide of Mach-Zehnder modulator. Hybridization of an anisotropic mode solver and a Laplace solver is developed, allowing accurate calculation of the optical-RF modes interaction. Modelling results show that 20V applied voltage gives  $\Delta n_{\text{eff}} = 1.57 \times 10^{-3}$  and  $r_{\text{eff}} = 48.69 \text{ pm/V}$ .

### Introduction

Epitaxial growth of BaTiO<sub>3</sub> (BTO) films on Si (001) substrate is recently reported [1, 2], making BTO operable in silicon integrated device. Here we present accurate numerical studies of the electro-optical modulator.

### Summary

Fig.1 illustrates one waveguide of Mach-Zehnder modulator. Low-index BTO film ( $n_{\text{BTO}} \sim 2.3$ ) is sandwiched between silicon strip waveguide and SOI substrate ( $n_{\text{Si}} \sim 3.5$ ) to compose a horizontal slot waveguide.

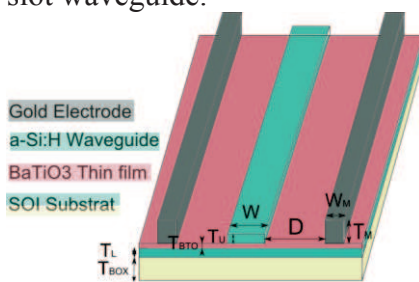


**Fig. 1.** Schematic of the slot waveguide of Mach-Zehnder modulator

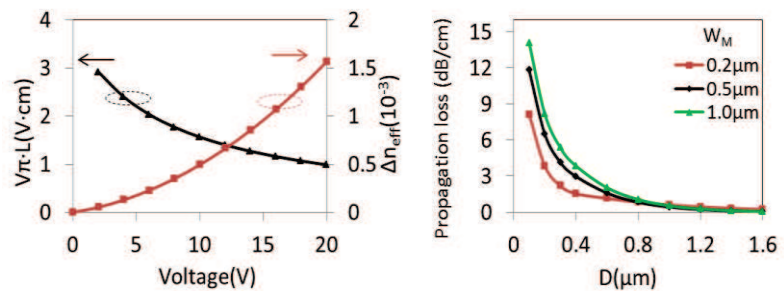


**Fig.2.** (a) Simulated electro-optical effect for TM-like mode  
(b) Propagation loss versus gap D for different  $W_M$

Starting with Pockell's coefficients of the bulk material, the electro-optic responses of proposed device are stimulated and presented in Fig.2(a). With applied DC voltage of 0-20V, TM-like propagation mode shows a variation of effective index  $\Delta n_{\text{eff}} = [0, 1.57 \times 10^{-3}]$ , and the modulator parameter  $V\pi L = [2.9 \text{ V}\cdot\text{cm}, 0.9 \text{ V}\cdot\text{cm}]$ . We reveal thus an effective Pockels coefficient  $r_{\text{eff}} = 48.69 \text{ pm/V}$  at 20V, comparable to the experimental data. Fig.2(b) shows a wider gap D decreases the propagation loss. With a large D ( $>1.0 \mu\text{m}$ ), electrodes width  $W_M$  plays less important role as electrodes are far away from the propagation mode to absorb. 0.42 dB/cm loss was derived with  $D=1.0 \mu\text{m}$  and  $W_M=0.5 \mu\text{m}$ . However, a large D means, at the same time, less electrical/optical overlap, and then less efficient electro-optic effect.

Accurate calculation has been carried out, including the index variation of non-diagonal permittivity material (BaTiO<sub>3</sub> in this case) induced by the bias voltage, and the impact of the design parameters on proposed device performance.

### References

- [1] Niu Gang, et al. "Epitaxy of BaTiO<sub>3</sub> thin film on Si (001) using a SrTiO<sub>3</sub> buffer layer for non-volatile memory application." *Microelectronic Engineering* 88.7 (2011): 1232-1235.
- [2] Abel Stefan, et al. "A strong electro-optically active lead-free ferroelectric integrated on silicon." *Nature communications* 4 (2013): 1671.

## Mono and multielectrode SOA structure optimization for wide optical bandwidth operation

P. Morel<sup>1,\*</sup>, R. Brenot<sup>2</sup>, F. Lelarge<sup>2</sup>, T. Motaweh<sup>1</sup>, A. Lagrost<sup>1</sup>

<sup>1</sup> *École Nationale d'Ingénieurs de Brest (ENIB), UEB, Lab-STICC UMR CNRS (6285), Brest, France*

<sup>2</sup> *Alcatel Thales, III-V Lab, Route Départementale 128, 91767 Palaiseau Cedex, France*

[\\*morel@enib.fr](mailto:morel@enib.fr)

We investigate the optical bandwidth optimization of new Multi Quantum Well (MQW) Semiconductor Optical Amplifiers (SOA) as a function of the electrode length in mono and multi-electrode cases.

### Introduction

New MQW-SOA structures have been developed under UltraWIDE project (ANR 2010 VERS 011 06) showing a wide optical bandwidth. The spectral shape of the gain of these components, unlike bulk SOAs, evolves with current and shows a plateau for a given injected current [1]. In this case, optimizing these SOA structures in term of lengths needs a dedicated algorithm.

### Results

We have first calculated the MQW-SOA model parameters to fit on a monoelectrode SOA of length 1 mm. We present now the optimization results of mono (fig 1) and multielectrode (fig 2) cases, where the optimization criteria are the maximal gain fixed to 20 dB and the greatest possible optical bandwidth. In both cases, the current density in each electrode has been automatically adjusted to provide the best result for each electrode length configuration. Fig 1 presents the optimal bandwidth defined at -1 dB as a function of the SOA length (monoelectrode case). The optimal result shows a bandwidth of 73 nm for a SOA length slightly greater than 1.2 mm. Fig 2 shows the optimal bandwidth for the bielectrode case, as a function of the length of each electrode. The best configuration corresponds to a constant sum of the two electrode lengths still around 1.2 mm. The comparison between the two cases finally shows that the bielectrode case does not enhance significantly the optical bandwidth. It can though be used to improve the noise figure or saturation power as we will show.

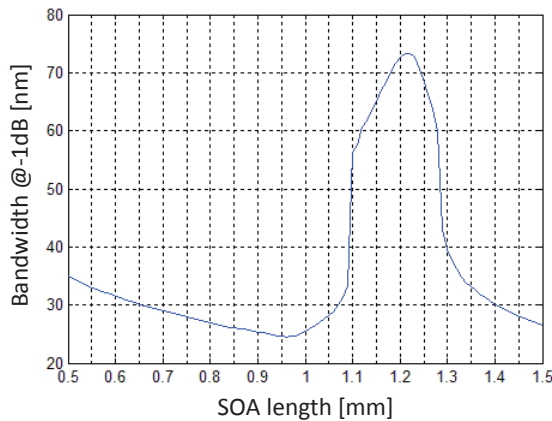


**Fig. 1.** Optical bandwidth as a function of monoelectrode SOA length.

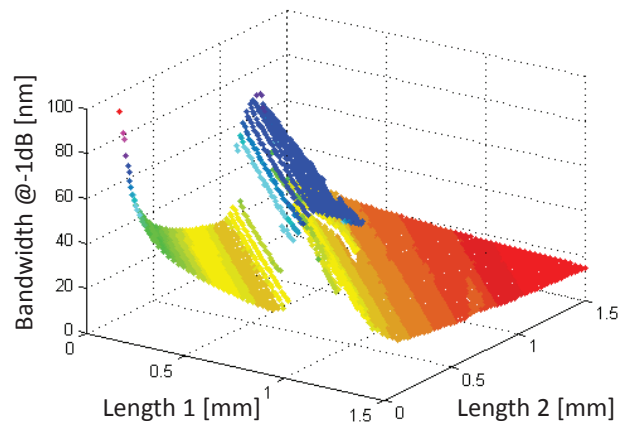


**Fig. 2.** Optical bandwidth as a function of bielectrode SOA lengths.

### References

- [1] T. Motaweh, P. Morel, A. Sharaiha, M. Guégan, *A Semi-Phenomenological Model for the Material Gain of Broadband MQW-SOAs*, NUSOD 2013, Vancouver, Canada, 2013

## Study of optical properties of textured Si solar cell with micro pillars

F. J. Cabrera-Espana, B. M. A. Rahman and A. Agrawal\*  
 School of Engineering and Mathematical Sciences, City University London  
 \*[Arti.agrawal.1@city.ac.uk](mailto:Arti.agrawal.1@city.ac.uk)

In this paper, we report the optical properties of a silicon (Si) solar cell when varying the parameters of a micro pillar array on the cell surface using the FDTD technique.

### Summary

Texturing techniques are important for trapping the incident light. There are various techniques available such as: placing nanowires [1], micro pillars ( $\mu$ Ps) [2], etc on the cell surface. In this study we consider, texturing Si  $\mu$ Ps on the surface of a Si solar cell, placed in hexagonal arrays. Reflectance (R) is obtained when varying the surface coverage (SC) between 20 and 80 % and pillar diameters between 1 and 3  $\mu$ m for constant pillar height.

### Results

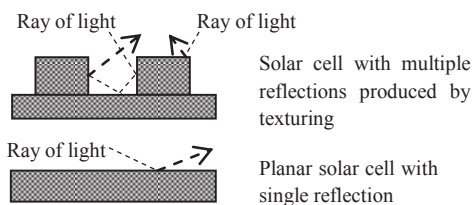


**Fig. 1** Multiple reflections and single reflection

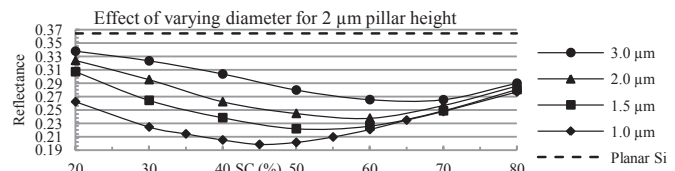


**Fig. 2** Effect on R varying diameter for different pillar height

The purpose of using  $\mu$ P arrays is to trap the light in the area between the pillars by multiple reflections (see Fig.1). Figure 2 shows R as a function of SC for different pillar diameters. If the area between the pillars is too large (i.e. low SC such as 20%), there are few multiple reflections due to the large distance between pillars. However, if the area is too low (i.e. high SC such as 80%), more light is reflected from the top of the  $\mu$ P and less multiple reflections take place. When there is a balance between light penetrating and the area between pillars (i.e. optimizing multiple reflections) the reflectance is minimum. For the studied SCs and diameters, 1  $\mu$ m diameter shows the lowest R, which is why more SC values are considered for this diameter. For any of the studied diameters, the R decreases when the pillar diameter decreases.

### Conclusion

The benefits of  $\mu$ P arrays cells over planar cells and the parametric influence on R are shown. The SC of the  $\mu$ P arrays is the parameter with largest impact on the optical R of the Si solar cell for any given diameter. The diameter also is to be taken into account because when it decreases, R decreases as well.

### References

- [1] E. Garnet and P. Yang (2010) *Light trapping in Silicon Nanowire Solar cell*, Nano letter, Vol. 10, 1082-1087.
- [2] J. Shin *et al.* (2012) *Experimental study of design parameters in Silicon Micropillar Array Solar Cells produced by Soft lithography and metal-assisted chemical etching*, IEEE Journal of photovoltaics, Vol. 2, No.2, 129.

## Perfectly Matched Layers in Negative Index Metamaterials

É. Bécache<sup>1</sup>, P. Joly<sup>1</sup>, V. Violes<sup>1</sup>,

<sup>1</sup> POEMS, UMR 7231 CNRS-INRIA-ENSTA ParisTech, Palaiseau, France  
valentin.violes@ensta-paristech.fr

We study the Perfectly Matched Layers (PMLs) in the framework of Negative Index Metamaterials. As expected, the standard PMLs are unstable due to the presence of backward waves. An asymptotic analysis allows us to understand this phenomenon and to propose new stable PMLs.

### Summary

The simulation of waves in unbounded domains requires methods to artificially truncate the computational domain, for instance the Perfectly Matched Layers (PMLs) which are effective and stable for non dispersive isotropic media. For non dispersive anisotropic media, a necessary stability condition was established in [1]: a PML is always unstable in presence of backward waves. We are interested here in Negative Index Metamaterials (NIMs) which are dispersive and show backward waves. So we sought to extend the stability result of [1] to very general dispersive models and to a larger class of PMLs. To simplify the presentation, we consider the 2D Maxwell's equations (TE mode) in time domain coupled with a simple model of NIMs: the Drude model. It is defined in the frequency domain by  $\varepsilon(\omega) = \varepsilon_\infty(1 - \omega_e^2/\omega^2)$  and  $\mu(\omega) = \mu_\infty(1 - \omega_m^2/\omega^2)$ . For this model, numerical simulations confirm the instabilities of the standard PMLs (cf Fig. 1). Those can be understood as complex changes of variable leading to the following modification of the spatial derivatives

$$\partial_x \longrightarrow \left(1 + \frac{\sigma_x(x)}{i\omega}\right)^{-1} \partial_x \quad \text{and} \quad \partial_y \longrightarrow \left(1 + \frac{\sigma_y(y)}{i\omega}\right)^{-1} \partial_y.$$

Inspired by previous works like [2], we propose more general changes of variable

$$\partial_x \longrightarrow \left(1 + \frac{\sigma_x(x)}{i\omega\psi(\omega)}\right)^{-1} \partial_x \quad \text{and} \quad \partial_y \longrightarrow \left(1 + \frac{\sigma_y(y)}{i\omega\psi(\omega)}\right)^{-1} \partial_y,$$

where  $\psi(\omega)$  is a function to be chosen judiciously. Using an asymptotic analysis, we have generalised the necessary stability condition for those new PMLs. This analysis allows us to understand the instabilities observed for standard PMLs in NIMs and to propose a choice of functions  $\psi(\omega)$  which takes into account the backward waves. Numerical simulations confirm the stabilization of the PMLs (cf Fig. 1). Our results can be easily generalized to a larger class of NIMs like the Lorentz model.

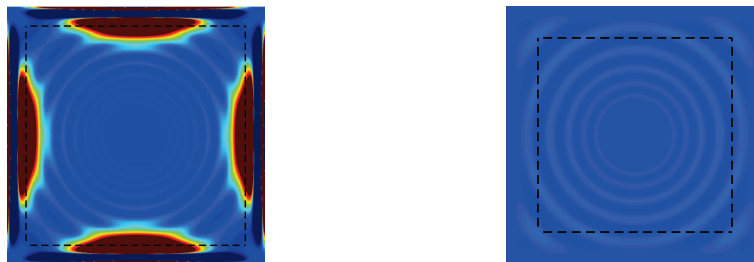


Fig. 1. Left : the standard PMLs are unstable. Right : the new PMLs are stable.

### References

- [1] É. Bécache, S. Fauqueux, P. Joly, *Stability of perfectly matched layers, group velocities and anisotropic waves*, Journal of Computational Physics, vol. 188-2, p. 399–433, 2003
- [2] S.A. Cummer, *Perfectly matched layer behavior in negative refractive index materials*, Antennas and Wireless Propagation Letters, IEEE, vol. 3(1), p. 172–175, 2004

## Dielectric tensor retrieval for gyrotropic 3D photonic crystals

A.A. Shcherbakov<sup>1,\*</sup>, A.V. Tishchenko<sup>2</sup>

<sup>1</sup>*Moscow Institute of Physics and Technology, Dolgorudnyi, Russia*

<sup>2</sup>*University Jean Monnet, University of Lyon, Saint-Etienne, France*

\*[alex.shcherbakov@phystech.edu](mailto:alex.shcherbakov@phystech.edu)

We propose a new method of complete dielectric tensor retrieval for gyrotropic 3D dielectric photonic crystals in the optical domain. The method is based on rigorous solution of the wave equation in a complex 3D periodic artificial media and subsequent calculation of effective medium parameters.

### Introduction

Artificial 3D periodic media with specific anisotropic properties are promising candidates for replacing natural materials in various optical applications. Recent progress in fabrication of such materials [1,2] establishes reliable experimental methods for complex 3D periodic media fabrication at micro and nanoscales. This progress needs to be supported by computational techniques which are able to predict and optimize artificial media optical properties. Currently there is a need in efficient methods capable to rigorously calculate effective dielectric tensor for 3D periodic material with complex period filling [3]. To fulfill this gap in this work we propose a new numerical method which is based on our previous results.

### Summary

New method of complete dielectric tensor retrieval for gyrotropic 3D dielectric photonic crystals in optical domain is based on the Generalized Source Method [4] applied in the 3D Fourier space [5]. An approach proposed in [5] allows calculating amplitudes of the Fourier harmonics in an arbitrary dielectric 3D periodic structure in linear time with respect to the problem geometry complexity for a given exciting external plane wave. Thus, by calculating complex poles of the amplitude response relative to the incident wave wavenumber we obtain mode propagation constants in a given propagation direction. Analysis of modal amplitudes provides us with directions of the principal axes of the dielectric tensor. Separation of the symmetric and antisymmetric parts of the dielectric tensor in a given coordinate frame allows distinguishing the gyration part, and further rotation of the tensor to the principal axes gives all the components of the effective gyration vector.

### References

- [1] S. Takahashi, et. al, *Direct creation of three-dimensional photonic crystals by a top-down approach*, Nat. Mater., **8**, 721-725, 2009
- [2] M.D. Turner, et. al. *Miniature chiral beamsplitter based on gyroid photonic crystals*, Nat. Photonics, **7**, 801-805, 2013
- [3] J.A. Reyes-Avendano, et. al., *From photonic crystals to metamaterials: the bianisotropic response*, New J. Phys. **13**, 073041, 2011
- [4] A.V. Tishchenko, *Generalized source method: new possibilities for waveguide and grating problems*, Opt. Quantum Electron., **32**, 1971-1980, 2000
- [5] A.A. Shcherbakov, A.V. Tishchenko. *Fast modeling of electromagnetic scattering in 3D Fourier space*, ELS'XIV Conference, Lille, France, June 17 –21, 2013

## Plasmon resonances on metal sphere aggregates in a dielectric matrix

S. Bakhti, N. Destouches, A.V. Tishchenko\*

University Jean Monnet, University of Lyon, Saint-Etienne, France

\*[Alexandre.Tishchenko@univ-st-etienne.fr](mailto:Alexandre.Tishchenko@univ-st-etienne.fr)

We study properties of collective plasmon resonances on groups of metal spheres. The method is based on rigorous solution of electromagnetic scattering problem combined with an accurate pole finding algorithm to retrieve precisely resonance characteristics and modal near fields.

### Introduction

The electromagnetic excitation of metal particles induces a resonant collective oscillation of the conduction electrons, resulting in a local increase of the electromagnetic near field. These resonances, called localized surface plasmon resonance (LSPRs) appear in the visible spectrum and depend on the size, shape and nature of the metal and the host material [1]. This unique property is widely used in many application areas such as SERS, bio-sensing, biomedicine and nano-photonics. The modeling of the optical properties of the nanoparticles is rigorously determined using electromagnetic theory by developing solution in terms of spherical harmonics. The Extended Boundary Condition Method (EBCM) or Null-Field Method (NFM) is based on surface integrals in spherical coordinates and the electromagnetic response of a particle is formulated in form of T-Matrix [2].

### Summary

We apply the method developed in the earlier study of resonances on single metal particles [3] to extract numerically the characteristics of different plasmon modes of silver nanoparticle assemblies directly from the scattering parameters (cross sections and optical near-field) calculated using EBCM. This gives precisely the position and width of the resonance and the near field for each excited plasmon mode (Fig. 1). Finally, we introduce a general phenomenological approach to describe plasmon resonances.

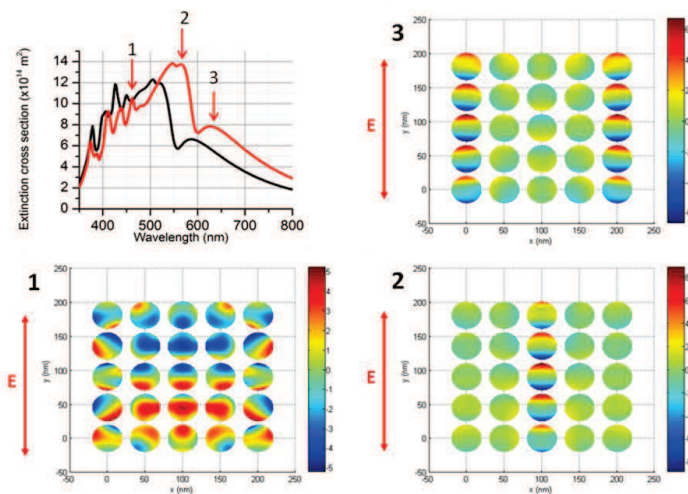


Fig. 1. Extinction cross section of a set of 25 Ag spheres and the near field intensity in three different plasmon modes.

### References

- [1] Kelly K.L, et al. *The optical properties of metal nanoparticles: the influence of size, shape and dielectric environment*, J. Phys. Chem. B **107**, 668-677, 2203
- [2] Mishchenko M.I., et al. *T-matrix computations of light scattering by nonspherical particles: A review*. J. Quant. Spectr. Rad. Tr., **55**, 535-575, 1996
- [3] Benghorieb S., et al. *Extraction of the 3D plasmon field*. Plasmonics, **6**, 445-455, 2011

## Explanation of ultra narrow-band reflection from a 1d grating based on a modal method and symmetry considerations

T. Kämpfe<sup>1,\*</sup>, A.V. Tishchenko<sup>1</sup>, O. Parriaux<sup>1</sup>

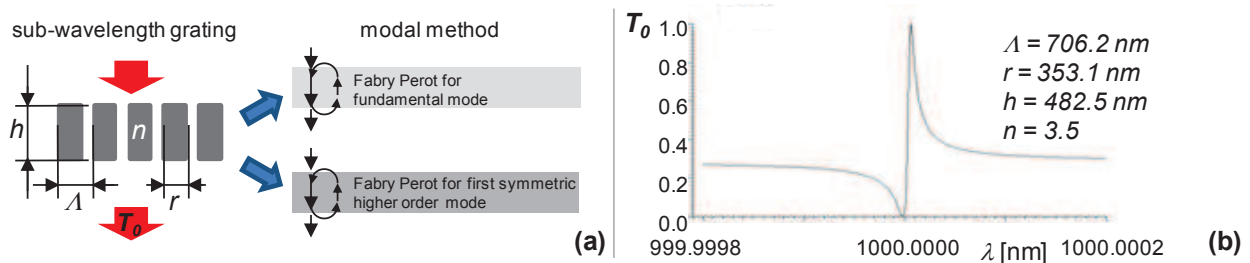
<sup>1</sup> University of Lyon, Lab. H. Curien UMR CNRS 5516, F-42000 Saint-Etienne

\*[thomas.kampfe@univ-st-etienne.fr](mailto:thomas.kampfe@univ-st-etienne.fr)

A 1D, high index contrast subwavelength binary corrugation can exhibit arbitrarily narrow reflection resonances. The necessary parameters are given analytically using the interference of the two involved grating modes and symmetry considerations of their reflection and transmission coefficients.

### Introduction

A 1D, high index contrast subwavelength binary grating exhibits under normal incidence narrow reflection peaks characterized by a huge field accumulation in the high index corrugation [1]. The analysis in [2] attributes the resonance sharpness to the resonance of a super-mode, which is a particular combination of the two involved eigenmodes of the grating. Based on this idea, the present contribution will explain why those resonances can be infinitely narrow.



(a): Considered grating with parameter definition, (b): example of an extremely narrowband resonance

### Summary

The occurrence of the narrowband resonances can be understood by considering the first two vertically propagating modes, created by the periodic refractive index variation of the grating (Fig. 1(a)). The resonances can be identified by the number of roundtrips  $m_0$  and  $m_2$  in the corresponding Fabry Perot resonators [3]. The interaction between the modes and their transmission to the outside can be described by transmission and reflection coefficients at the substrate-grating and grating-cover interface, while their propagation simply corresponds to a phaseshift. By using energy conservation at the interfaces and certain symmetry considerations, the ideal zero-width fano-type resonance is found if the following grating heights  $h_{res,0}$  and  $h_{res,1}$  are equal :

$$h_{res,0} = \left( m_0 \pi + \arg \left( \frac{t_{c2}}{t_{c0}r_{02} - t_{c2}r_{00}} \right) \right) / 2\pi n_{eff,0} \quad h_{res,2} = \left( m_2 \pi + \arg \left( \frac{t_{c0}}{t_{c2}r_{02} - t_{c0}r_{22}} \right) \right) / 2\pi n_{eff,2}$$

( $t_{cx}$  – transmission coeff. of mode  $x$  to cover and substrate;  $r_{xy}$  – reflection coeff. from mode  $x$  to  $y$ ;  $n_{eff,x}$  – effective index of mode  $x$ ). As will be shown in the presentation the equality of those two heights is systematically fulfilled for the considered grating structure, which explains the inevitable occurrence of ultra-narrowband resonances and allows the determination of their parameters in an exhaustive, analytic fashion.

### References

- [1] E. Bonnet et al., Opt. Quant. Electr., vol. 35, pp. 1025-1036 (2003)
- [2] C. Hasnain et al., Adv. in Opt. and Phot., vol. 4, pp. 379 -439 (2012)
- [3] O. Parriaux et al., Opt. Express, Vol. 20, pp. 28070-28081 (2012)

## Analytical Model for the Field of Microstructured Optical Fibers: Evaluation and Enhancement

Dinesh Kumar Sharma<sup>\*</sup>, Anurag Sharma

*Physics Department, Indian Institute of Technology Delhi, New Delhi-110016, India*

*\*dk81.dineshkumar@gmail.com, asharma@physics.iitd.ac.in*

We present an improved version of our earlier developed analytical field model for achieving better accuracy in the simulated results, by extending number of air-holes rings in the microstructured optical fiber (MOF) cross-section and by adding an additional shifted Gaussian term in the modal field.

### Introduction

We have earlier developed an analytical field model [1] for the fundamental mode of index-guiding MOFs, based on considering three rings (3-Rings) in the fiber structure and one ring of lobes in the modal field, to study the modal properties of MOFs. Here, we proposed the modified form of the model and show that the accuracy of the model is significantly improved particularly for those cases where the field extends deeper into the cladding region.

### Summary

Our field model gives appreciably good results which match well with experimental and simulation results, but the accuracy deteriorates for smaller values of pitch or smaller air-filling fraction ratios as the field spreads more into the holey cladding [2,3]. In such cases the model which has only one ring of side lobes is not adequate; one must include more rings of side lobes in the modal field. We have therefore extended our model by including more layers of air-holes in the model to bring the model closer to the real fibers. We thus consider five rings (5-Rings) around the central missing hole in the MOF geometry and two rings of lobes in the modal field to account the spreading of field, which is given by the following expression:

$$\Psi(r, \varphi) = \exp(-\alpha r^2) - A \exp(-\alpha_1 (r - \sigma \Lambda)^2) (1 + \cos 6\varphi) - B \exp(-\alpha_2 (r - \eta \Lambda \sqrt{3})^2) (1 - \cos 6\varphi)$$

where  $A, \alpha, \alpha_1, \sigma, B, \alpha_2$  and  $\eta$  are the field parameters;  $\Lambda$  is the separation between the two adjacent air-holes. We use the variational techniques to obtain the optimized values of these parameters and the propagation constant of the fundamental mode for a given wavelength.

### Results and Conclusion

Using the enhanced form of the analytical field model we computed the splice losses between a standard fiber such as, SMF-28 having core diameter of  $8.3 \mu\text{m}$  and core and cladding refractive indices of 1.5362 and 1.5306, respectively and an MOF (see Fig.1). For comparison, we have included the results obtained using full-vector FEM [3]. The results are in better agreement compared to our earlier 3-ring model, reflecting the validity of enhancement in the model. Further work is in progress.

### References

- [1] A. Sharma and H. Chauhan, *Opt. Quantum Electron.*, **41**, 235 (2009).
- [2] D.K. Sharma and A. Sharma, *Opt. Quantum Electron.*, **44**, 451 (2012); also *OWTNM 2013*.
- [3] Hoo *et al.*, *Microw. Opt. Technol. Lett.*, **40**, 378 (2004).

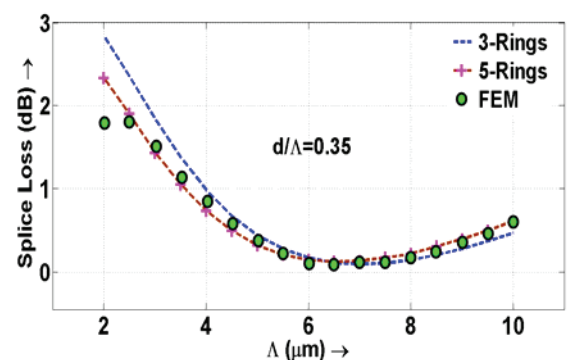


Fig.1. Splice loss as a function of pitch.

## Approximate Method for Modal Analysis of Nanoscale Surface Plasmon-Polariton Waveguides

K. Gehlot<sup>1,2</sup>, A. Sharma<sup>1</sup>,

<sup>1</sup> Indian Institute of Technology Delhi, New Delhi, India

<sup>2</sup> University of Rajasthan, Jaipur, India

<sup>1</sup>gehlot.kanchan@gmail.com, <sup>2</sup>asharma@physics.iitd.ac.in

We present an efficient approximate analysis for surface plasmon-polariton (SPP) waveguides using semi-vector optimal variational method. An example of dielectric loaded SPP waveguide is presented in detail. Results of the present analysis show good agreement with rigorous numerical results.

### Introduction

For an SPP waveguide, the effective index method (EIM) provides simple and approximate modal analysis. However, the EIM does not work well for the modes close to the cut-off and also in [1] it has been shown that the EIM can be implemented in two ways, named as EIM-1 and EIM-2 and both the analysis give different results. To avoid this ambiguity and obtain better results, we propose to use the semi-vector optimal variational method (SV-VOPT) [2] for the modal analysis of SPP waveguides.

### Results and Discussion

In the semi-vector analysis of the SV-VOPT method, the modal field is assumed to be separable in two orthogonal directions. In this paper, we present the SV-VOPT analysis for a dielectric loaded SPP (DLSP) waveguide. In the DLSP waveguide a polymer ridge is placed on a gold film to reduce the waveguide mode size in lateral cross-section. In Fig 1, the variation of mode effective index,  $n_{eff} = \text{Re}(\beta/k)$  and propagation length,  $L = 1/2\text{Im}(\beta)$ , with polymer ridge thickness  $t$ , are shown. The schematic of the DLSP waveguide is shown in the inset. This method gives accurate results even for the modes close to the cut-off and, unlike EIM, converges to the same results if started with different initial approximations.

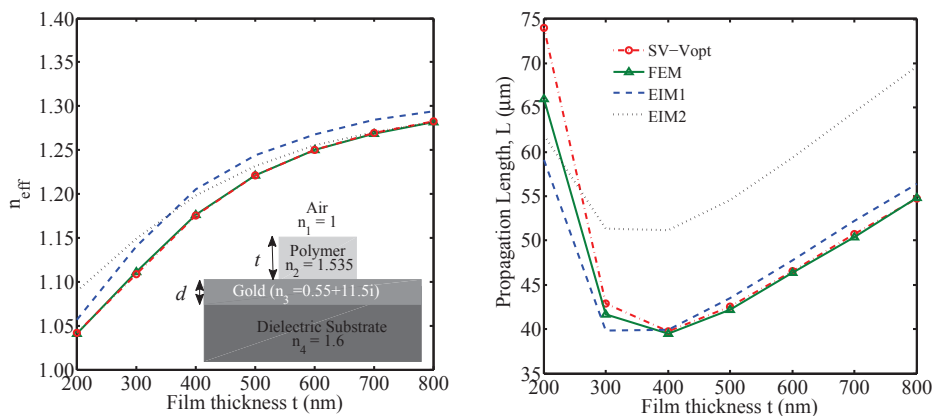


Fig. 1. Variation of  $n_{eff}$  and  $L$  with polymer ridge thickness  $t$ .

### References

- [1] T. Holmgaard, S. I. Bozhevolnyi, *Phys. Rev. B* **75**, 245405 (2007).
- [2] K. Gehlot, A. Sharma, *Opt. Express* **21**, 9807-9812 (2013)

## Characteristics of Dual-Core Hybrid Plasmonic Liquid Crystal Photonic Crystal Fiber

B. M. Younis<sup>1,2</sup>, A. M. Heikal<sup>1,3</sup>, Mohamed Farhat O. Hameed<sup>1,3</sup>, Maher Abdelrazak<sup>2</sup>,  
S. S. A. Obayya<sup>1\*</sup>

<sup>1</sup>Centre for Photonics and Smart Materials, Zewail City of Science and Technology, Sheikh Zayed District, 6th of October City, Giza, Egypt. \*sobayya@zewailcity.edu.eg

<sup>2</sup>Electronics and Communications Engineering Department, Faculty of Engineering, Mansoura University, Mansoura, Egypt

<sup>3</sup>Mathematics and Engineering Physics Department, Faculty of Engineering, Mansoura University, Mansoura, Egypt

In this paper, a novel design of dual-core hybrid plasmonic liquid crystal photonic crystal fiber (HPLC-PCF) is reported and analyzed using full vectorial finite element method (FVFEM). The HPLC-PCF has a metal wire between the two cores. In addition, two large holes in the two cores are infiltrated by nematic liquid crystal (NLC) of type E7. The effects of the structure geometrical parameters, temperature and rotation angle of the direction of the NLC on the modal characteristics of the proposed design is investigated in detail. The analyzed parameters are effective index, attenuation, and coupling coefficient. It is evident from the simulation results that the HPLC-PCF has high tunability with temperature and external electric field due to the infiltration with the NLC.

### Design Considerations

Figure 1 shows the proposed HPLC-PCF. The suggested PCF has a soft glass of type FK51A as a background material and the cladding air holes of diameter  $d_1$  are arranged in hexagonal shape. In addition, a Gold metal wire of diameter  $d_c$  is inserted between the two cores. Moreover, two large holes of diameter  $d_2$  infiltrated by NLC are inserted in the two cores. The Sellmeier equation for the NLC can be obtained from [1], and the Drude model for the Gold is taken from [2]. The Sellmeier equation of FK51A can be obtained from [3]. The modal characteristics of the suggested design will be introduced in the conference.

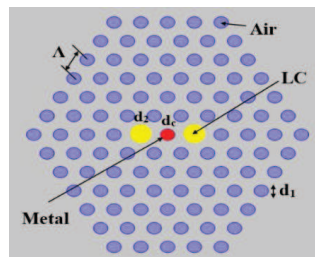


Fig.1 Cross section of the HPLC-PCF

### References:

- [1] M. F. O. Hameed, S. S. A. Obayya "Polarization Splitter Based on Soft Glass Nematic Liquid Crystal Photonic Crystal Fiber" *IEEE photonics J.* vol. 1, no. 6/2009.
- [2] Alireza Hassani and Maksim Skorobogatyi, "Design criteria for microstructured-optical-fiber based surface-plasmon-resonance sensors" *Vol. 24, No. 6/June 2007/J. Opt. Soc. Am. B.*
- [3] Sanjib Das, Anindya Jyoti Dutta, Nurmohammed Patwary, M. Shah Alam, "Characteristic Analysis of Polarization and Dispersion Properties of PANDA Fiber Using Finite Element Methods", *The AUST Journal of Science and Technology, Vol. 3, No. 2/Jan 2013.*

## Polarization Characteristics of Elliptical Spiral Plasmonic Photonic Crystal Fiber

F.Faeq K. Hussain<sup>1,2</sup>, A. M. Heikal<sup>3,4</sup>, Mohamed Farhat O. Hameed<sup>3,4</sup>, J. El-Azab<sup>1</sup>, W. S. Abdelaziz<sup>1</sup>, S. S. A. Obayya<sup>3\*</sup>

<sup>1</sup>National Institute of Laser Enhanced Sciences, Cairo University, Egypt

<sup>2</sup>Physics Department, Faculty of Science, Al-Muthana University, Iraq.

<sup>3</sup>Centre for Photonics and Smart Materials, Zewail City of Science and Technology, Sheikh Zayed District, 6th of October City, Giza, Egypt,  
\*sobayya@zewailcity.edu.eg

<sup>4</sup>Mathematics and Engineering Physics Department, Faculty of Engineering, Mansoura University, Egypt

In this paper, a novel design of elliptical spiral plasmonic photonic crystal fiber (ESP-PCF) is reported and analyzed. The suggested design has a gold metal wire in the cladding region. The polarization characteristics of the proposed design are studied using full vectorial finite element method (FVFEM). The effects of the structure geometrical parameters on the polarization characteristics of the ESP-PCF are investigated in detail. In addition, the coupling properties between x-polarized and y-polarized core modes are reported.

### Design and Simulated Results

Figure 1 (a) shows the proposed structure with an elliptical core region. The ESP-PCF has eight spiral arms. Each arm consists of four circular air holes with diameter  $d_h$ . The center of the next hole in each arm is located at the normal distance  $d_r$  to the line between the centers of two neighboring holes in the previous ring as shown in fig. 1(a). The ESP-PCF has a single gold wire in the first ring close to the core region. Figure 1 (b) and (c) show the dispersion property and attenuation of the horizontally polarized and vertically polarized modes, respectively. The simulated results show that the vertically polarized and horizontally polarized core modes are separated in certain wavelength values which can be used in pass-band and stop-band filter applications. More results will be presented in the conference.

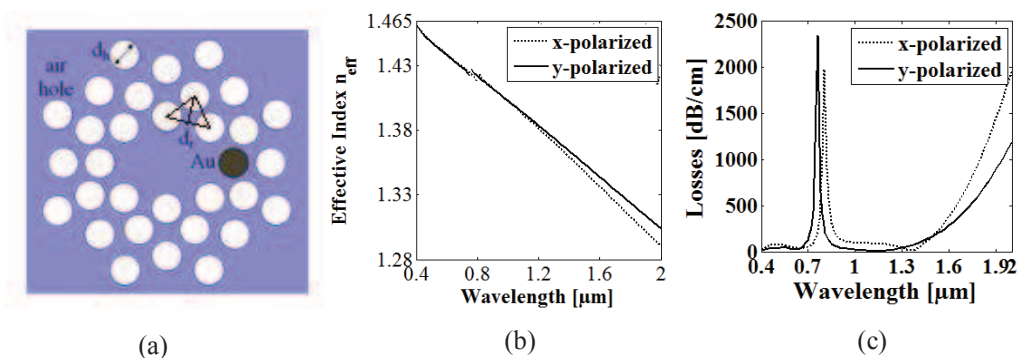


**Fig. 1** (a) Schematic diagram of the proposed structure, wavelength dependence of (b) effective index and (c) losses of the x-polarized and y-polarized core modes filled with gold wire into the air hole layer.

## Blocked Schur for Noniterative Bidirectional Beam Propagation Method

Afaf M. A. Saeed S. S. A. Obayya

Center for Photonics and Smart Materials, Zewail City of Science and Technology, Giza, Egypt  
sobayya@zewailcity.edu.eg

A new finite-element bidirectional beam propagation method (FE-BiBPM) is presented for multiple longitudinal optical waveguide discontinuities. The proposed method is relying on the Blocked Schur (BS) algorithm [1] to compute the square root of the characteristic matrices at the discontinuity section for the noniterative BiBPM based on the scattering operators [2]. As will be demonstrated latter, the proposed BS-FE-BiBPM is very accurate, versatile, efficient, fast and stable. Moreover, our newly proposed BS-FE-BiBPM provides more accurate physically treatment of evanescent waves than other BiBPMs.

### Summary

Using Schur decomposition which introduces a triangular matrix with a diagonal of the eigenvalues of the characteristic matrix is more accurate while dealing with the evanescent modes in optical waveguides. Furthermore, the ability of Schur algorithm to compute any desired square root for general matrices leads to avoid any associated errors depending on the choice of the reference index in other BiBPMs. However, the Schur method suffers from taking long execution time. Alternatively, we use the Blocked Schur (BS) algorithm [1] which was found to be up to 6 times faster than Schur method. Therefore, our newly proposed BS-FE-BiBPM will be faster than other BiBPMs when higher-orders of rational approximations are a must to deal correctly with strongly reflecting optical structures.

To ensure the accuracy and stability of the proposed BS-FE-BiBPM, a distributed-feedback structure (DFB) [3] of Fig. 1(a) is simulated. For the excited TE mode, Fig. 1(b) shows the reflectivity of the DFB structure compared with those obtained through coupled wave theory [3] and the rotated padé primes of order [5/5] [3]. Our results are closer to the results of the coupled wave theory, while the iterative method of padé approximation produced a slight shift. Moreover, for the actual total power, our approach is more accurate and stable than those obtained by padé order of [1,1] or [5/5] as shown in Fig. 1(c).

### References

- [1] Edwin Deadman, NicholasJ. Higham, and Rui Ralha. Blocked schur algorithms for computing the matrix square root. 7782:171–182, 2013.
- [2] Pui Lin Ho and Ya Yan Lu. A stable bidirectional propagation method based on scattering operators. *Photonics Technology Letters, IEEE*, 13(12):1316–1318, 2001.
- [3] H. El-Refaei, D. Yevick, and Ian Betty. Stable and noniterative bidirectional beam propagation method. *Photonics Technology Letters, IEEE*, 12(4):389–391, 2000.

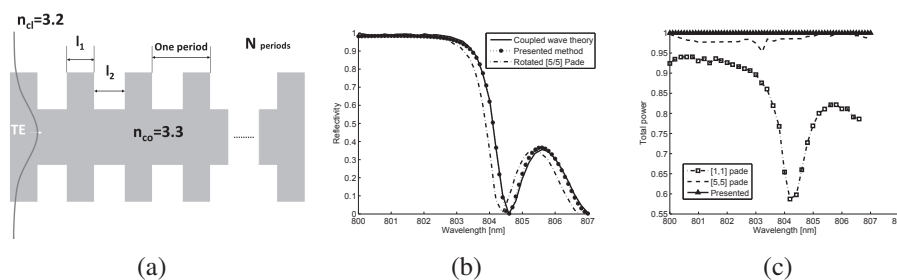


Fig. 1. DFB structure; (a) Configuration of the structure; (b) Reflectivity for the DFB structure with 256 periods; and (c) Normalized total power.

## Compact TM-Pass Polarizer Based on Silicon-on-Insulator Photonic Wire

Shaimaa I. H. Azzam<sup>1,2</sup>, S.S.A.Obayya<sup>1\*</sup>

<sup>1</sup>Centre for Photonics and Smart Materials, Zewail City of Science and Technology, Sheikh Zayed District, 6<sup>th</sup> of October City, Giza, Egypt. \*[sobayya@zewailcity.edu.eg](mailto:sobayya@zewailcity.edu.eg)  
<sup>2</sup> Faculty of Engineering, Mansoura University, Mansoura, Egypt

A TM-pass polarizer based on silicon-on-insulator (SOI) photonic wire is introduced and analyzed. The proposed polarizer structure is very simple relying on the deposition of a layer of a high refractive index material into the silica substrate. The polarizer is relatively short with device length of only 0.5 mm. The analysis indicated an extinction ratio (ER) of 20 dB for the TE polarization state and an insertion loss (IL) of 0.2 dB for TM state. Fabrication of the introduced polarizer is compatible with standard CMOS fabrication process.

### Design and simulation results

An optical polarizer is an integral part of modern silicon-based circuits to prohibit the propagation of one of the two supported polarization states. Allowing only one polarization state through the photonic circuits, the problem of polarization dependence in silicon photonic circuits can be minimized. Various structures for transverse electric (TE) and transverse magnetic (TM) polarizers have been introduced. In this work we propose a TM-pass polarizer based on SOI photonic wire. The proposed polarizer structure is very simple relying on the deposition of layer of a high refractive index material, namely silicon, into the silica substrate. The optimization of the thickness of this layer and its position relative to the silicon core can achieve an effective coupling between the TE-like fundamental mode and this high-index layer. The TM-like mode can still be propagated with minimal losses.

The SOI photonic wire has both width and height fixed at 400 nm. Silicon and silica refractive indices are taken as 3.45 and 1.45, respectively at the operating wavelength 1.55 μm while the cladding is air. The thickness and the position of the deposited silicon layer are varied to obtain the point at which the TM-like mode has low losses while the TE-like mode suffers maximum losses. The optimized performance is achieved at silicon layer thickness of 250 nm at 250 nm from the silicon core. The calculated ER and IL of the polarizer are 20 dB and 0.2 dB, respectively, at a relatively short device length of 0.5 mm. The proposed TM-pass polarizer is CMOS-compatible which makes it a simple candidate for photonic circuits.

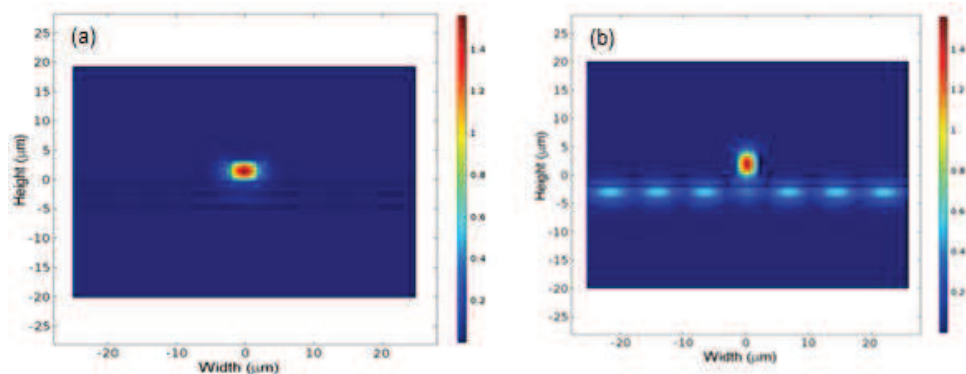


Figure 1 Major magnetic field distributions for (a) the TM-like mode ( $H_x$ ) and (b) the TE-like mode ( $H_y$ ) showing the high leakage of the TE-like mode due to coupling with the silicon layer in the substrate.

### 3D-active beam propagation method to simulate QD-polymer waveguides

I. Suárez and J.P. Martínez-Pastor

UMDO, Instituto de Ciencia de los Materiales, Universidad de Valencia, 46071  
Valencia, Spain

[isaac.suarez@uv.es](mailto:isaac.suarez@uv.es)

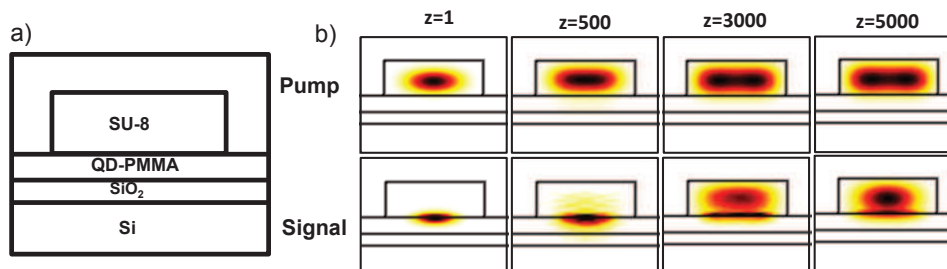
In this work different active waveguides based on the incorporation of colloidal quantum dots (QDs) in polymers are analyzed. For this purpose a model to simulate the absorption/emission of light by QDs is incorporated in an active beam propagation method (BPM) to study and optimize the photonic structures.

#### Introduction

The incorporation of colloidal quantum dots (QDs) in polymers has a great interest nowadays because the resulting nanocomposite joins the interesting properties of the nanoparticles (room temperature emission and tuning of absorption/emission wavelength with QD size and base material) with the technological feasibility of polymers. In this way we demonstrated the implementation of active planar and bidimensional waveguides by embedding the nanostructures in PMMA [1] or SU-8 [2]. Moreover, the waveguides can be improved by including passive polymer claddings in the waveguides in order to collect radiated photoluminescence and to propagate the light through longer distances [3]. For this purpose it is useful to simulate the generation and propagation of signal together with the propagation of the pump beam to optimize the structures. In this work a model to take account of the excitonic photogeneration and spontaneous emission in the QDs is incorporated in a 3D-BPM to optimize the geometrical parameters of the photonic structures. Finally, waveguides are fabricated and characterized corroborating our modeling.

#### Summary of results

Different types of waveguides based on CdSe (emission at 600 nm) in PMMA are analyzed using an active 3D-active BPM. On the basis of this modeling, fabrication and testing of different QD-PMMA waveguides were carried out for comparison theory-experiment purposes. For example the figure shows power cross section of the pump and the signal beams in a bilayer structure composed by SU-8 ridge waveguides on a QD-PMMA layer deposited on a SiO<sub>2</sub>/Si substrate (Fig. a). The pump is coupled in the ridge exciting the signal in the nanocomposite. At long propagation lengths (z) signal is evanescently coupled to the patterns (Fig. b) [3].



#### References

- [1] I. Suárez, H. Gordillo, R. Abargues, S. Albert, and J. Martínez-Pastor, *Nanotechnology*, 22, 435202 (2011).
- [2] H. Gordillo, I. Suárez, R. Abargues, P.J. Rodríguez-Cantó, S. Albert, and J.P. Martínez-Pastor, *J. Nanomater.*, 2012, 960201 (2012).
- [3] H. Gordillo, I. Suarez, R. Abargues, P.J. Rodríguez-Cantó, G. Almuneau and J.P. Martínez-Pastor, *J. Lightwave Technol*, 31, 2515-2525 (2013).

## Spectral Model of Non-linear Phenomena in a Power-Over-Fiber System

L. Ghisa<sup>1,\*</sup>, F. Audo<sup>1</sup>, H. Prod'homme<sup>1</sup>, A. Perennou<sup>1</sup>, V. Quintard<sup>1</sup>, M. Guegan<sup>1</sup>

<sup>1</sup>Ecole Nationale d'Ingénieurs de Brest (ENIB), UMR CNRS 6285 Lab-STICC, Université européenne de Bretagne, Technopôle Brest-Iroise, C.S. 73862, F-29238 Brest cedex 3, France

\*laura.telescu@enib.fr

We developed a spectral model of the non-linear optical phenomena occurring in a Power-Over-Fiber system in the case of a simultaneous transmission of data in a 10 km long single mode optical fiber. The comparison of the obtained results with the experimental ones confirms the accuracy of the implemented model.

### Context

For the extension of submarine cabled observatories, we recently built and validated a prototype using only one single mode optical fiber to transport both the energy to supply a remote instrument and the data. This Power-Over-Fiber system allows a bidirectional real time communication between the 10 km distant instrument and its base station [1]. The simultaneous propagation on the same physical link of the power supply and the data signals may induce some non-linear phenomena due to the high power values usually involved. The objective of this kind of system is of course to provide maximum of energy to the instrument without degrading the data quality. In this context, in order to find the best values for the prototype parameters (power, wavelength, physical and technological characteristics of the fiber link) to optimize power supply and data transmission, we developed a spectral model of the non-linear optical phenomena occurring in such a link.

### Simulation principle and results

The model takes into account some optical phenomena such as Raman scattering, Brillouin scattering, propagation attenuation and Rayleigh scattering over the entire spectral band of interest

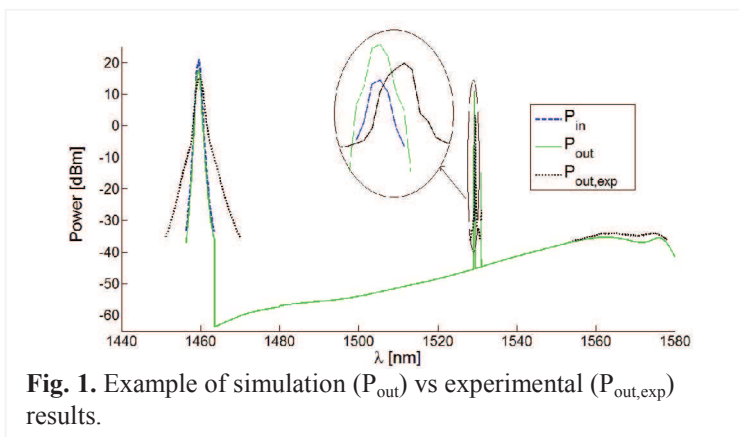


**Fig. 1.** Example of simulation ( $P_{out}$ ) vs experimental ( $P_{out,exp}$ ) results.

and can be used with a multi-wavelength pumping system and with co- and contra- directional optical data inputs. To compute the propagation evolution of the optical waves, the fiber is split in an optimal number of segments. An iterative method is used to study the energy exchanges between the different optical waves in the case of bidirectional propagation. We choose only one direction for the optical power transmission and one data wavelength to be co-directional (down-stream data)

with the optical pump and the other one to be contra-directional (up-stream data). Figure 1 presents an example of comparison between the simulation and experimental results obtained for an input pump power of 2 W at 1480 nm, a down-stream data at 1549 nm (dashed blue line for the both) and an up-stream data at 1551 nm (not displayed on the figure). There is a good agreement between simulation results (solid green line) and the experimental ones (dashed black line). Future work will be devoted to use this model to determine the optimum choice of wavelengths for the data before an in-situ implementation of our Power-Over-Fiber system prototype.

### Reference

- [1] F. Audo et al, *Raman amplification in an optically high-powered data link dedicated to a 10 km long extension for submarine cabled observatories*, J. Opt., Vol. 15, pp. 55703, April 2013.

## Analysis of Surface Plasmon Polariton Modes on a Metal Thin Film Covered with Uniaxially Anisotropic Material

Hsuan-Hao Liu<sup>1</sup> and Hung-chun Chang<sup>2,\*</sup>

<sup>1</sup>Graduate Institute of Photonics and Optoelectronics, National Taiwan University, Taipei, Taiwan 10617, R.O.C.

<sup>2</sup>Department of Electrical Engineering, Graduate Institute of Photonics and Optoelectronics, and Graduate Institute of Communication Engineering, National Taiwan University, Taipei, Taiwan 10617, R.O.C.

\*[hungchun@ntu.edu.tw](mailto:hungchun@ntu.edu.tw)

Surface plasmon polariton modes which can exist on a metal thin film covered with half-space uniaxially anisotropic material and having isotropic substrate are analyzed using an eigenmode solver based on the finite element method. Possible leaky modes are carefully determined and discussed.

### Introduction

Although the surface plasmon polariton (SPP) wave existing at an interface between metal and isotropic dielectric material has been well known, the related phenomenon when the dielectric becomes anisotropic is relatively less investigated. We have recently analyzed SPPs at an interface between metal and a uniaxially anisotropic dielectric material and obtained possible leaky-mode solutions in addition to the pure guided modes [1]. When the optic axis of the uniaxial dielectric is rotated in the plane of the interface, analytical characteristic equations can be derived. In [1], we demonstrated that complex modal effective indices obtained using the finite-element-method (FEM) eigenmode solver we developed agree excellently with the analytical solutions. This FE solver was formulated using three electric-field (or magnetic-field) components and incorporated with suitable perfectly matched layers (PMLs) for solving planar structures involving anisotropic materials with arbitrary permittivity tensor. In this paper, we extend our SPP-mode study to two-interface structures such as a metal thin film with cover and substrate materials. The cover region is made of uniaxially anisotropic dielectric material, such as 5CB liquid crystal [2]. Such structure can have applications in designing tunable SPP devices.

### Results

Fig. 1(a) shows the two-planar-interface structure and coordinate systems for one numerical example. The  $x = d$  and  $x = -d$  planes are the upper and lower interfaces, respectively, of the silver thin film with thickness  $2d$ . The  $x > d$  region is made of 5CB liquid crystal material and the  $x < d$  substrate region is silica. The SPP modes propagate along the  $z$ -direction. The operating wavelength is taken to be  $\lambda = 0.644 \mu\text{m}$  and  $2d = 80 \text{ nm}$ . The FEM solver obtained  $\text{Re}[n_{\text{eff}}]$  and modal loss in  $\text{dB}/\mu\text{m}$  versus  $\theta$  curves for  $\phi = 90^\circ$  are shown in Fig. 1(b), where  $n_{\text{eff}}$  is the effective index, or the modal index. The red dashed curve in Fig. 1(b) is a cutoff line determined by the uniaxial material. That part of the  $\text{Re}[n_{\text{eff}}]$  curve below the cutoff line ( $\theta > \sim 64^\circ$ ) corresponds to a leaky SPP mode.

### References

- [1] H.-H. Liu and H.-C. Chang, *IEEE Photon. J.*, vol.5, 4800806, Dec. 2013.
- [2] P. Yeh and C. Gu, *Optics of Liquid Crystal Displays*, Wiley, New York, NY, USA, 1999, p. 61.

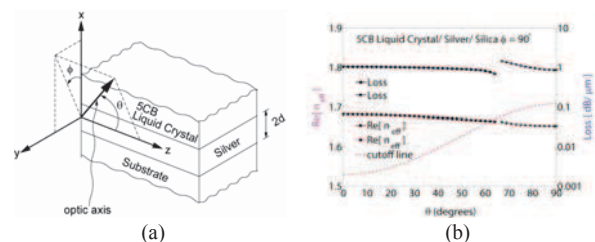


**Fig. 1.** (a) Schematic of the two-planar-interface structure. (b) FEM calculated  $\text{Re}[n_{\text{eff}}]$  and modal-loss results for SPP modes versus the rotated angle of the optic axis.

## Design and Analysis of a Coupled Strip-Slot Waveguide Structure for Dispersion Compensation

Nandam Ashok, Vipul Rastogi\* and Vidhi Mann

<sup>1</sup>Indian Institute of Technology Roorkee, Roorkee, 247667, India

\*vipul.rastogi@osamember.org

We have carried out the analysis of a coupled strip-slot waveguide using finite difference time domain method. Resonance between the slab and slot modes results in a high negative dispersion of  $-4.8 \times 10^5$  ps/(km-nm) over an FWHM bandwidth of 13 nm at 1538-nm centre wavelength.

### Introduction

Silicon based photonic devices have attracted considerable interest in integrated optics technology. Recently slot optical waveguides have received significant interest in silicon photonics because of their capability of confinement and guiding of light in a low index slot region. Slot waveguides are attractive for several on-chip applications including bio-sensor, polarization rotator, giant birefringence, and dispersion engineering [1]. Zhang, et al. have proposed a dispersive slot waveguide structure and showed a dispersion of  $-1.8 \times 10^5$  ps/(km-nm) [2]. In this paper we propose a coupled strip-slot configuration that shows 2.5 times larger dispersion. The study would be useful in designing a compact integrated receiver-based dispersion compensator to compensate the residual dispersion in a fiber link on a per-channel basis.

### Numerical Results

The proposed slot waveguide structure in silicon on silica (SOI) material system is shown in Fig. 1. The slot mode of the structure resonantly couples to the strip mode at 1538 nm wavelength. This results in a high negative dispersion for the symmetric supermode of the structure. The total dispersion coefficient of the structure has been calculated by finite difference time domain method for strip width  $d = 258$  nm slot width 22 nm and strip-slot separation 500 nm. Figure 2 shows the dispersion coefficient as a function of wavelength. We can see a high negative dispersion of  $-4.8 \times 10^5$  ps/(km-nm) and an FWHM bandwidth of 13 nm. The magnitude of dispersion obtained is more than 2.5 times larger than that reported in Ref. [2].

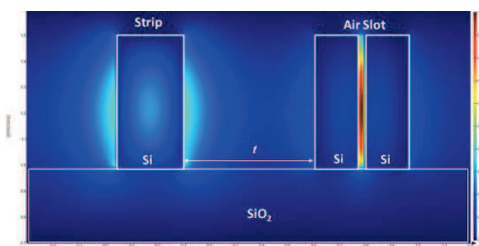


Fig. 1. Coupled strip-slot structure with modal field profile

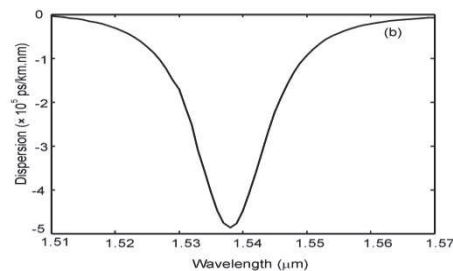


Fig. 2. Total dispersion of the structure

### Conclusion

We have designed and numerically analyzed a coupled strip-slot waveguide, which shows an enormously high negative dispersion. The structure can be used as integrated optic dispersion compensator and linear pulse compressor.

### References

- [1] S. Mas, J. Caraquitená, J. V. Galán, P. Sanchis, and J. Martí, "Tailoring the dispersion behavior of silicon nanophotonic slot waveguides," *Opt. Express*, vol. 18, pp. 20839 - 20844, 2010.
- [2] L. Zhang, Y. Yue, Y. Xiao-Li, R. G. Beausoleil, A. E. Willer, "Highly dispersive slot waveguides" *Opt. Express*, vol. 17, pp. 7095-7101, 2009.

## Low-frequency photonic bands in metallic lattices: a tight-binding description

K. Wang<sup>1,\*</sup>

<sup>1</sup>Laboratoire de Physique des Solides, UMR CNRS/Université Paris-Sud, Orsay, France

\*[mailto: kang.wang@u-psud.fr](mailto:kang.wang@u-psud.fr)

### Introduction

We study the low-frequency photonic band structures in square and hexagonal metallic lattices, by both numerical and tight-binding approaches. The structures are constructed upon two sets of adjustable structure unities, allowing probing the contribution of different structure configurations to the band formation.

### Results

The band structures and evolutions are comparatively investigated with respect to local resonances and their variations following the modulations of the sizes and shapes of the structure unities. We show that the lowest frequency bands are formed by *s*-like resonance modes sustained by the structure unities, of which the contributions vary following local structure modulations, and, under certain conditions, the second bands (above the first photonic band gaps) are formed by *p*-like modes sustained by the same unities. The *s* and *p* bands can both be described in the frame work of a tight-binding model, allowing band structure analyses in terms of relations between local resonance modes and their mutual correlations.

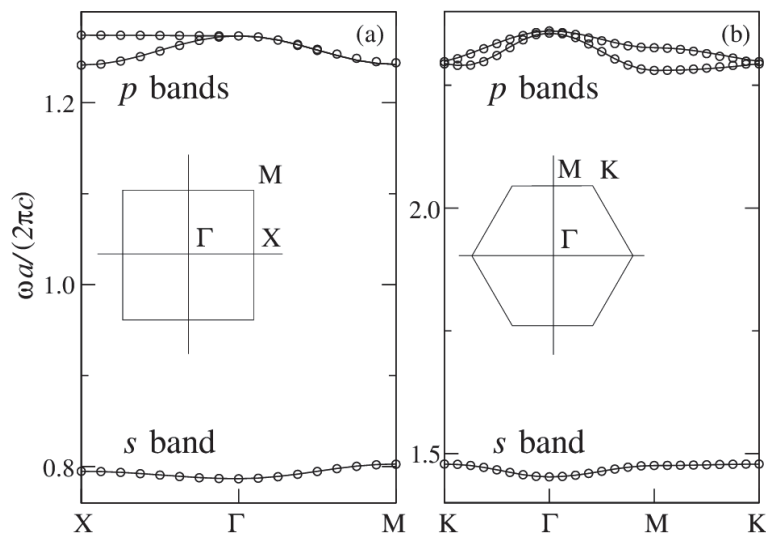


**Fig. 1.** The *s* and *p* bands for the square [(a)] and hexagonal [(b)] metallic lattices with high local symmetry. The numerical solutions are represented by circles, while the curves calculated with the tight-binding model are depicted by solid lines.

### Conclusion

This work demonstrates that the origin of the low frequency bands and gaps can be explicitly analyzed from the perspective of local structure arrangements, that determine both the local resonance conditions and their mutual correlation relations. The plasma gaps and the first photonic band gaps arise naturally from specific local structure patterns. From this point of view, low frequency light waves in metallic lattices can be compared to tightly bound electrons in solids.

## “Talbot Effect” in the Time Domain

Enakshi K Sharma<sup>1\*</sup> and Jyoti Anand<sup>2</sup>

<sup>1</sup> Department of Electronic Science, University of Delhi South Campus, Delhi-110021, India

<sup>2</sup> Keshav Mahavidyalaya, University of Delhi, Delhi 110034, India

\* [enakshi54@yahoo.co.in](mailto:enakshi54@yahoo.co.in)

We looked at the equivalence of the self-imaging “Talbot Effect” in space to the propagation of a temporal comb in a coaxial optical fiber at an appropriate wavelength. The consequent “Talbot Effect” in time can generate a comb of varying periodicity from a given comb by appropriate choice of the length of the fiber.

### Summary

The Talbot Effect or self-imaging of a periodic aperture was discovered as early as 1836 by Henry Fox Talbot. A periodic aperture can be represented by Fourier series and by use of the Fresnel-Kirchhoff diffraction integral in the paraxial approximation it can be seen that the pattern repeats itself after multiples of certain defined distance known as the “Talbot Length” [1]. We looked for a equivalence in the propagation of a Gaussian temporal comb in the fundamental LP<sub>01</sub> mode of a coaxial optical fiber, defined by  $f(t) = e^{j\omega_0 t} \left[ E_0 e^{-t^2/\tau_0^2} * \sum_{n=-\infty}^{+\infty} \delta(t - nT) \right]$ , at a wavelength (or frequency  $\omega_0$ ) where the dispersion curve shows a minima (Fig. 1b). At this wavelength the propagation constant,  $\beta(\omega)$ , can be accurately expanded in a Taylor series expansion about  $\omega_0$  retaining only the second order term  $\alpha_0 = \left. \frac{d^2\beta}{d\omega^2} \right|_{\omega=\omega_0}$ . The mathematical analysis leads to a term similar to that in self-imaging to show that for a specific combination of periodicity of the comb, T, and length of the fiber, one can define a “Talbot Length”,  $z_T = \frac{T^2}{2\pi|\alpha_0|}$  and its multiples, where the original input comb is regenerated; at intermediate lengths, combs of different periodicity are generated [Fig.1(c)]. Fig. 1d shows the intensity variation of the combs as a color contour plot with propagation distance and time often referred to as “Talbot Carpet” in space domain. The effect can be used to generate a comb of different periodicity from a given comb depending on the length of the coaxial fiber.

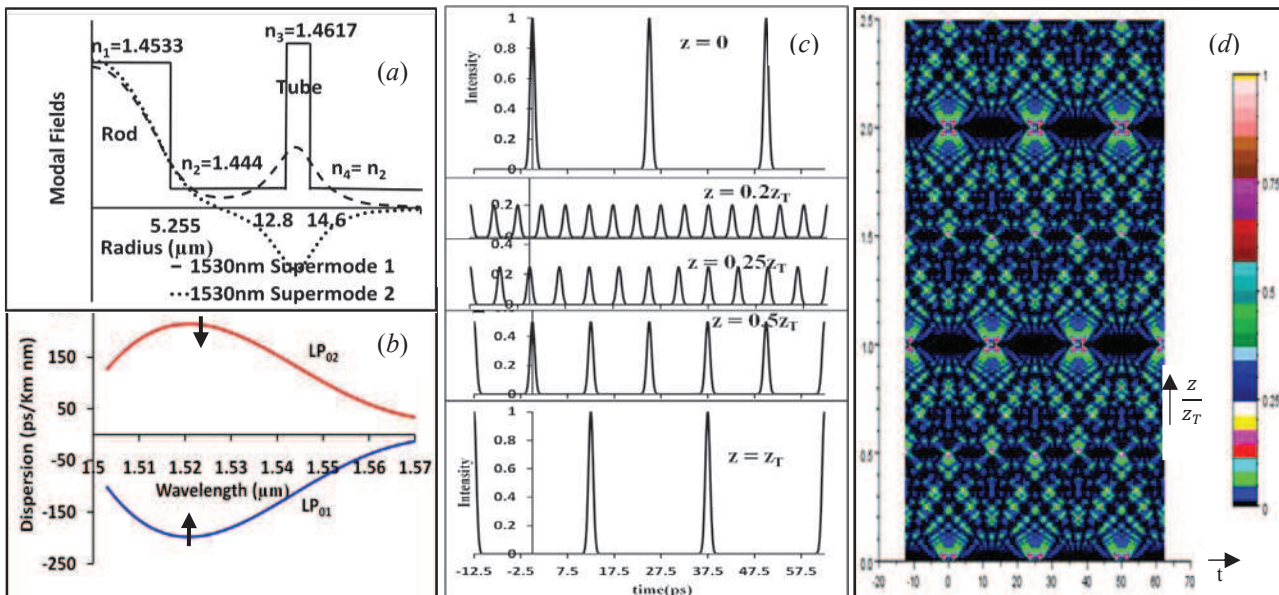


Fig. 1 (a) Coaxial optical fiber and its modes (b) Variation of Dispersion of the modes with wavelength (c) Intensity variation of output pulse with time at fractional multiples of Talbot Length (d) Talbot Carpet.

### References

[1] J. Wen, Y. Zhang and M. Ziao, *Advances in Optics and Photonics*, 5, 83-150, 2013.

## Optimization of Micro-Structured Waveguides in Lithium Niobate

M. Dubov, H. Karakuzu, S. Boscolo\*

Aston Institute of Photonic Technologies, Aston University, Birmingham B4 7ET, United Kingdom

\*s.a.boscolo@aston.ac.uk

We describe how the guiding properties of buried, micro-structured waveguides that can be formed in a lithium niobate crystal by direct femtosecond laser writing can be optimized for low-loss operation in the mid-infrared region beyond  $3\ \mu\text{m}$ .

### Summary

Lithium niobate ( $\text{LiNbO}_3$ ) offers incredible versatility as a substrate for integrated nonlinear optics. Owing to its robustness and unique flexibility, the direct femtosecond (fs) laser inscription method is one of the most efficient techniques for three-dimensional volume micro-structuring of transparent dielectrics. In crystals, by writing multiple tracks with a slightly reduced refractive index (RI) around the unmodified volume of material it is possible to produce a depressed-index cladding with the central volume serving as the core of a waveguide (WG). In this work, we present a practical approach to the numerical optimization of the guiding properties of depressed-cladding, buried WGs in  $z$ -cut  $\text{LiNbO}_3$  crystals [1]. The approach accounts for both the relationship between track size  $D$  and induced RI contrast  $\delta n$ , a suitable variation of the track size among different cladding layers, and the intrinsic losses due to fs laser inscription. The experimentally found dependencies of  $D$  and  $\delta n$  on the laser pulse energy were used, which make such parameters correlated if the (sample translation) inscription speed is fixed. A natural strategy to extend the spectral range of low-loss operation of the WG is to allow the track diameter to differ from one ring to another with the exterior rings that have large tracks. The rate of growth of the track size from the innermost to the outermost ring was parameterized with a single parameter  $p > 0$ , so that the track diameter  $D_n$  in the  $n$ -th ring is:  $D_n = D_{\min} + ((n - 1)/(N_{\text{clad}} - 1))^p (D_{\max} - D_{\min})$ ,  $n \in [1, N_{\text{clad}}]$ , where  $N_{\text{clad}}$  is the number of cladding layers, and  $D_{\max}$  and  $D_{\min}$  are the respective maximum and minimum diameters. Maxwell's equations were solved using the COMSOL simulation software based on the finite element method to find out the complex effective RIs  $n_{o,e}^{\text{eff}}$  of the modes of the structure for the O and E polarization states. The confinement losses, i.e., the losses due to the finite transverse extent of the confining structure, were computed from the imaginary part of effective RI. The results presented in Fig. 1 reveal that the spectral region where the confinement losses in both O and E polarizations are acceptably low (below 1 dB/cm) can extend up to a wavelength of  $3.5\ \mu\text{m}$  for optimized, hexagonal WG structures with seven rings of tracks. This makes such structures suitable for mid-infrared applications.

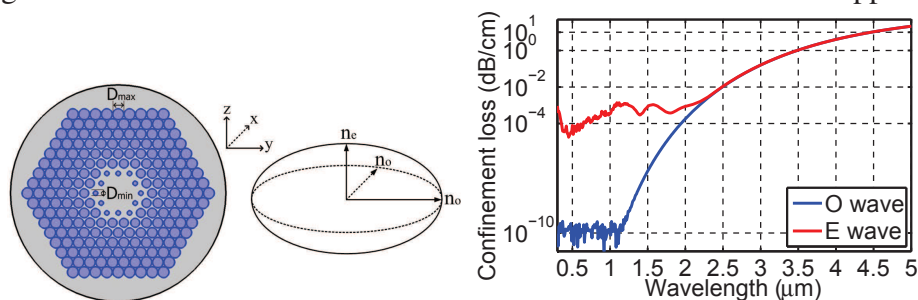


Fig. 1. Left: Cross-section of WG structure with seven rings of tracks with different diameters ( $p = 0.01$ ), and ellipsoid of refractive indices of  $z$ -cut  $\text{LiNbO}_3$  crystal. Right: Confinement losses for O and E waves as a function of wavelength for a seven-ring WG structure with  $p = 0.01$  and RI contrast changing from one ring to another following the change in track size. Other parameters are: maximum RI contrast  $\delta n = -0.01$ ,  $D_{\max} = 2.4\ \mu\text{m}$ ,  $D_{\min} = 1\ \mu\text{m}$ .

### References

[1] H. Karakuzu, M. Dubov, S. Boscolo, L. A. Melnikov, Y. A. Mazhirina, *Opt. Mater. Express* **4**, 541 (2014).

## Studies on dipolar interactions in arrays of sub-wavelength plasmonic nanoparticles

J. Fiala, P. Kwiecien, I. Richter\*

Czech Technical University in Prague, Faculty of Nuclear Sciences and Physical Engineering,  
Department of Physical Electronics, Břehová 7, 11519 Prague 1, Czech Republic

\* [richter@fjfi.cvut.cz](mailto:richter@fjfi.cvut.cz)

In this contribution, we use an interacting dipole approximation in order to reveal an interplay between resonances localized in individual nanoparticles (NP) and lattice resonances originating in the array. We also effectively combine the analysis of NP dimers, with this coupled dipole approach.

### Introduction

Metals and especially metal NP are interesting in plasmonic physics since they exhibit strong surface plasmon (SP) resonance. Optical properties of a NP array depend on the orientation of the particles and their shape, with respect to impinging light as well as on their arrangement. We have developed an analytical model based on previous work of Garcia de Abajo [1] which reveals interplay between a NP plasmon resonance and a lattice resonance – a coupled dipole approximation (CDA) [2]. In this work, we calculated that under a proper periodicity of a NP lattice, such arrays can exhibit narrow resonances with asymmetric Fano-type line shapes in the spectra [2]. The phenomena of field enhancement and spatial confinement are related to dipolar fields and resonances, being governed by the generation of localized SP and their mutual coupling.

### Results

In order to describe the physics of plasmon bounded modes in detail, a simple analytical model of two coupled NP (dimers), inspired in [3], is proposed, too. Polarizabilities and cross-sections are calculated under the action of a monochromatic plane wave which exhibit resonances indicating light trapping and field enhancement. Modes of coupled oscillations and corresponding eigenfrequencies are computed together with resonance shifts, with respect to NP distances. We further extend our analytical description gamut to several shapes of NP (e.g. nanorods, nanoshells). The benefit of the CDA lies in the separate description of resonances localized on the particles and resonances of the lattice. Therefore, polarizabilities of non-trivially shaped nanoparticles can be computed using the analytical expressions from either the Mie theory or from the rigorous numerical calculations (such as FDTD or RCWA), and inserted into the analytical model, predicting an enhanced or suppressed optical transmission. More complicated structures of dimers and trimers can be described in terms of properly excited coupled modes and eigenfrequencies, too.

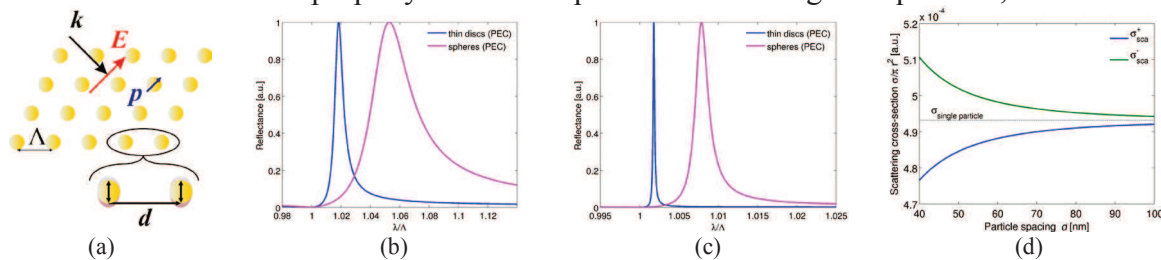


**Fig. 1:** (a) Schematic picture of arrayed resonant structure based on surface plasmon resonance; spectral reflectance characteristics, for the lattice constant  $\Lambda=800$  nm, and particle diameters (b)  $d/\Lambda=1/5$ ; and (c)  $d/\Lambda=1/8$ . (d) Scattering cross sections of a NP dimer, with respect to interparticle spacing.

**Acknowledgements:** This work was financially supported by the Czech Science Foundation (project P205/12/G118).

### References

- [1] F.J. Garcia de Abajo, *Rev. Mod. Phys.* **79**, 1267-1290, (2007).
- [2] J. Fiala, P. Kwiecien, I. Richter, *Proceedings of PIERS 2013 in Stockholm* (the 34th PIERS Conference in Stockholm, Sweden, 12-15 August, 2013), 439-442, (2013).
- [3] M. Apostol, S. Ilie, A. Petrut, M. Savu, S. Toba, *Proceedings of Meta 2013 Conference* (4th International Conference on Metamaterials, Photonic Crystals, and Plasmonics, UAE), (2013).

# Analysis of plasmonic slot waveguide couplers in linear and nonlinear regimes

J. Petráček<sup>1</sup>, P. Kwiecien<sup>2</sup>, I. Richter<sup>2,\*</sup>, Y. Ekşioğlu<sup>1</sup>

<sup>1</sup> Brno University of Technology, Faculty of Mechanical Engineering, Institute of Physical Engineering, Technická 2, 616 69 Brno, Czech Republic

<sup>2</sup> Czech Technical University in Prague, Faculty of Nuclear Sciences and Physical Engineering, Department of Physical Electronics, Břehová 7, 11519 Prague 1, Czech Republic

\* [richter@jfji.cvut.cz](mailto:richter@jfji.cvut.cz)

Numerical investigation of plasmonic directional couplers consisting of two dielectric slab waveguides separated with metallic claddings, in both linear and nonlinear regimes, has been performed, in terms of their geometrical as well as physical parameters.

## Introduction

Among nanophotonic structures, recently, plasmonic waveguides [1] of various geometries and configurations have found an increasing scientific interest in many areas of applications, due to their abilities to subwavelength light confinement and manipulations. Considering only planar structures, such as plasmonic slot waveguides studied here (Fig. 1a), with a dielectric core guide, surrounded with metallic slabs, have already shown effective performance. Due to strong metallic losses, however, there is always an inherent trade-off between confinement and propagation characteristics [1,2]. Since such plasmonic structures can strongly increase local fields, inherently-weak nonlinear optical effects can be significantly enhanced, and thus applied in many potential applications [3]. Here we consider Kerr-type nonlinearity (i.e. intensity dependent refractive index, of both dielectric as well as metal components) in conjunction with nanoplasmonics.

## Results

The analysis is done with our in-house technique, based on the extension of the eigenmode expansion (EME) method to Kerr-type nonlinearity (NL-EME), with the help of rigorous coupled-mode theory. The simulations are confirmed with the nonlinear finite difference time domain (FDTD) technique [4]. Based on our recent study [5], understanding the physics of such devices, comparing both linear and nonlinear performance, is a very important issue. We have studied power-dependent switching characteristics of the relative output power with respect to the level of nonlinearity, and the ways of improvements.

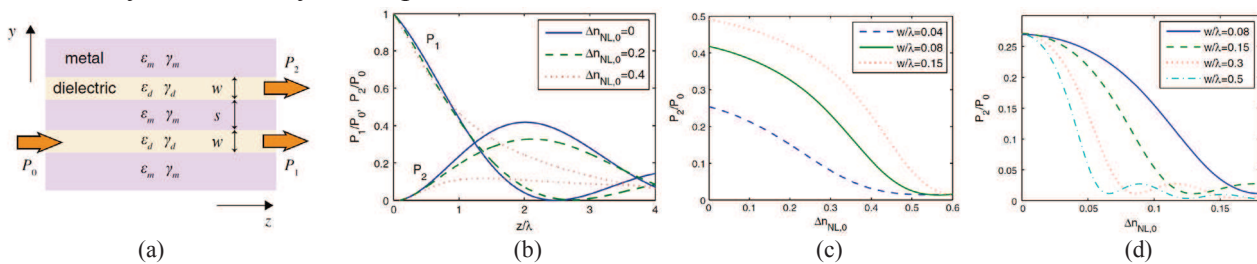


**Fig. 1:** (a) Schematic picture of an analyzed plasmonic coupler - two dielectric waveguides of widths  $w$  separated with the metallic cladding (width  $s$ ), with linear ( $\epsilon_m$  and  $\epsilon_d$ ) and nonlinear (Kerr) coefficients -  $\gamma_m$  and  $\gamma_d$ ; (b) relative output powers  $P_1/P_0$  and  $P_2/P_0$  with respect to the normalized propagation distance; (c) the switching characteristics  $P_2/P_0$  with respect to the nonlinearity level; and (d) improvement of the switching characteristics with a material of silicon nanocrystals in an amorphous silica matrix.

**Acknowledgements:** This work was financially supported by the Czech Science Foundation (project P205/12/G118 – P.K., I.R.), the Ministry of Education, Youth, and Sports of the Czech Republic (project LD14008 – J.P.), and Brno University of Technology (project CZ.1.07/2.3.00/30.0039 – Y.E.).

## References

- [1] P. Berini, I. De Leon, *Nature Photonics* **6**, 16, (2011).
- [2] J. Čtyroký, P. Kwiecien, I. Richter, *J. Europ. Opt. Soc. - Rap. Public.* **8**, 13024, (2013).
- [3] M. Kauranen, A.V. Zayats, *Nature Photonics* **6**, 737, (2012).
- [4] Crystal Wave - Photon Design software [<http://www.photond.com/>].
- [5] J. Petráček, *Applied Physics B* **112**, 593, (2013).

## Nonlinear metal slot waveguides: bifurcations and higher order modes

W. Walasik<sup>1,2</sup>, Y. V. Kartashov<sup>2</sup>, G. Renversez<sup>1</sup>

<sup>1</sup> Aix-Marseille Université, CNRS, Ecole Centrale, Institut Fresnel, 13013 Marseille, France

<sup>2</sup> ICFO — Institut de Ciències Fotòniques, Universitat Politècnica de Catalunya, 08860 Castelldefels (Barcelona), Spain

[gilles.renversez@fresnel.fr](mailto:gilles.renversez@fresnel.fr)

We study the nonlinear waves propagating in symmetric metal slot waveguides with a Kerr-type dielectric core. We develop two independent semi-analytical models to describe the properties of such waveguides. We especially show that the dispersion curve of the first asymmetric mode is invariant with respect to the slot width for high powers and we provide analytical approximations of this curve.

### Introduction

The studies of nonlinear waves combining both plasmon and soliton features started in 1980s [1, 2]. The interest in the field started to grow again thanks to the results provided in Ref. [3]. Even if no experimental demonstration of plasmon–solitons has been published yet [4], in the mid term, such states can have several applications, e.g. in nonlinear couplers or in a four wave mixing process. The structure studied in Ref. [3] is a nonlinear dielectric core surrounded by two semi-infinite metal regions. It will be called here the nonlinear slot waveguide (NSW). Recently, some stationary waves in such waveguides with a Kerr-type focusing nonlinear core were studied in details [5, 6]. It has been shown that symmetric, antisymmetric and asymmetric plasmon–solitons can propagate in the NSW. The asymmetric nonlinear mode appears from the symmetric one through a symmetry-breaking bifurcation at a critical power. This bifurcation phenomenon has already been described in several nonlinear waveguides as early as in the eighties.

### Methods

Using Maxwell's equations and a simple description of the optical Kerr effect to study NSW, we developed a simplified semi-analytical model, where field shapes in the core are described by the Jacobi elliptic special functions. We also developed an exact approach where the field shapes in the core are found with the aid of direct integration of Maxwell's equations.

### Results

Qualitatively the results of the simplified, but analytical approach and the exact approach are the same. We present a number of previously unknown higher order symmetric, antisymmetric and asymmetric modes in the NSW. The dispersion curves and the field shapes for these modes are obtained for the first time. Both our models predict the bifurcation of asymmetric modes from the symmetric node-less modes. We show that the bifurcation occurs not only for the first but also for higher order nonlinear modes. We show that the first nonlinear asymmetric mode dispersion curves have invariant parts with respect to the core width, and we describe these parts using analytical formula.

### References

- [1] J. Ariyasu, C. T. Seaton, G. I. Stegeman, A. A. Maradudin, and R. F. Wallis. *J. Appl. Phys.*, 58(7):2460, 1985.
- [2] D. Mihalache, M. Bertolotti, and C. Sibilia. volume XXVII, pages 229–313. Elsevier, Amsterdam, 1989.
- [3] E. Feigenbaum and M. Orenstein. *Opt. Lett.*, 32(6):674, 2007.
- [4] W. Walasik, V. Nazabal, M. Chauvet, Y. Kartashov, and G. Renversez. *Opt. Lett.*, 37(22):4579, 2012.
- [5] A. R. Davoyan, I. V. Shadrivov, and Y. S. Kivshar. *Opt. Express*, 16:21209, 2008.
- [6] I. D. Rukhlenko, A. Pannipitiya, M. Premaratne, and G. Agrawal. *Phys. Rev. B*, 84:113409, 2011.

## Modeling of a cavity-resonator-integrated guided-mode resonance filter

N.Rassem<sup>1</sup>, A-L.Fehrembach<sup>1,\*</sup>, E.Popov<sup>1</sup>

<sup>1</sup>Université d'Aix-Marseille, CNRS, Centrale Marseille, Institut Fresnel, Marseille, France

\*[nadege.rassem@fresnel.fr](mailto:nadege.rassem@fresnel.fr)

**Abstract:** Cavity-resonator-integrated guided-mode resonance filters (CRIGFs) are promising structures that afford a very fine spectral width less than 0.3 nm. Yet they are difficult to rigorously model due to their large length more than 100 wavelengths. We show how the RCWA method can be used to simulate the CRIGF response efficiently.

### CRIGF structure and method

Studies we conduct are focused on a new kind of resonant grating, called CRIGFs. CRIGFs were introduced in 2011 and are composed by a guided-mode resonance filter (GMRF) integrated between two distributed Bragg reflectors (DBR) (see Fig. 1) [1,2]. The GMRF is a subwavelength grating with period  $d$  and the DBR period is  $d/2$ . The length of the GMRF section is around 15 wavelengths and each DBR has a 70 wavelengths length. On each side of the GMRF, we inserted a phase section to optimize the reflectivity of the CRIGF. The advantage of this structure as compared to periodic resonant gratings is that we create a localized mode in the GMRF, due to the reflectors, that can be excited by a Gaussian beam focused on the GMRF. Contrary to periodic resonant gratings, CRIGFs have a greater angular tolerance.

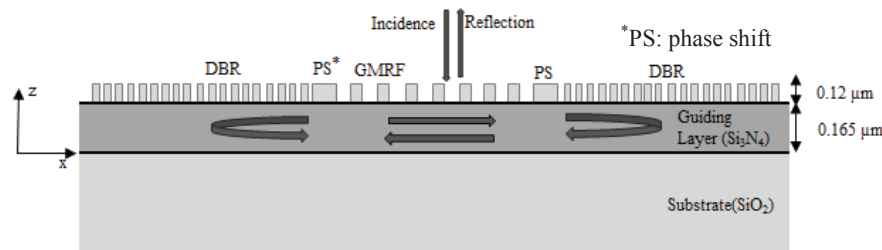


**Fig. 1.** Schematic view of the structure and different sections: DBR, PS, GMRF. Definition of materials.

To numerically model this non-periodic large structure (around 150 wavelengths), we use the RCWA method that is a Fourier rigorous method usually used to solve scattering from periodic structures. In fact, we consider the CRIGF structure represented on fig. 1 as the basic pattern of a periodic structure (super cell method). For the calculation to be accurate, the field in each basic cell must be independent from that in the other cells. This condition is in part realized thanks to the presence of the DBR, and is fully realized by adding Perfectly Matched Layers (PMLs) between the DBRs of two adjacent cells.

In the post, we will show that the method convergence is relatively rapid and allows calculations within a reasonable time (around 3 minutes per wavelength), even for highly focused beams. We will also present calculations aiming at understanding the basic physical principles governing the properties of CRIGFs: field maps, maps of the reflectivity with respect to the wavelength and angle of incidence, dependence of the properties with respect to different parameters of the structure (optical indexes, phase shift, fill factor ...) and of the size of the Gaussian incident beam (waist).

### Conclusion

With a RCWA code, we calculated the performances of CRIGFs structure using the super cell method with PMLs between each basic cell. Our calculation time is much smaller than that necessary with the FDTD method used by other groups [1]. We believe our work is a decisive step toward the control of the diffractive properties of CRIGFs and the design of CRIGFs adapted to practical applications.

### References

- [1] X. Buet et al. "High angular tolerance and reflectivity with narrow bandwidth cavity-resonator-integrated guided-mode resonance filter", *Optics Express*, 20:9322-9327, 2012.
- [2] K.Kintaka et al. "Cavity-resonator-integrated guided-mode resonance filter for aperture miniaturization", *Opt. Expr.*, 20, 1444, 2012.

# Vertical Mode Expansion Method for Diffraction of Light by Biperiodic Circular Cylindrical Structures

Xun Lu, Hualiang Shi, Ya Yan Lu

*Department of Mathematics, City University of Hong Kong, Kowloon, Hong Kong*  
*mayylu@cityu.edu.hk*

For biperiodic structures with circular cylindrical inclusions, we present a vertical mode expansion method based on expanding the field in 1D vertical modes. The method is an alternative to the Fourier modal method.

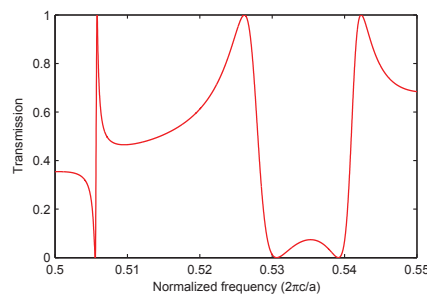
## Introduction

For analyzing crossed gratings or other biperiodic structures, the Fourier modal method (FMM) is suitable if the structure consists of one or more layers where each layer is invariant in the vertical  $z$  direction (assuming the structure is periodic in the horizontal  $xy$  plane). However, the FMM requires 2D modes which are expensive to calculate. We present a vertical mode expansion method (VMEM) which expands the field in 1D modes which are functions of  $z$ . The VMEM has been used in previous works for different applications [1, 2, 3]. We extend the VMEM to structures with a biperiodic array of circular cylindrical inclusions for plane incident waves given in the media above or below the structure.

## Method and results

Let  $\Omega$  be the horizontal cross section of one period of the biperiodic structure, and let  $\Omega$  be divided into a circular disk  $\Omega_1$  and its exterior  $\Omega_0$  (separated by the circle  $\Gamma$ ). The VMEM consists of following steps: (1) truncate  $z$  by PMLs and calculate the TE and TM modes for the two vertical profiles corresponding to  $\Omega_0$  and  $\Omega_1$ ; (2) calculate the Dirichlet-to-Neumann (DtN) maps on  $\Gamma$  for 2D scalar Helmholtz equations in  $\Omega_0$  and  $\Omega_1$  corresponding to each vertical modes; (3) expand the field inside and outside the circular cylinder and match the field on the vertical wall of the cylinder. As the total field is not outgoing and is inconsistent with PMLs, the field is only expanded after a 1D solution (related to the incident wave) is first subtracted.

As in [4], we consider a photonic crystal slab with a square lattice (lattice constant  $a$ ) of circular holes (radius  $0.2a$ ), where the slab thickness is  $0.5a$  and the dielectric constant of the slab is 12. Assuming the slab is parallel to the  $xy$  plane, we use the VMEM to calculate the transmission spectrum for a normal incident plane wave. The results shown in the figure below agree well with those of [4].



## References

- [1] S. Boscolo and M. Midrio, *J. Lightwave Technol.*, **22**, 2778-2786, 2004.
- [2] L. Yuan and Y. Y. Lu, *J. Opt. Soc. Am. B*, **27**, 2568-2579, 2010.
- [3] X. Lu, H. Shi, and Y. Y. Lu, *J. Opt. Soc. Am. A*, **31**, 2014.
- [4] S. Fan and J. D. Joannopoulos, *Phys. Rev. B*, **65**, 235112, 2002.

## Geometrical interpretation of Fano resonances in plasmonic nanostructures

V. Grigoriev, S. Varault, G. Boudarham, B. Rolly, B. Stout, J. Wenger and N. Bonod\*

*Université d'Aix-Marseille, CNRS, Centrale Marseille, Institut Fresnel, Marseille, France*

\*[nicolas.bonod@fresnel.fr](mailto:nicolas.bonod@fresnel.fr)

The scattering properties of plasmonic nanostructures arranged in 2D periodic arrays are analyzed by expanding their response into perfectly emitting and absorbing modes. It is shown that the frequencies of these modes determine the shape of reflection and transmission spectra in the same way as the positions of point-like charges determine the electric field around them.

### Introduction

Plasmonic nanostructures offer a unique ability to engineer the optical properties at the scale which is smaller than the wavelength of light. They are often fabricated as arrays of scatterers periodically arranged on a surface. The profile of the scatterers can be made in the form of split-ring resonators, dolmen-like structures or various oligomers to control the coupling between different resonances and to observe such effects as electromagnetically induced transparency, absorption, etc.

### Summary

We show that the scattering spectra for all of these structures can be described by analytical formulas. Our approach is based on the ability to expand the frequency response of nanostructures into perfectly emitting and absorbing modes [1,2]. These modes exist in the domain of complex frequencies and create similar singularities as the positive and negative electric charges in 2D space. It is the analogy with electrostatics that helps to understand the interaction between multiple resonances better and to explain various resonant effects [2].

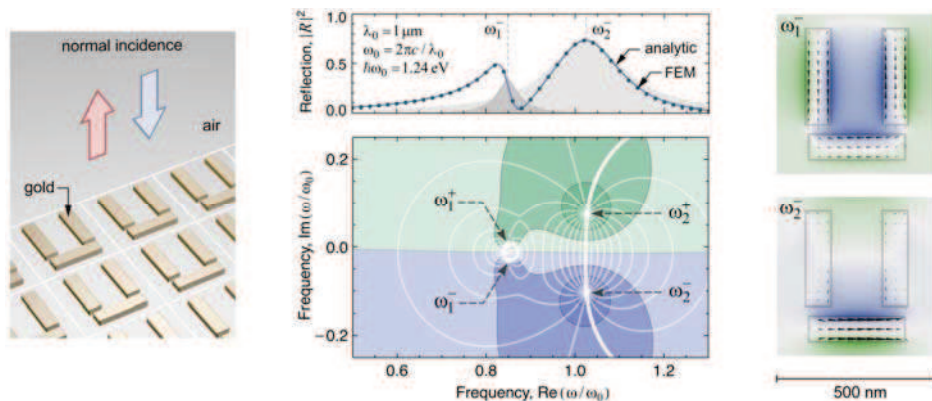


**Fig. 1.** An array of dolmen-like structures. The reflection spectrum for normal incidence, and its decomposition into perfectly emitting and absorbing modes. The field profiles of quadrupolar and dipolar modes.

### References

- [1] V. Grigoriev, A. Tahri, S. Varault, B. Rolly, B. Stout, J. Wenger, N. Bonod, “Optimization of resonant effects in nanostructures via Weierstrass factorization,” *Phys. Rev. A* 88, 011803(R) (2013)
- [2] V. Grigoriev, S. Varault, G. Boudarham, B. Stout, J. Wenger, N. Bonod, “Singular analysis of Fano resonances in plasmonic nanostructures,” *Phys. Rev. A* 88, 063805 (2013)

## Polarizability tensors of metallic U-shaped scatterers

S. Varault, B. Rolly, G. Boudarham, G. Demésy, B. Stout, and N. Bonod\*

*Université d'Aix-Marseille, CNRS, Centrale Marseille, Institut Fresnel, Marseille, France*

\*[nicolas.bonod@fresnel.fr](mailto:nicolas.bonod@fresnel.fr)

In this work, we derive the polarization tensors of magneto-electric metallic antennas when illuminated by a plane wave and highlight the importance of the multipolar contributions of the coupling with the incident field, even for metallic particles of size  $(\lambda/10)$ .

### Introduction

The derivation of the polarizability tensor of metallic particles is of high interest for studying their optical properties or designing optical antennas.

### Summary

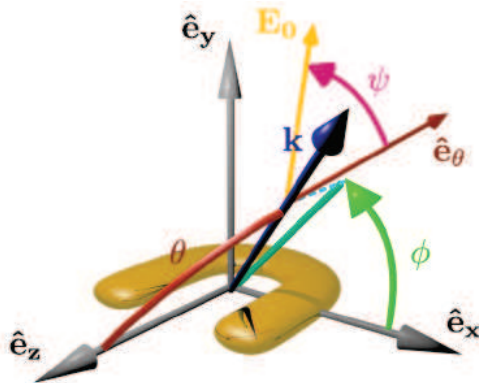
We first show that the classical expression of dipolar moments:

$$\begin{bmatrix} \mathbf{p} \\ \mathbf{m} \end{bmatrix} = \begin{bmatrix} \bar{\alpha}^{ee} & \bar{\alpha}^{em} \\ \bar{\alpha}^{me} & \bar{\alpha}^{mm} \end{bmatrix} \begin{bmatrix} \mathbf{E}^0 \\ \mathbf{H}^0 \end{bmatrix}$$

cannot apply in the case of U-shaped metallic scatterers, since several terms in the polarization tensor depend on the incidence conditions. We apply the more general formulation:

$$\begin{aligned} p_i &= \alpha_{ij}^{ee} E_j^0 + a_{ijk} \nabla_k E_j^0 + \alpha_{ij}^{em} H_j^0 + b_{ijk} \nabla_k H_j^0 + \dots \\ m_i &= \alpha_{ij}^{me} E_j^0 + c_{ijk} \nabla_k E_j^0 + \alpha_{ij}^{mm} H_j^0 + d_{ijk} \nabla_k H_j^0 + \dots \end{aligned}$$

up to the quadrupolar order and retrieve with a fitting procedure the different dipolar and quadrupolar terms. In the case of subwavelength sized particles, we are able to present an corrected expression of the first classical relation, where the dependence over the incidence is taken into account in the different elements of the tensor.



$$\bar{\alpha}_{cor} = \begin{bmatrix} \alpha_{xx}^{ee} + a_{xxz} \cos \theta & 0 & 0 & 0 & \alpha_{xy}^{em} + b_{xyz} \cos \theta & 0 \\ 0 & 0 & 0 & 0 & 0 & 0 \\ 0 & 0 & \alpha_{zz}^{ee} & 0 & 0 & 0 \\ 0 & 0 & 0 & 0 & 0 & 0 \\ \alpha_{yx}^{me} + c_{yxz} \cos \theta & 0 & 0 & 0 & \alpha_{yy}^{mm} + d_{yyz} \cos \theta & 0 \\ 0 & 0 & 0 & 0 & 0 & 0 \end{bmatrix}$$

### References

- [1] S. Varault, B. Rolly, G. Boudarham, G. Demésy, Brian Stout, and N. Bonod, "Multipolar effects on the dipolar polarizability of magneto-electric antennas," *Opt. Express* **21**, 16444-16454 (2013)

## Coherent perfect absorption of light by nanoparticles

V. Grigoriev<sup>1</sup>, N. Bonod<sup>1</sup>, J. Wenger<sup>1</sup>, B. Stout<sup>1\*</sup>

<sup>1</sup> Université d'Aix-Marseille, CNRS, Centrale Marseille, Institut Fresnel, Marseille, France

\*[brian.stout@fresnel.fr](mailto:brian.stout@fresnel.fr)

Coherent 'Perfect' Absorption (CPA) corresponds to a fundamental upper bound of the absorption cross section,  $\sigma_{\text{abs}} \leq 3\lambda^2/8\pi$ . CPA constrains the absorber permittivity to specific values, but these values can be found in a few materials at certain wavelengths or designed as effective parameters at any wavelength.

### Introduction

Electromagnetic hot spots can be produced in a variety of structured nano-materials. Coherent 'Perfect' Absorbers (CPA) provide a means to efficiently transform electromagnetic energy of these hot spots into another form (joule heat, photo-electric, fluorescence).<sup>[1]</sup>

### Results

We show that CPA satisfies a fundamental upper bound of the absorption cross section ( $\sigma_{\text{abs}} \leq 3\lambda^2/8\pi$  for a dipole channel), and that it constrains the permittivity of the absorber to discrete values that can be determined via Weierstrass factorization.<sup>[2]</sup> As an example, we plot in Fig.1, the required CPA permittivity for the electric dipole mode in a spherical scatterer as a function of the particle's size parameter,  $ka$  where  $k$  is the host medium wavenumber, and  $a$  the particle radius.

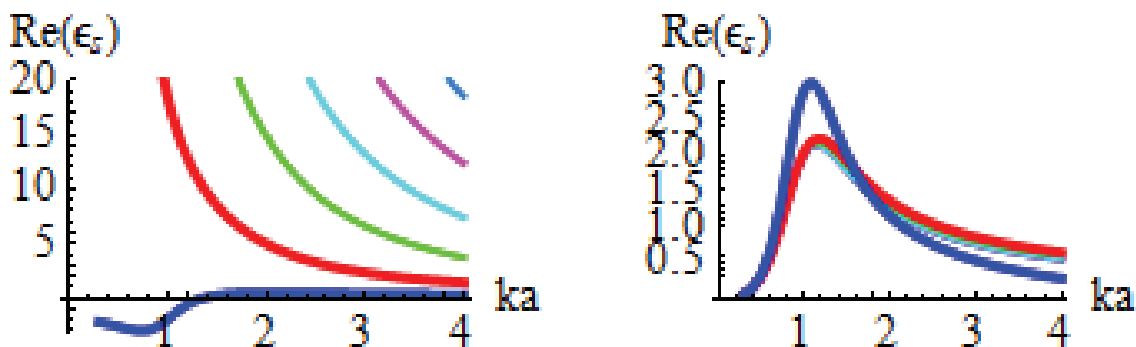


Fig. 1. Permittivity required for electric dipole CPA as a function of the size parameter  $ka$

We also derive and present new analytic approximations that can be used to approximate the CPA conditions and which aid in determining the required effective media properties of designed materials.

### Summary

We describe the underlying physics of the CPA phenomenon and show that it can be achieved using realistic materials. New approximate formulas based on the exact Weierstrass decomposition method are introduced to facilitate the CPA designs at essentially arbitrary frequencies.

### References

- [1] Y.D. Chong *et al.*, "Coherent Perfect Absorbers: Time-Reversed Lasers," PRL. **105**, 053901 (2010).  
 [2] V. Grigoriev *et al.*, Optimization of resonant effects in nanostructures via Weierstrass factorization, Ph.Rev.A, **88**, 011803 (2013).

## Controllable emission directivity with a hybrid magnetic-electric dielectric scatterer

J. Benedicto<sup>1</sup>, B. Rolly<sup>1</sup>, J.-M. Geffrin<sup>1</sup>, R. Abdeddaim<sup>1</sup>, B. Stout<sup>1</sup>, N. Bonod<sup>1</sup>,  
<sup>1</sup> *Universit d'Aix-Marseille, CNRS, Centrale Marseille, Institut Fresnel, Marseille, France*  
[jessica.benedicto@fresnel.fr](mailto:jessica.benedicto@fresnel.fr)

We demonstrate experimentally and theoretically that the energy radiated by an electric dipole can be emitted either toward the forward or the backward direction, by controlling either the emission frequency or the emitter-to-particle distance.

### Introduction

It was recently showed that dielectric particles of moderate refractive index exhibiting electric and magnetic modes can satisfy the so-called Kerker's conditions that lead to complete forward scattering or strong the backward scattering depending on the frequency of the incident plane wave [1, 2]. These conditions were recently extended to the case of near field excitation and it was demonstrated that this novel class of electric and magnetic resonant scatterers offer higher gains in directivity than classical electric or magnetic resonant particles [3].

### Results

We propose to design a hybrid electric-magnetic dielectric antenna, sub-wavelength in size, composed by a single spherical scatterer exhibiting a very moderate refractive index  $n = 2.45$ , that we characterize in a anechoic in radio frequencies. This refractive index can be observed with many materials in a wide range of frequencies, but more importantly, it leads to a broadening of the Mie resonances which allows a coupling between the dipole emitter with the electric and magnetic dipolar and quadrupolar modes in the dielectric resonator. We show that this interplay between this different modes allows to control the emission direction by tuning either the emission frequency [4], or the emitter-to-particle distance.

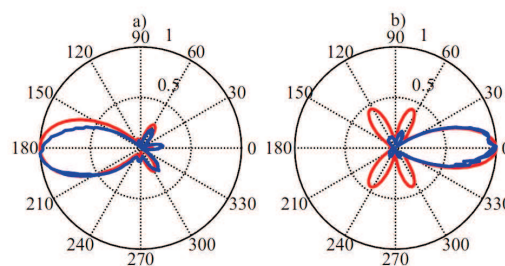


Fig. 1. Norm of the electric field scattered for an emitter-to-particle gap of 10 mm in the E-plane : (a) Back-scattering observed at 9.74 GHz, (b) Forward scattering observed at 8.7 GHz.

### References

- [1] R. Gomez-Medina *et al.* *Electric and magnetic dipolar response of germanium nanospheres: interference effects, scattering anisotropy, and optical forces.* *Journal of Nanophotonics*, **5**, 053512 (2011).
- [2] J. Geffrin *et al.* *Magnetic and electric coherence in forward-and back-scattered electromagnetic waves by a single dielectric subwavelength sphere.* *Nature communications* **3**, 1171 (2012).
- [3] B. Rolly, B. Stout and N. Bonod, *Boosting the directivity of optical antennas with magnetic and electric dipolar resonant particles* *Optics Letters*, **20**, 20376-20386 (2012).
- [4] B. Rolly, J.-M. Geffrin, R. Abdeddaim, B. Stout and N. Bonod, *Controllable emission of a dipolar source coupled with a magneto-dielectric resonant subwavelength scatterer* *Scientific reports* **3** (2013).

## Polarization-dependent spectra of photonic crystal with anisotropic plasmonic defect layer

S. Moiseev<sup>1,2\*</sup>, V. Ostatochnikov<sup>1</sup>, D. Sementsov<sup>1</sup>

<sup>1</sup>*Ulyanovsk State University, Ulyanovsk, Russia*

<sup>2</sup>*Kotelnikov Institute of Radio Engineering and Electronics of Russian Academy of Sciences, Ulyanovsk, Russia*

\*[serg-moiseev@yandex.ru](mailto:serg-moiseev@yandex.ru)

Polarization-dependent features appearing when the electromagnetic wave is reflected from and transmitted through a 1D photonic crystal with a defect layer formed by nonspherical metal nanoparticles are theoretically studied.

The composite material with uniformly oriented elongated metal nanoparticles behaves like a dichroic crystal. In this work the possibility of using plasmonic nanocomposite with nonspherical metal inclusions as a tuning defect in a photonic crystal (PC) is considered and the features of the behavior of electromagnetic eigenmodes in an artificial layered periodic structure with a finite number of periods and a plasmonic defect are analyzed.

It is shown that the presence of a plasmonic composite layer creates additional resolved levels in forbidden zones of the nondefective artificial layered periodic structures (by analogy with additional resolved levels in solids), which correspond to localized modes associated with the defect. By combining different types of defects and their positions in the structure as well as selecting the material, it is possible to efficiently control the optical properties of PC. According to Fig. 1, reflection and transmission spectra of the defective layered periodic structure exhibits high polarization contrast. For radiation of the region near the spectral line of the defect mode, this PC absorbs the light polarized parallel to the long axis of spheroids, and for the light polarized parallel to the short axis of spheroids the structure is transparent.

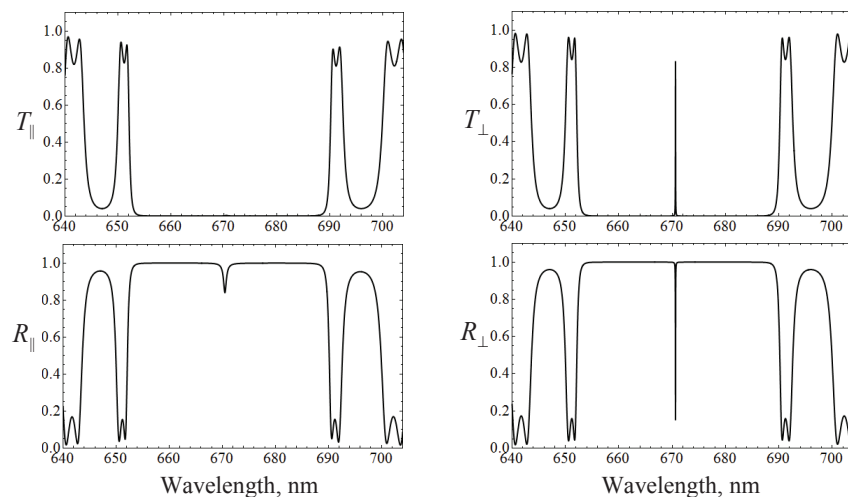


**Fig. 1.** Polarization-dependent spectral reflectance  $R$  and transmittance  $T$  of the defective layered periodic structure for the light polarized parallel to the long axis of spheroids (left plots) or to the short axis of spheroids (right plots). The computational parameters: volume concentration of nanoparticles equals  $5 \cdot 10^{-5}$ , the ratio of the length of polar semi-axis and equatorial semi-axis of spheroids equals 3.

This work was supported by the Ministry of Education of the Russian Federation.

## Controlling interface reflectance by plasmonic composite structure

S. Moiseev<sup>1,2\*</sup>

<sup>1</sup>*Ulyanovsk State University, Ulyanovsk, Russia*

<sup>2</sup>*Kotelnikov Institute of Radio Engineering and Electronics of Russian Academy of Sciences, Ulyanovsk, Russia*

\*[serg-moiseev@yandex.ru](mailto:serg-moiseev@yandex.ru)

The possibility of using continuous and discontinuous nanocomposites with nonspherical metal inclusions as anti-reflection coatings is theoretically studied.

Nanocomposites with extraordinary electromagnetic properties can find a variety of applications, in particular for manufacturing nonreflecting (absorptive) materials, controlling the optical beam intensity and propagation direction, etc. In this work, a detailed theoretical investigation of optical properties of a matrix metal-dielectric medium with nonspherical metal inclusions is performed, and the possibility to realize functional structures with beneficial effects in the visible region is considered.

The dependence of optical properties of the continuous composite with spheroidal metal nanoparticles randomly distributed over the whole matrix volume on the geometric (shape and concentration of nanoparticles) and material (permittivities of the matrix and metal nanoparticles) parameters are calculated within the effective-medium approximation. Discontinuous nanocomposite structure is considered to be formed by one, two, or more monolayers of uniformly oriented metal nanoparticles of nonspherical form suspended in a continuous media. In order to calculate the coefficients of the direct light transmission and specular reflection for a stack made of monolayers, we combine the quasi-crystalline approximation applied for calculations of the transmission properties of individual monolayers, with the transfer-matrix technique used for subsequent calculations of the transmission properties of multilayer structures.

The results of calculation show that composite medium with nonspherical metal inclusions can be used as anti-reflection (anti-glare) coating. Metal nanoparticles incorporated in the anti-reflection coating significantly reduce the Fresnel reflection in some spectral range due to a destructive interference effect (as shown at Fig. 1). Constructively, anti-reflection coating may represent a microscopic region in the optical medium (in a prism, optical fiber, integrated waveguide, etc.) doped with metal nanoparticles.

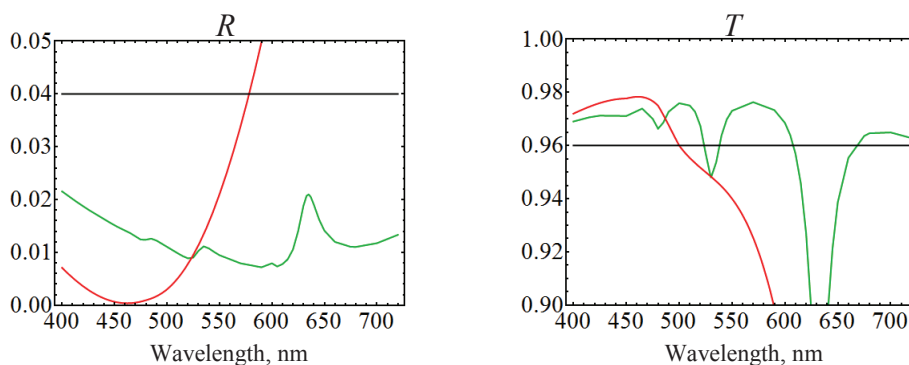


**Fig. 1.** Calculated reflectance  $R$  and transmittance  $T$  of the anti-reflective coatings for normal incidence of light. Red lines correspond to the case of continuous composite with spheroidal silver nanoparticles. Green lines correspond to the case of single monolayer of cylindrical silver nanoparticles. The reflectance and transmittance of the substrate are shown for comparison by black lines.

This work was supported by the Ministry of Education of the Russian Federation.

## **Author index**

|                 |          |                        |
|-----------------|----------|------------------------|
| Abass           | A.       | O-7.3                  |
| Abdeddaim       | R.       | P-39                   |
| Abdelaziz       | W.S.     | P-21                   |
| Abdelrazak      | M.       | P-20                   |
| Agrawal         | A.       | P-13                   |
| Anand           | J.       | P-29                   |
| Arlandis        | J.       | O-3.1                  |
| Asadchy         | V.       | O-3.0                  |
| Ashok           | N.       | P-27                   |
| Audo            | F.       | P-25                   |
| Azzam           | S. I. H. | P-23                   |
| Bakhti          | S.       | P-16                   |
| Bécache         | E.       | P-14                   |
| Bedu            | F.       | O-7.2                  |
| Begou           | T.       | O-7.2                  |
| Bellanca        | G.       | O-8.2, P-06            |
| Benedicto       | J.       | P-39                   |
| Benghalia       | A.       | P-01, P-02             |
| Benisty         | H.       | O-1.0                  |
| Benson          | T.       | P-10                   |
| Bernardin       | T.       | O-8.1                  |
| Boguslawski     | M.       | O-3.3                  |
| Bonnet-Ben Dhia | A.-S.    | O-5.1                  |
| Bonod           | N.       | P-36, P-37, P-38, P-39 |
| Bos             | J.       | O-6.2                  |
| Boscolo         | S.       | P-30                   |
| Bouchon         | P.       | O-7.0                  |
| Boudarham       | G.       | P-36, P-37             |
| Breno           | R.       | P-12                   |
| Cabrera-Espana  | F.J.     | P-13                   |
| Carvalho        | C.       | O-5.1                  |
| Centeno         | E.       | O-3.1                  |
| Chang           | H.-C.    | P-26                   |
| Chesnel         | S.       | O-5.1                  |
| Chevalier       | P.       | O-7.0                  |
| Ciarlet Jr. 1   | P.       | O-5.1                  |
| Commandré       | M.       | O-7.2                  |
| Čtyroký         | J.       | O-6.4                  |
| Dallaporta      | H.       | O-7.2                  |
| Degiron         | A.       | O-1.0                  |
| Demésy          | G.       | O-7.2, P-37            |
| Denz            | C.       | O-3.3                  |
| Destouches      | N.       | P-16                   |
| Desyatnikov     | A.S.     | O-3.3                  |
| Diebel          | D.       | O-3.3                  |
| Djouablia       | L.       | P-01                   |
| Dubov           | M.       | P-30                   |
| Duffy           | A.       | O-4.2                  |
| Ekşioğlu        | Y.       | P-32                   |
| El-Azab         | J.       | P-21                   |
| Farhat          | M. O. H. | P20, P-21              |
| Fatome          | J.       | O-8.1                  |
| Fehrembach      | A.-L.    | P-34                   |
| Fiala           | J.       | P-31                   |

|                 |          |                   |
|-----------------|----------|-------------------|
| Finot           | C.       | O-8.1             |
| Fliss           | S.       | O-6.1             |
| Gabalís         | M.       | O-8.2, P-03       |
| Geffrin         | J.-M.    | P-39              |
| Gehlot          | K.       | P-19              |
| Ghisa Telescu   | L.       | P-25              |
| Gomez Rivas     | J.       | O-7.3             |
| Granet          | G.       | O-5.2             |
| Grigoriev       | V.       | P-36, P-38        |
| Guegan          | M.       | P-25              |
| Haidar          | R.       | O-7.0             |
| Hammer          | M.       | P-07, O-8.0       |
| Hassan          | K.       | O-8.1             |
| Hecquet         | C.       | O-7.2             |
| Heikal          | A.M.     | P-20, P-21        |
| Hoekstra        | H.J.W.M. | O-8.0             |
| Hu              | Z.       | O-8.3             |
| Hu              | X.       | P-11              |
| Huang           | L.       | P-04              |
| Hussain         | F.F. K.  | P-21              |
| Jaeck           | J.       | O-7.0             |
| Joly            | P.       | P-14              |
| Jouablia        | L.       | P-02              |
| Kämpfe          | T.       | P-17              |
| Karabchevsky    | A.       | O-1.2             |
| Karakuzu        | H.       | P-30              |
| Kartashov       | Y.V.     | P-33              |
| Kaya            | S.       | O-8.1             |
| Kolosovsky      | E.       | P-09              |
| Koška           | P.       | O-1.1, O-6.4      |
| Kwiecien        | P.       | O-6.4, P-31, P-32 |
| Labbani         | A.       | P-01, P-02        |
| Lagrost         | A.       | P-12              |
| Lantéri         | S.       | O-6.0             |
| Léger           | R.       | O-6.0             |
| Lelarge         | F.       | P-12              |
| Lévesque        | Q.       | O-7.0             |
| Leykam          | D.       | O-3.3             |
| Liu             | H.-H.    | P-26              |
| Lu              | Y. Y.    | O-8.3, P-05, P-35 |
| Lu              | X.       | P-35              |
| Lupu            | A.       | O-1.0             |
| Maes            | B.       | O-7.3             |
| Malaguti        | S.       | O-8.2             |
| Mann            | V.       | P-27              |
| Mansoor         | R.       | O-4.2             |
| Martin          | O.J.F.   | O-5.0             |
| Martínez-Pastor | J.P.     | P-24              |
| Melati          | D.       | O-4.1             |
| Melloni         | A.       | O-4.1             |
| Moiseev         | S.       | P-40, P-41        |
| Morel           | P.       | P-12              |
| Morichetti      | F.       | O-4.1             |
| Motaweh         | T.       | P-12              |

|                |         |                         |
|----------------|---------|-------------------------|
| Mounkala       | E.      | O-7.1                   |
| Myslivets      | S.A.    | O-3.2                   |
| Nefedov        | I.S.    | O-3.2                   |
| Nerukh         | A.      | P-10                    |
| Nicolet        | A.      | O-7.2                   |
| Nielsen        | M.      | O-8.1                   |
| Obayya         | S.S.A.  | P-20, P-21, P-22, P-23  |
| Orobtchouk     | R.      | P-11                    |
| Ostatochnikov  | V.V.    | P-40                    |
| Pardo          | F.      | O-7.0                   |
| Parini         | A.      | O-8.2, P-06             |
| Parriaux       | O.      | O-7.1, P-17             |
| Payne          | F.P.    | P-04                    |
| Pelouard       | J.-L.   | O-7.0                   |
| Perennou       | A.      | P-25                    |
| Peterka        | P.      | O-1.1                   |
| Petráček       | J.      | O-6.3, P-32             |
| Petruskevicius | R.      | O-8.2, P-03             |
| Popov          | A.      | O-3.2                   |
| Popov          | E.      | P-34                    |
| Prod'homme     | H.      | P-25                    |
| Quintard       | P.      | P-25                    |
| Ra'di          | Y.      | O-3.0                   |
| Rahman         | B.M.A.  | P-13                    |
| Rassem         | N.      | P-34                    |
| Rastogi        | V.      | P-27                    |
| Renversez      | G.      | P-33                    |
| Richter        | I.      | O-6.4, P-31, P-32       |
| Rodriguez      | S.R.K.  | O-7.3                   |
| Rolly          | B.      | P-36, P-37, P-39        |
| Rose           | P.      | O-3.3                   |
| Saeed          | A. M.A. | P-22                    |
| Saenz          | J. J.   | O-4.0                   |
| Sasse          | H.      | O-4.2                   |
| Scheid         | C.      | O-6.0                   |
| Sementsov      | D.      | P-40                    |
| Shalaev        | M. I.   | O-3.2                   |
| Sharma         | D. K.   | P-18                    |
| Sharma         | A.      | P-18, P-19              |
| Sharma         | E. K.   | P-29                    |
| Shcherbakov    | A. .A.  | P-15                    |
| Shi            | H.      | P-35                    |
| ShklyaeV       | A.      |                         |
| Slabko         | V.V.    | O-3.2                   |
| Song           | D.      | P-05                    |
| Stout          | B.      | P-36, P-37, P-38, P-39  |
| Suárez         | I.      | P-24                    |
| Tardieu        | C.      | O-7.0                   |
| Tischenko      | A. V.   | O-7.1, P-15, P-16, P-17 |
| Tisserand      | S.      | O-7.2                   |
| Tretyakov      | S.      | O-3.0                   |
| Tsarev         | A.      | O-1.3, P-08, P-09       |
| Urbonas        | D.      | O-8.2, P-03             |
| Vagionas       | C.      | O-6.2                   |

|            |       |            |
|------------|-------|------------|
| Varault    | S.    | P-36, P-37 |
| Vial       | B.    | O-7.2      |
| Vincent    | G.    | O-7.0      |
| Vinoles    | V.    | P-14       |
| Viquerat   | J.    | O-6.0      |
| Walasik    | W.    | P-33       |
| Wang       | K.    | P-28       |
| Weeber     | J.-C. | O-8.1      |
| Wenger     | J.    | P-36, P-38 |
| Wilkinson  | J.S.  | O-1.2      |
| Younis     | B.M.  | P-20       |
| Zayats     | A.    | O-2.0      |
| Zervas     | M.N.  | O-1.2      |
| Zolla      | F.    | O-7.2      |
| Zolotariov | D.    | P-10       |



## Many Thanks to our Partners :

### **Aix-Marseille Université**

Jardin du Pharo  
58, bd Charles Livon  
13284 Marseille Cedex 07  
France  
<http://www.univ-amu.fr>

### **Université Nice Sophia Antipolis**

Pôle Universitaire St Jean d'Angély  
24 avenue des Diables Bleus  
06300 Nice  
France  
<http://unice.fr>

### **PHOENIX SOFTWARE**

P.O. Box 545  
7500 AM Enschede  
The Netherlands  
Phone: +31 53 483 64 60  
Fax: +31 53 433 74 15  
Email: [info@phoenixbv.com](mailto:info@phoenixbv.com)  
<http://www.phoenixbv.com>

### **PHOTON DESIGN**

34 Leopold Street  
Oxford, OX4 1TW  
United Kingdom  
Phone: +44 1865 324990  
Fax: +44 1865 324991  
Email: [info@photond.com](mailto:info@photond.com)  
<http://www.photond.com>

### **OPTITEC**

Technopôle de Château Gombert  
38, rue F. Joliot Curie  
13388 Marseille cedex 13  
France  
<http://www.pole-optitec.com>

### **C'Nano PACA**

Campus de Luminy  
Case 913  
13288 Marseille cedex 9  
France  
<http://www.cnano-paca.fr>



OUR PARTNERS:



**OWTNM2014**

